

Aus dem Experimental and Clinical Research Center (ECRC) und  
der Medizinischen Klinik m. S. Nephrologie und Internistische  
Intensivmedizin der Medizinischen Fakultät  
Charité – Universitätsmedizin Berlin

DISSERTATION

Die Rolle von TRPC6 bei Nierenschäden  
The role of TRPC6 in kidney damage

zur Erlangung des akademischen Grades  
Doctor medicinae (Dr. med.)

vorgelegt der Medizinischen Fakultät  
Charité – Universitätsmedizin Berlin

von

Herrn Zhihuang Zheng  
aus Fujian, China

Datum der Promotion: 03.03.2023

## Table of Contents

Table of Contents .....	1
List of abbreviations.....	3
List of figures .....	5
Abstract .....	6
Zusammenfassung .....	7
1. Introduction .....	8
2. Aims and Hypothesis .....	11
3. Methodology .....	12
4. Results .....	15
4.1 TRPC6 deficiency and IRI-induced acute kidney damage .....	15
4.2 TRPC6 deficiency and IRI-induced acute kidney inflammation.....	15
4.3 TRPC6 inhibition and IRI-induced acute kidney damage.....	16
4.4 TRPC6 inhibition and IRI-induced acute kidney inflammation .....	16
4.5 TRPC6 inhibition and UUO-induced kidney damage .....	16
4.6 TRPC6 inhibition and UUO-induced kidney inflammation.....	17
4.7 TRPC6 inhibition and UUO-induced kidney fibrosis.....	17
5. Discussion.....	18
5.1 Short summary .....	18
5.2 TRPC6 blocker and pharmacological efficacy .....	18
5.3 TRPC6 and glomerular/tubular damage .....	20
5.4 TRPC6 and renal inflammation.....	20
5.5 TRPC6 and renal fibrosis.....	21
5.6 Future perspectives and clinical applications.....	23
6. Bibliography .....	24
7. Statutory Declaration.....	30
8. Selected Publication.....	32
8.1 Publication #1 .....	32
8.2 Publication #2 .....	58
9. Curriculum Vitae.....	80
10. Complete list of publications .....	82
11. Acknowledgements.....	83

## List of abbreviations

Acta2	Mouse gene nomenclature for $\alpha$ -smooth muscle actin
AKI	Acute kidney injury
AKI-to-CKD	Acute kidney injury to chronic kidney disease
CCL2	Chemokine (C-C motif) ligand 2
Ccl5	Mouse gene nomenclature for (C-C motif) ligand 5
Ccn2	Mouse gene nomenclature for connective tissue growth factor
Ccr2	Mouse gene nomenclature for (C-C motif) receptor 2
CCR2	Chemokine (C-C motif) ligand 2 receptor
CKD	Chronic kidney disease
Col1a2	Mouse gene nomenclature for collagen I
Col3a1	Mouse gene nomenclature for collagen III
Col4a3	Mouse gene nomenclature for collagen IV
CTGF	Connective tissue growth factor
Cxcl1	Mouse gene nomenclature for (C-X-C motif) ligand 1
DKD	Diabetic kidney disease
DMSO	Dimethyl sulfoxide
ERK	Extracellular signal-regulated kinase
Fn1	Fibronectin
FSGS	Focal segmental glomerulosclerosis
GOF	Gain-of-function
GPCR	G-protein coupled receptor
Havcrt2	Mouse gene nomenclature for kidney injury molecule 1
ICAM-1	Intercellular adhesion molecule 1
IL-6	Interleukin 6
IRI	Ischemia/reperfusion injury
KIM-1	Kidney injury molecule 1
Lcn2	Mouse gene nomenclature for neutrophil gelatinase-associated lipocalin
LOF	Loss-of-function
MCP-1	Monocyte chemoattractant protein-1
MEK	Mitogen-activated protein kinases/extracellular signal-regulated kinase
NGAL	Neutrophil gelatinase-associated lipocalin
NZO	New Zealand obese
PAS	Periodic acid Schiff

PBS	Phosphate–buffered saline
qRT-PCR	Real time quantitative reverse transcription polymerase chain reaction
ROS	Reactive oxygen species
S100a8/9	S100 calcium-binding protein A8/9
SPF	Specific-pathogen-free
TECs	Tubular epithelial cells
TEM	Leukocyte transendothelial migration
TGF- $\beta$	Tissue growth factor $\beta$
TNF- $\alpha$	Tumor necrosis factor-alpha
TRP	Transient receptor potential
TRPC6	Transient receptor potential cation channel, subfamily C, member 6
UUO	Unilateral ureteral obstruction
VCAM-1	Vascular cell adhesion molecule 1
WT	Wild-type



**List of figures**

Figure 1: Structural and functional aspects of TRPC6.....8  
Figure 2: Chemical structure of SH045 and (+)-Larixol.....10  
Figure 3: Study design: TRPC6 inhibition in kidney damage.....11  
Figure 4: Membrane homo- or heteromeric TRPC channels.....19  
Figure 5: TRPC6 associated mechanisms of renal inflammation and fibrosis.....23

## Abstract

Acute kidney injury (AKI) and chronic kidney disease (CKD) are worldwide common cause of death, strongly increases the risk of cardiovascular disease, and associated with a substantial economic burden. Severe AKI can progress to CKD. CKD is commonly the consequence of diabetes, high blood pressure, or glomerulonephritis, which initiate kidney injury that results in a period of months or years to inflammation, fibrosis, and ultimately to nephron loss. The initiation and progression of kidney fibrosis appear to involve a complex, so far incompletely characterized interaction between injured tubules, fibroblasts, pericytes, endothelial cells and inflammatory cells. During past years, novel drug targets such as the transient receptor potential cation channel, subfamily C, member 6 (TRPC6) emerged, as it was associated with focal segmental glomerulosclerosis. However, the function of TRPC6 channel in kidney injury is still unknown. Moreover, the effectiveness a novel selective TRPC6 inhibitor (larixyl N-methylcarbamate, SH045) has not been studied in animal models of the human disease such as the ischemia reperfusion injury (IRI) or the unilateral urethra obstruction (UUO) model. We used *Trpc6*<sup>-/-</sup> mice and SH045 to evaluate short-term outcomes of ischemia reperfusion injury (IRI)-induced AKI. Our results demonstrated that neither *Trpc6* deficiency nor pharmacological inhibition of TRPC6 influences the short-term outcomes in AKI. These findings improve the understanding of the role of TRPC6 in acute kidney damage. We also used the inbred New Zealand Obese (NZO) mouse strain better mimicking human metabolic syndrome and CKD pathophysiology to model subchronic kidney injury. This type of kidney injury was induced by unilateral urethra obstruction (UUO). As opposed to AKI, SH045 ameliorated renal inflammation and fibrogenesis in UUO mouse model. The renal expression of the pro-fibrotic markers and chemokines were markedly decreased by SH045 treatment. Furthermore, renal immune cells infiltration and tubulointerstitial fibrosis were decreased in SH045 treated NZO-UUO mice. We conclude that TRPC6 pharmacological inhibition (SH045) is a promising antifibrotic strategy to treat progressive tubulo-interstitial fibrosis.

## Zusammenfassung

Akute Nierenschädigung (AKI) and chronische Nierenerkrankung (CKD) sind weltweit eine häufige Todesursache, erhöhen das Risiko von Herz-Kreislauf-Erkrankungen stark und sind mit einer erheblichen wirtschaftlichen Belastung verbunden. Eine schwere AKI kann zu einer CKD führen. CKD ist in der Regel die Folge von Diabetes, Bluthochdruck oder Glomerulonephritis, die eine Nierenschädigung auslösen, die über Monate oder Jahre hinweg zu Entzündungen, Fibrose und schließlich zum Verlust von Nephronen führt. Der Anfang und Fortschreiten der Nierenfibrose scheint eine komplexe, bisher unvollständig charakterisierte Wechselwirkung zwischen verletzten Tubuli, Fibroblasten, Perizyten, Endothelzellen und Entzündungszellen zu sein. In den vergangenen Jahren wurden neue Wirkstoffziele wie der transiente Rezeptorpotential-Kationenkanal, Unterfamilie C, Mitglied 6 (TRPC6) entdeckt, der mit fokalen segmentalen Glomerulosklerose assoziiert wurde. Die Funktion des TRPC6-Kanals bei Nierenverletzungen ist jedoch noch unbekannt. Darüber hinaus wurde die Wirksamkeit eines neuartigen selektiven TRPC6-Inhibitors (Larixyl-N-Methylcarbammat, SH045) in Tiermodellen der menschlichen Erkrankung, wie der Ischämie-Reperfusionsschädigung (IRI) oder dem Modell der einseitigen Harnröhrenobstruktion (UUO), nicht untersucht. Wir verwendeten *Trpc6*<sup>-/-</sup> Mäuse und SH045, um kurzfristige Folgen durch Ischämie-Reperfusionsschädigung (IRI)-induzierte AKI festzustellen. Unsere Ergebnisse zeigten, dass weder TRPC6-Mangel noch pharmakologische Hemmung von TRPC6 die kurzfristigen Folgen der AKI beeinflussen. Diese Ergebnisse verbessern das Verständnis der Rolle von TRPC6 bei akuten Nierenschäden. In der UUO-Studie verwendeten wir den neuseeländischen fettleibigen (NZO) Mausstamm, der das humane metabolische Syndrom und die CKD-Pathophysiologie besser imitiert. Im Gegensatz zu AKI verbesserte SH045 die Nierenentzündung und Fibrogenese im UUO-Mausmodell. Die renale Expression von pro-fibrotischen Markern und Chemokine wurde durch die SH045-Behandlung deutlich verringert. Darüber hinaus waren die Infiltration von renalen Immunzellen und die tubulointerstitielle Fibrose bei den mit SH045 behandelten NZO-UUO-Mäusen verringert. Wir schließen daraus, dass die pharmakologische Hemmung von TRPC6 (SH045) eine vielversprechende antifibrotische Strategie zur Behandlung der progressiven tubulo-interstitiellen Fibrose darstellt.

# 1. Introduction

Transient receptor potential (TRP) channels are a group of non-selective cation channels which promote cellular influx of calcium ( $\text{Ca}^{2+}$ ) and monovalent cations [1]. In mammalian TRP superfamily, 28 members share some structural similarity with each other. Transient receptor potential canonical 6 (TRPC6) channel, a member of TRPC subfamily, triggers large amounts of  $\text{Ca}^{2+}$  influx in the cell often as a response to G-protein coupled receptor (GPCR) activation [2] (Figure 1).

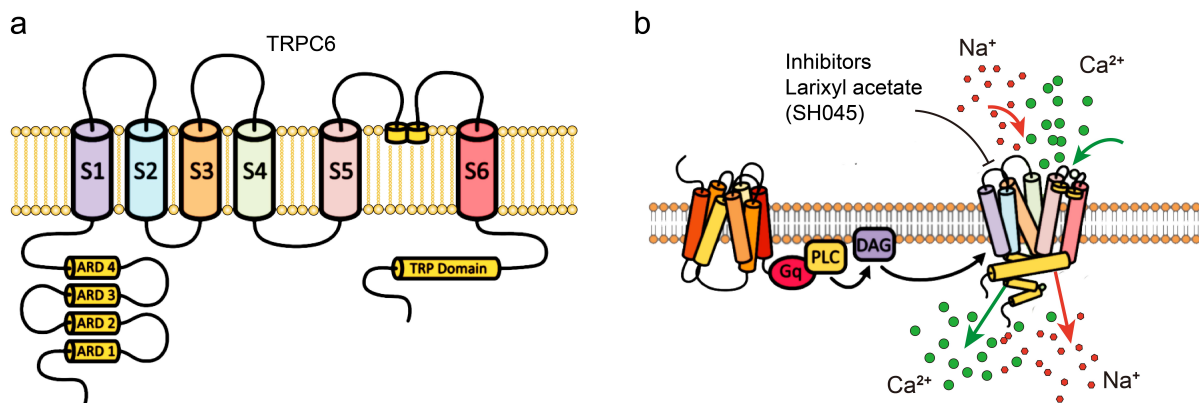


Figure 1: Structural and functional aspects of TRPC6. (a) A schematic representation of the TRPC6 structure on the membrane. TRPC6 possesses 6 membrane-spanning and 3 conserved domains. (b) Regulators of TRPC6 channel activity. G-protein-coupled receptors (GPCR) regulate TRPC6 activity by stimulating phospholipase C (PLC) to generate diacylglycerol (DAG). SH045 is a novel TRPC6 inhibitor. Modified with permission from MDPI, International Journal of Molecular Sciences, 2021, Vol 22, Issue 4, 2074, Shekhar S, et al., Copyright (2021)[3].

TRPC6 is highly expressed in renal podocytes where it interacts with major slit diaphragm proteins podocin and nephrin [4]. Increasing evidence suggests that both gain-of-function (GOF) and loss-of-function (LOF) in TRPC6 mutations lead to the proteinuria development, further resulting in progressive kidney failure and focal segmental glomerulosclerosis (FSGS) [5, 6]. In addition, angiotensin II, reactive oxygen species (ROS), and other factors in the setting of diabetic kidney disease (DKD) stimulate renal podocytes with drastic increase in  $\text{Ca}^{2+}$  influx through TRPC6 channel, causing podocytes hypertrophy with foot process effacement [7]. Therefore, TRPC6 has been extensively investigated as a target in chronic glomerular diseases.

However, to date, very little is known about the functional role of TRPC6 in acute or progressive kidney injury, especially in tubulo-interstitial damage.

Acute kidney injury (AKI), a common complication in intensive-hospitalized patients, has emerged as a major public health problem which affects millions of patients worldwide [8]. It contributes to the risk increase of chronic kidney disease (CKD) and, once development of kidney dysfunction, therefore, decreases life expectancy [9]. Ischemia/reperfusion injury (IRI), as a major cause of AKI, often occurs in the context of multiple organ failure, sepsis, and renal transplantation [10, 11]. Renal tubular epithelial cells (TECs) are susceptible to IRI because of their active energy metabolism [12]. Numerous studies showed that  $\text{Ca}^{2+}$  overload induced ROS, oxidative stress, and mitochondrial dysfunction are the key contributors to cellular damage and apoptosis during IRI [13, 14]. It suggests that limiting cellular  $\text{Ca}^{2+}$  over accumulation in TECs may decrease the ischemic injury and support recovery of TEC integrity and function.

Inflammation is now believed to play a major role in the pathophysiology of ischemic injury. AKI is known to be associated with intrarenal and systemic inflammation [15, 16]. Notably,  $\text{Ca}^{2+}$ -signalling was identified to be involved in the regulation of inflammatory responses [17, 18]. Yamamoto et al. demonstrated that cellular influx of  $\text{Ca}^{2+}$  controls the ROS-induced signalling cascade, which is responsible for chemokine production and promote inflammation [19]. As a  $\text{Ca}^{2+}$ -permeable channel, TRPC6 regulates neutrophil recruitment and leukocyte transendothelial migration during the inflammatory response [20-22]. TRPC6 deficiency in murine neutrophils exhibited lower  $\text{Ca}^{2+}$  transients during the initial adhesion by affecting CXCR2 or CXCL1-induced neutrophil adhesion, arrest and transmigration [20, 21]. In addition, a transient increase in endothelial cytosolic free  $\text{Ca}^{2+}$  concentration ( $\uparrow[\text{Ca}^{2+}]_i$ ) mediated by TRPC6 is required for leukocyte transendothelial migration (TEM) [22]. Hence, hyperfunction of TRPC6 channel accompanied by an increase in  $\text{Ca}^{2+}$  influx may aggravate inflammation and increase kidney damage.

To the best of our knowledge, no studies have demonstrated the role of TRPC6 channel in acute mouse model of kidney injury. Improved understanding is important for identifying whether TRPC6 have potential as a therapeutic target to prevent or ameliorate AKI and progressive kidney damage.

In addition, the prominent role of TRPC6 in kidney fibrosis was highlighted by recent work [23, 24]. Kidney fibrosis – the hallmark of progressive kidney damage – which is often observed in metabolic syndrome (e.g., diabetes or hypertension) might be a target of TRPC6 functional inhibition. Our previous study using *Trpc6*<sup>-/-</sup> mice showed that TRPC6 deficiency ameliorated tubule-interstitial fibrosis and immune cellular infiltration in the unilateral urethral obstruction (UUO) model [25]. Recently, a methylcarbamate congener of (+)-larixol, named SH045, has been developed as a novel, highly potent, and subtype-selective inhibitor of TRPC6 channel (Figure 2) [26, 27]. However, no studies report its effect on kidney diseases. Understanding the effect of SH045 in kidney fibrosis is essential for developing novel therapies to CKD.

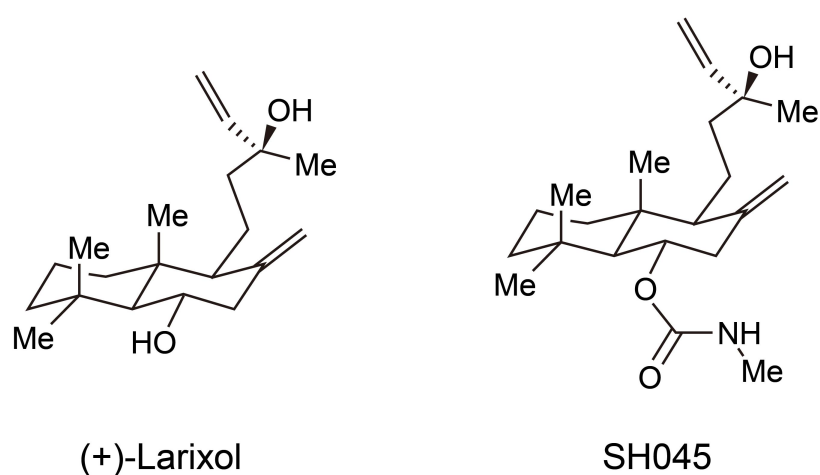


Figure 2: Chemical structure of SH045 and (+)-Larixol. The (+)-larixol and its congener SH045, both belonging to the class of labdane diterpenes, showed a structural similarity. Adapted from Fig. 1, WILEY, ChemMedChem, 2018, Vol 13, Issue 10, 1028-1035, Häfner S, et al. (2018)[26].

Certain animal models, such as the New Zealand obese (NZO) inbred mouse strain, are especially valuable for translational research. The NZO murine strain carries several susceptible genes for diabetes, obesity, and hypertension, similar to metabolic syndrome and CKD in humans [28]. Furthermore, it is known that human metabolic syndrome, including diabetes, obesity, and hypertension, is closely related to CKD. Therefore, UUO induced subchronic kidney damage in NZO mice could serve as a valuable model to mimic early stage of human CKD pathophysiology.

## 2. Aims and Hypothesis

The main purpose of this project was to uncover the role of TRPC6 channels in acute and subchronic kidney damage.

Surgical renal ischemia/reperfusion injury (IRI) and unilateral ureter obstruction (UUO) models were used to induce murine AKI and kidney fibrosis, respectively. Renal function, histological changes, immune cells infiltration, cytokines/chemokine expression, and fibrosis markers were determined and evaluated. In addition, myogenic tone was measured by isolated kidney perfusion. The following hypothesis (also summarised in Figure 3) were tested:

1. Genetic deficiency or pharmacological inhibition of TRPC6 improves renal outcomes in terms of kidney function, tubular injury, immune cells infiltration, and cytokines or chemokine upregulation in IRI-induced AKI model.
2. Pharmacological inhibition of TRPC6 ameliorates renal parenchyma damage, inflammation, and tubulo-interstitial fibrosis in UUO-induced early CKD model.

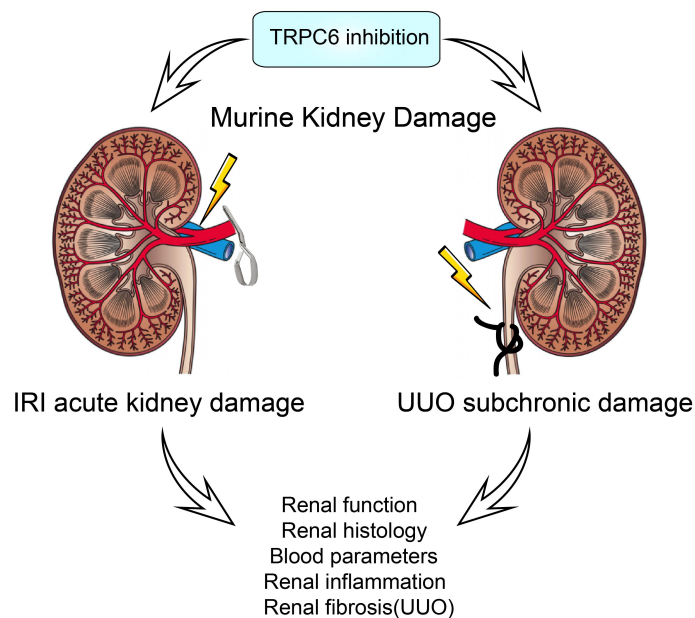


Figure 3: Study design: TRPC6 inhibition in kidney damage. The acute kidney damage mouse model is induced by ischemia/reperfusion injury (IRI). The subchronic kidney damage mouse model is induced by unilateral ureter obstruction (UUO). Outcomes of kidney damage are evaluated by renal function, blood parameters, renal histology, inflammation, and fibrosis.

### 3. Methodology

#### Animal models

To IRI-induced AKI model

From age-matched 12- to 14-week-old *Trpc6*<sup>-/-</sup> mice (male, homozygosity in a mix C57BL/6J:129Sv genetic background) and control wild-type (WT) mice (male, C57BL/6J) were used for AKI studies. The generated and characterized *Trpc6*<sup>-/-</sup> mice underwent IRI was introduced as described previously [25, 29]. Briefly, the abdomen was opened after anaesthesia and analgesia. The left renal pedicle was exposed and clamped for 17.5 minutes or 20 minutes with a non-traumatic aneurysm clip (FE690K, Aesculap, Germany) after right-sided nephrectomy. Then the clip was release and kidney reperfusion was confirmed visually. Afterwards, the abdomen and the skin were sutured separately with a 5/0 braided-silk sutures. The murine body temperature was monitored and maintained at 37 °C during surgery. Kidneys and blood samples were collected upon mouse euthanization (overdose of isoflurane and additional cervical dislocation) 24 hours after surgery for further analysis.

To UUO-induced kidney fibrosis model

The New Zealand obese (NZO) mice (Male, NZO/BomHIDife genetic background) were used as described previously [25]. Briefly, the abdomen was opened and left ureter covered by adipose tissue was exposed after analgesia and deep anaesthesia. Next, left ureter was ligated twice close to the renal pelvis by using a 5-0 polyglycolic acid suture wire. The carprofen was used in the drinking water (0.05 mg/ml) over the following two days. All UUO-NZO mice were divided into two groups as follows: UUO+Vehicle and UUO+SH045 (20 mg/kg, i.p. once per day). The UUO mice were treated with TRPC6 inhibitor SH045 once abdomen was closed and continuously received administration for 7 days. The UUO+Vehicle group was treated by vehicle under the same conditions as SH045. Seven days after mouse euthanization, blood and urine samples were collected for further analysis. Left kidney was considered as UUO kidney and the right one as control. Kidneys were cut and divided into three portions. Upper part was frozen in isopthan for immunohistochemistry. Middle part was immersed in 4% phosphate-buffered saline (PBS)-buffered formalin for histology. Last part was snap-frozen in liquid nitrogen for RNA preparation.



All experimental mice were kept in specific-pathogen-free (SPF) condition with a 12:12-h light-dark cycle, and with free access to purified food and water. Our animal study (No. G0175/18) was approved by Berlin Animal Review Board of Germany. In addition, the restrictions in the Berlin State Office for Health and Social Affairs (LaGeSo) reviewed and approved all animal experiments [30]. All experiments were performed in accordance with ARRIVE guidelines [31].

### **TRPC6 blockers and blood measurements**

SH045 (Rudolf-Boehm-Institute for Pharmacology and Toxicology, Leipzig University, Germany) was initially dissolved in 5% Cremophor EL<sup>®</sup> solution and used in IRI-induced AKI model by intravenous injection (2 mg/kg) and in UUO mouse model by intraperitoneally injection (20 mg/kg). BI-749327 (MCE, New Jersey, USA), another TRPC6 blocker, was dissolved in corn oil and administrated via oral gavage (30mg/kg) in IRI-induced AKI mouse model.

To evaluate the impact of TRPC6 pharmacological inhibition on electrolytes and renal function in AKI and UUO mouse models, blood parameters were measured and analyzed by using a clinically approved i-STAT analyzer system with Chem8+ cartridges (Abbott, Wiesbaden, Germany). The blood parameters included potassium, sodium, ionized calcium, chloride, total carbon dioxide, urea nitrogen, glucose, creatinine, hemoglobin, hematocrit, and anion gap.

### **Renal histopathology**

Briefly, kidney samples were harvested and fixed in 4% paraformaldehyde, then, embedded in paraffin, and cut into 2- $\mu$ m slice. Periodic acid Schiff (PAS) was performed using standard protocol. Histological scoring was used to evaluate kidney damage in a blinded fashion and 10 consecutive 400 $\times$  fields per slice were randomly selected for quantification. The severity of histological damage were graded from 0 to 3 according to the distribution of lesions: 0=none; 1, <25%; 2, 25–50%; 3, >50% [32]. In IRI-induced AKI, the damage parameters includes tubular epithelium flattening, tubular dilation, cellular cast formation, epithelial loss of brush border, nuclear lysis, and basement membrane rupture. In UUO mouse model, the kidney damage was evaluated using following morphological parameters: glomerular mesangial expansion, tubular epithelium flattening, tubular lumen dilation, and cast formation. In addition, to assess renal fibrosis in UUO kidneys, Sirius red staining was performed and analyzed using the same method.

## **Quantitative RT-PCR**

As previously described [33, 34], total RNA was extracted and purified from kidney according to manufacturer's instruction by using the RNeasy RNA isolation kit (Qiagen, Hilden, Germany). The concentration of RNA was examined by NanoDrop-1000 spectrophotometer (Thermo Fisher Scientific, Waltham, USA). Two micrograms of total RNA from each sample were transcribed to cDNA by using High Capacity RNA-to-cDNA™ Kit (Applied Biosystems, Waltham, USA). The qPCR for target gene was performed using the TaqMan or SYBR green Master Mix in Applied Biosystems QuantStudio 5 Real-Time PCR System (Applied Biosystems, Waltham, USA).

## **Immunohistochemistry and immunofluorescence**

Immunohistochemistry and immunofluorescence were performed on paraffin-embedded tissues using standard techniques. Briefly, 2- $\mu$ m kidney sections were deparaffinized in xylene, rehydrated in graded ethanol, and boiled in sodium citrate (pH 6.0) at 98°C for antigen retrieval. After blocking incubation using 10% normal donkey serum, kidney sections were incubated with primary antibodies at 4 °C overnight. For immunohistochemistry, tissue sections were subsequently exposed to a biotinylated secondary antibody. An ultrasensitive streptavidin peroxidase detection system was used for detection and visualization according to manufacturer's instruction. For immunofluorescence, after incubation with primary antibodies, tissue sections were further incubated with a secondary antibody and counterstained with DAPI. Slices were visualized using a Zeiss Axioplan-2 imaging microscope with the computer program AxioVision 4.8 (Zeiss, Jena, Germany).

## **Statistical analysis**

The GraphPad Prism 5.04 software (GraphPad Software Inc., San Diego, CA, USA) was used to statistical analysis. Study groups were analyzed by one-way ANOVA using Turkey's post-hoc test or two-way ANOVA using Sidak's multiple comparisons post hoc test. Data are presented as mean  $\pm$  SEM. *P* values < 0.05 were considered as statistically significant.

- For complete and detailed methodology, please see the publications [33, 34].

## 4. Results

### 4.1 TRPC6 deficiency and IRI-induced acute kidney damage

First, we performed qRT-PCR to determine whether *Trpc6* expression changes after IRI-induced AKI in wild-type (WT) mice. In kidney tissue 24 hours after IRI, *Trpc6* mRNA expression was unchanged compared to the sham operated mice. At baseline, biochemical blood parameters in *Trpc6*<sup>-/-</sup> mice were also similar compared to WT mice. However, concentrations of sodium and ionized Ca<sup>2+</sup> were higher in *Trpc6*<sup>-/-</sup> mice but still in normal, physiological range. WT and *Trpc6*<sup>-/-</sup> mice developed similar level of hyperkalaemia 24 h after IRI. To evaluate renal function, we measured serum creatinine by i-STAT analyzer system. *Trpc6*<sup>-/-</sup> mice showed matching serum creatinine level compared to WT mice after renal IRI ( $P = 0.18$ , two-way ANOVA), suggesting that *Trpc6* deficiency had no impact on renal function in AKI model. Similarly, the renal mRNA expression of tubular damage markers kidney injury molecule 1 (KIM-1) and neutrophil gelatinase-associated lipocalin (NGAL) showed no difference between WT and *Trpc6*<sup>-/-</sup> mice after IRI. In addition, renal histological assessment revealed comparable tubular damage score in *Trpc6*<sup>-/-</sup> and WT mice after IRI. Thus, we concluded that *Trpc6* deficiency exhibits no protective effect on acute tubular damage.

### 4.2 TRPC6 deficiency and IRI-induced acute kidney inflammation

Previous studies demonstrated that immune cells infiltration (e.g., neutrophils) plays critical role in AKI-induced renal damage [15]. Therefore, we evaluated neutrophils infiltration after IRI. Neutrophils in kidney tissue were immunolabelled with the Ly6B.2 marker. Results show the accumulation of Ly6B.2 positive cells in *Trpc6*<sup>-/-</sup> IRI kidney which was similar to WT group, suggesting renal neutrophils infiltration was not influenced by *Trpc6* deficiency. In addition, we also measured expression of classic inflammatory indicators e.g., S100 calcium-binding protein A8 and A9 (*S100a8/a9*), interleukin 6 (*Il6*), tumor necrosis factor-alpha (*Tnf- $\alpha$* ), intercellular adhesion molecule 1 (*Icam1*), vascular cell adhesion molecule 1 (*Vcam1*), chemokine (C-C motif) ligand 2 (*Ccl2*), and chemokine (C-C motif) ligand 2 receptor (*Ccr2*). Renal mRNA expressions of these chemokine/cytokines (*S100a8*, *S100a9*, *Tnf- $\alpha$* , *Il6*, *Vcam1*, *Icam1*, *Ccl2*, and *Ccr2*) in *Trpc6*<sup>-/-</sup> mice were equivalent to WT mice. These data indicate that *Trpc6* deficiency does not affect acute inflammation in IRI-induced AKI.

### **4.3 TRPC6 inhibition and IRI-induced acute kidney damage**

To verify the results obtained using genetic knockout mouse model, we further performed experiments using two structurally different pharmacological inhibitors of TRPC6 (SH045 and BI-749327) in AKI. Both SH045 and BI-749327 administration showed unaffected blood parameters after IRI. For instance, serum creatinine levels in IRI-induced AKI were similarly high in both groups (inhibitors treatment vs. vehicle treatment). Moreover, renal expression of tubular damage markers NGAL (*Lcn2*) and KIM-1 (*Havcr1*) was examined. By qRT-PCR analysis, results revealed markedly increased renal expression of *Lcn2* and *Havcr1* in both SH045-treated and vehicle-treated mice after AKI, whereas there was no difference between SH045 and vehicle treatment. Additionally, renal histological assessment revealed identical tubular damage score in SH045/BI-749327- and vehicle-treated mice after AKI. Thus, we concluded that TRPC6 pharmacological inhibition exhibited no protective effect on acute kidney damage upon 24 hours IRI.

### **4.4 TRPC6 inhibition and IRI-induced acute kidney inflammation**

Next, we performed immunofluorescence analysis to confirm data obtained in *Trpc6*<sup>-/-</sup> mice. Enhanced neutrophils infiltration was unaffected by SH045- or BI-749327-treatment after IRI-induced AKI. In alignment with *Trpc6* deficient mice, mRNA expressions of inflammatory markers (*S100a8*, *S100a9*, *Tnf- $\alpha$* , *Il6*, *Vcam1*, *Icam1*, *Ccl2*, and *Ccr2*) after TRPC6 pharmacological blockade group were equivalent to vehicle group after AKI. Therefore, renal IRI-induced acute inflammation is not affected by TRPC6 pharmacological inhibition.

### **4.5 TRPC6 inhibition and UUO-induced kidney damage**

To further investigate the role of TRPC6 in subchronic kidney damage, we performed UUO surgery on NZO mice. Thereafter, we applied SH045 to test whether TRPC6 pharmacological inhibition ameliorates renal fibrosis, glomerular or tubular damage, and inflammatory response. All blood parameters (e.g., serum creatinine, blood urea nitrogen, cystatin C) were normal in SH045-treated mice compared to vehicle-treated mice. In addition, urine albumin, and albumin-to-creatinine ration in SH045-treated mice were also similar between two groups, respectively. These data suggests no safety concerns of SH045 treatment *in vivo*. Histological staining and analysis revealed that glomerular and tubular damage scores in SH045-treated mice were

comparable to vehicle group. Besides, qRT-PCR analysis also demonstrated equivalent mRNA expression of kidney damage markers KIM-1 and NGAL (*Havcr1* and *Lcn2*) between groups, which suggest SH045 treatment did not alter kidney parenchymal damage.

#### **4.6 TRPC6 inhibition and UUO-induced kidney inflammation**

To evaluate renal inflammation 1 week after urethra obstruction, we first determined mRNA expression of chemokines or cytokines in kidney tissue. SH045 decreased the mRNA levels of chemokines or receptors (*Cxcl1*, *Ccl5*, and *Ccr2*,) in UUO kidneys compared to vehicle. Although the expressions of *Ccl2*, *Cxcl2*, and *Icam1* were slightly lower in SH045 UUO kidneys, these differences did not reach statistical significance ( $P = 0.057$ ,  $P = 0.068$  and  $P = 0.076$ , respectively). Renal ICAM-1 positive staining in SH045 treated UUO mice was significantly less than vehicle group. Moreover, renal immunofluorescence analysis revealed decreased interstitial accumulation of F4/80+ macrophages and CD4+ T cells in SH045-treated UUO kidneys compared to vehicle group. According to the data, TRPC6 inhibition with SH045 decreased inflammation in subchronic model of kidney injury.

#### **4.7 TRPC6 inhibition and UUO-induced kidney fibrosis**

Since kidney fibrosis is a typical lesion observed in UUO mouse model [35], we evaluated the gene markers including collagen I/III/IV (*Col1a2*, *Col3a1*, *Col4a3*), connective tissue growth factor (*Ccn2*),  $\alpha$ -smooth muscle actin (*Acta2*), and fibronectin (*Fn1*). The mRNA of these genes contributing to kidney fibrosis was upregulated after 7-day UUO. Of note, the expression of *Col1a2*, *Col3a1*, *Col4a3*, *Ccn2*, *Fn1*, and *Acta2* in the UUO kidneys was decreased by SH045 treatment, compared with vehicle group. In agreement with RT-qPCR, UUO kidneys displayed markedly increased Sirius red+ areas compared to control group, indicating that UUO caused considerable collagen deposition. SH045 effectively reduced this collagen deposition. Similarly, the immunofluorescence staining revealed increased fibronectin expression in UUO kidney, which was diminished by SH045 treatment. In addition,  $\alpha$ -SMA+ cells in UUO kidneys were decreased in SH045 treatment group when compared with vehicle group. Taken together, these findings strongly suggest that UUO-induced kidney fibrosis was diminished as TRPC6 functional blocked.

## 5. Discussion

### 5.1 Short summary

We used *Trpc6*<sup>-/-</sup> mice and SH045 (a pharmacological inhibitor of TRPC6) and BI-749327 (another TRPC6 inhibitor) to evaluate short-term AKI and UUO outcomes. We demonstrate that neither *Trpc6* deficiency nor pharmacological inhibition of TRPC6 influences the short-term outcomes of AKI (Hypothesis I). These data also suggest that overexpression and subsequent activation of TRPC6 channels may occur in later course of fibrosis after AKI.

Indeed, SH045 ameliorated renal fibrosis and inflammatory responses except of glomerular or tubular damage in UUO-model (Hypothesis II). SH045 markedly decreased expression of pro-fibrotic markers and chemokines in UUO kidneys of NZO mice. In addition, renal inflammatory cell infiltration and tubulointerstitial fibrosis were decreased in SH045 treated NZO mice. These findings imply that TRPC6 on immune cells (CD4+ or F4/80+) and fibroblasts may play a role in the development of renal chronic fibrosis.

### 5.2 TRPC6 blocker and pharmacological efficacy

Although the use of genetic mouse models is widespread, potential shortcomings of this methodology exist [36]. For instance, genetic knockout partially represents deficiency of target molecule which can lead secondary compensatory changes in gene expression [37]. Indeed, previous studies demonstrated that TRPC6 and other TRPC (e.g. TRPC3 or TRPC7) channels can form functional heteromultimers with different regulatory properties from the homomeric TRPC channels [38-40] (Figure 4). Expression of *Trpc3* is upregulated in *Trpc6*<sup>-/-</sup> mice, nevertheless it does not functionally replace *Trpc6* [41]. Given the complexity and potential interference of TRPC heteromultimers, functional inhibition by pharmacological inhibitors in homomeric or heteromeric TRPC6 channels may be better than gene knockout. Therefore, for exploring the role of TRPC6, high specific pharmacological blockade may have advantages in targeting TRPC6 over *Trpc6* knockout animals.

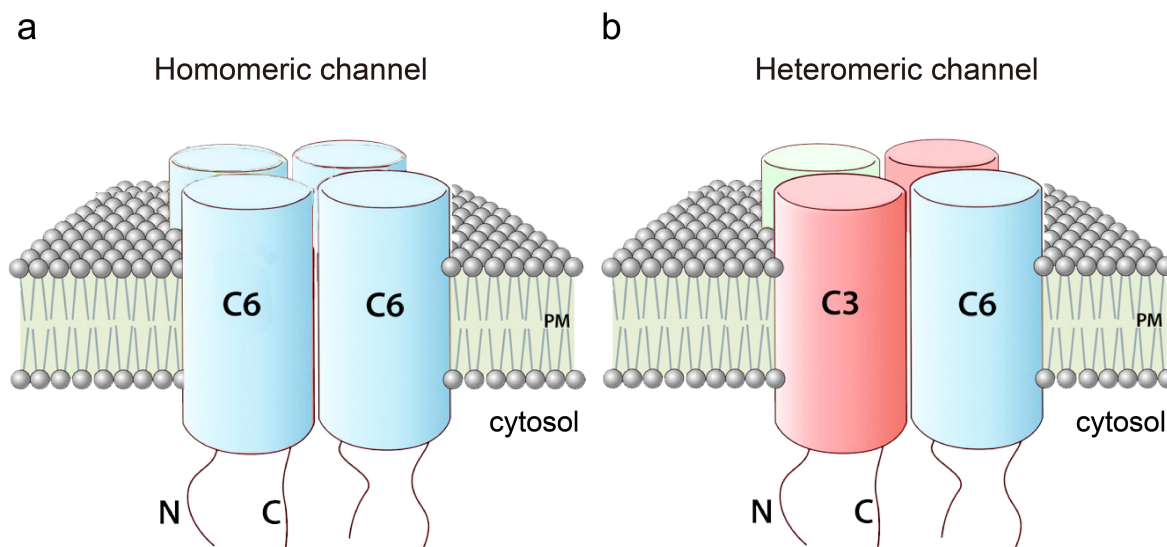


Figure 4: Membrane homo- or heteromeric TRPC channels. (a) Tetrameric structure of homomeric TRPC6 channels in the plasma membrane. (b) Proposed tetrameric structure of heteromeric TRPC3/6 channels in the plasma membrane. Adapted from Fig. 1, American Heart Association, *Circulation Research*, 2011, Vol 108, Issue 2, 265-72. Eder P, et al. (2011)[42].

Currently, several common chemical entities, blocking TRPC6, with only limited isotype-specificity to its closest relatives TRPC3/7. In order to target TRPC6 with high selectivity, recently, a methylcarbamate congener of (+)-larixol, named SH045, was obtained and identified in functional assays as a novel, highly potent, subtype-selective inhibitor of TRPC6 [26]. As a new inhibitor, the efficacy of SH045 in kidney tissue is the main focus of our attention. According to the reported  $IC_{50}$ -values (6-60 nM) and pharmacokinetic analysis of SH045 [26, 27], a concentration of 22 ng/g in tissues can be considered as pharmacologically effective. Assuming non-compartment modeling this concentration is expected to be equivalent to 60 nM (molecular weight of SH045 = 263). In our study SH045 concentration in kidney tissues was  $284.6 \pm 144.8$  ng/g after 30 min after the SH045 injection and  $16.3 \pm 14.6$  ng/g after 24 hours, respectively [34]. In addition, SH045 was identified extensively binding to kidney tissue and timely renal elimination from systemic circulation [43]. Beyond 2 hours after administration, an apparent amount of pharmacologically active SH045 passed the kidney filter. Therefore, the dosage of SH045 used *in vivo* was appropriate to inhibit the renal TRPC6 channels for the whole duration of the experiment.

### 5.3 TRPC6 and glomerular/tubular damage

Calcium ( $\text{Ca}^{2+}$ ) overload and reactive oxygen species (ROS) production have been identified as crucial factors for tubular epithelial damage in IRI-induced AKI [44, 45]. Kim et al. recently found that TRPC6 channel could be stimulated and activated by ROS and mediate podocytes injury in glomerular diseases [46]. Likewise, Liu et al. demonstrated that decreased cellular  $\text{Ca}^{2+}$  entry contributed to reducing astrocytic apoptosis, cytotoxicity and inflammatory responses in cerebral IRI using pharmacological blockage of TRPC6 [47]. Given that, we hypothesized nephroprotective properties of TRPC6 inhibition in ischemic AKI. Unexpectedly, no difference of renal function or tubular damage in *Trpc6*<sup>-/-</sup> mice when compared to WT mice underwent IRI [34]. Moreover, we also found no difference with respect to serum creatinine or tubular damage between AKI mice with or without pharmacological inhibition of TRPC6.

In IRI-induced AKI, tubular epithelial cells (TECs) are susceptible to injury due to ischemia-reperfusion and associated oxidative stress [48]. TRPC6 channel is identified expressed in the plasma membrane of most kidney cells, including podocytes, glomerular mesangial cells, and TECs [4]. Furthermore, Hou et al. demonstrated that TRPC6 deletion *in vitro* ameliorates renal proximal tubular cell apoptosis driven by  $\text{H}_2\text{O}_2$  [49]. Their findings *in vitro* contradict our results *in vivo* which exhibit no protective effects of TRPC6 inhibition in the ischemic AKI. Since  $\text{Ca}^{2+}$  signals are potent effectors of wound healing and tissue regeneration [50], TRPC6 associated effects may occur in recovery stage of kidney injury.

Nevertheless, numerous studies demonstrated that TRPC6 play a critical role in podocytes-associated glomerular diseases such as FSGS [51]. In line with a previous study of our group, SH045 did not affect the glomerular lesion or tubular dilatation in UUO mouse model [33]. An open question whether TRPC6 inhibition decreases long-term outcomes (> 1 week) of glomerular/tubular injury requires further investigation.

### 5.4 TRPC6 and renal inflammation

The occurrence and persistence of inflammation after renal injury contribute to renal repair and fibrogenesis, which plays an important role in renal prognosis [15, 52]. Numerous studies have found TRPC6 expressed on neutrophils and endothelium, which are involved in inflammatory responses by regulating immune cells



transendothelial migration, chemotaxis, phagocytosis, and cytokine release [20, 22]. Therefore, we hypothesized that TRPC6 inhibition regulates AKI associated inflammation. Our data showed no impact of TRPC6 inhibition/deficiency on renal neutrophils infiltration as well as S100A8/9 overexpression in AKI model [34]. Furthermore, renal expression of cytokines or chemokines confirmed absence of TRPC6 related benefits. Since injured TECs involved in recruiting inflammatory cells by releasing chemoattractant molecules [16, 53], too severe damage of TECs may explain failure of this strategy.

As opposed to AKI, *Trpc6* deficiency or pharmacological inhibition reduced CD3<sup>+</sup> T cells and F4/80<sup>+</sup> macrophages infiltration in 7-days UUO kidneys [25]. Besides, SH045 inhibited overexpression of chemokines/cytokines treatment. This agrees with a previous study using *Trpc6* deficient mice. Notably, neutrophil infiltration is one of the hallmarks of acute inflammation [54]. In contrast, subchronic inflammatory lesions are characterized by the infiltration of macrophages and T lymphocytes [15, 55]. We show that TRPC6 inhibition (SH045) reduce infiltration of CD4<sup>+</sup> T cells and F4/80<sup>+</sup> macrophages. It is highly likely that targeting these immune cells may also ameliorate chronic in addition to subchronic inflammatory stage. Furthermore, AKI to CKD progression occurs due to persistent inflammation [15, 16]. Hence, further investigations of TRPC6 effects on the renal chronic inflammatory response in the AKI-to-CKD progression may be of great clinical value.

## **5.5 TRPC6 and renal fibrosis**

Renal progressive fibrosis is the common pathological outcome of various acute and chronic kidney diseases independent of the underlying etiology. In general, renal fibrosis develops following activation of fibroblasts. They differentiate into myofibroblasts, which additionally participate in the inflammatory response to injury [56-58]. Next, upon activation by profibrotic factors (e.g., MCP-1(CCL2), CXCL2, CTGF, and TGF- $\beta$ ) myofibroblasts acquire a contractile/proliferative phenotype and become principal kidney collagen-producing cells, which are involved in the formation of the extracellular matrix [59].

Once tubulo-interstitial irreversible damage occurs, interstitial fibrosis is an important part of renal repair mechanisms, however, its excess leads to AKI-to-CKD progression. Interestingly, Wu et al. and our previous study suggested that TRPC6 inhibition using genetic deletion or pharmacological tools ameliorates renal interstitial

fibrosis [24, 25]. Growing evidence suggest that TRPC6 is responsible for cellular-increased  $\text{Ca}^{2+}$  flux in myo/fibroblasts [24, 60]. Moreover, a genome-wide screen identified TRPC6 is necessary and sufficient for TGF- $\beta$ 1 and angiotensin II-induced myofibroblast transdifferentiation. Activated TRPC6 channel is required for impaired dermal and cardiac wound healing [60]. Given that, TRPC6 in myo/fibroblasts could be a therapeutic target for fibrogenesis. Indeed, several studies confirmed the role of TRPC6 in pulmonary and skin fibrosis [61, 62]. Hence, the beneficial effects of TRPC6 inhibition seen in the UUO model likely involve fibroblast activation or transdifferentiation. Since renal fibrogenesis is an expected long-term outcome of AKI [63], this might explain the lack of *Trpc6*<sup>-/-</sup> effects on the short-term outcome of AKI in the present study. For this reason, we further hypothesized that functional blockade of TRPC6 may be beneficial in preventing AKI-to-CKD transition.

In UUO study, we used the NZO mouse strain with metabolic abnormalities including hypertension and diabetes [28]. UUO induced kidney fibrosis in NZO mice might be better to simulate human CKD pathophysiology. In UUO-NZO mice the results were consistent with our previous study [25]. SH045 attenuated renal fibrosis including collagen deposition and fibrosis-associated gene expression. Variety of these genes is activation stimuli derived from lymphocytes and macrophages [23]. Renal inflammation initiates and supports progression of fibrosis [23]. Interestingly, our results show that chemokine overproduction and immune cells infiltration were diminished by SH045 treatment. Consequently, one explanation for TRPC6 antagonizing renal fibrosis may include amelioration of the inflammatory process. Another likely mechanism involved in renoprotection is affecting myo/fibroblasts directly [60]. These mechanisms are schematically summarized in Figure 5.

On the other hand, TRPC6 blockade may decrease  $\text{Ca}^{2+}$  dependent activation of various molecular signaling e.g. MEK/ERK and Hippo pathways [64, 65] (Figure 5). Of note, MEK/ERK has been implemented in the differentiation and expansion of kidney fibroblasts [66]. UUO-induced kidney fibrosis can be ameliorated by trametinib (MEK inhibitor) through mammalian target of rapamycin complex 1 (mTORC1) and its downstream signaling. Moreover, Hippo signaling pathway was markedly activated with YAP persistent nuclear translocation in TECs during AKI-to-CKD transition [67-69]. Hippo pathway is an evolutionarily conserved signaling cascade regulating cell proliferation, apoptosis, and response to a wide range of extracellular and intracellular signals. Also, the function of cell polarity, cell-cell contact, mechanical

cues, G-protein-coupled receptors, and cellular energy status partially depend on Hippo pathway activation [70]. Similar to TRPC6, YAP, as the main downstream effector in Hippo pathway, its genetic mutation can lead to podocytes damage and further cause FSGS [6, 71]. Taken together, MEK/ERK and Hippo signaling pathways may involve the downstream mechanism of TRPC6 blocking kidney fibrosis but need further investigation.

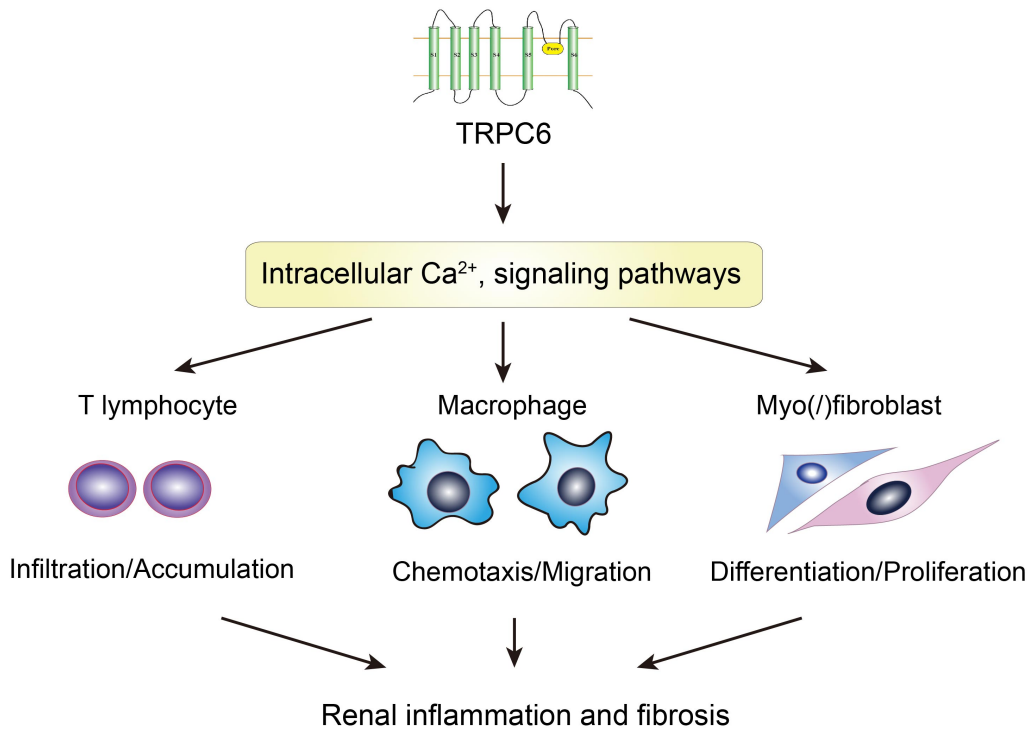


Figure 5: TRPC6 associated mechanisms of renal inflammation and fibrosis.

## 5.6 Future perspectives and clinical applications

We conclude that *in vivo* functional inhibition of TRPC6 might be a promising anti-fibrotic therapeutic agent to treat progressive kidney fibrosis. Although our results demonstrate TRPC6 inhibition has no protective effect in short-term outcome of ischemic AKI, our findings improve the understanding of the role of TRPC6 in acute kidney diseases. Future studies should investigate the effect of TRPC6 in long-term outcomes of AKI with chronic inflammation and fibrosis. Also, cell subset to target to ameliorate injury or enhance repair must be delineated. Our findings may have clinical implication for safety and prognosis of humans with *TRPC6* gene variations leading to familial forms of FSGS, with respect to the response of acute ischemic stimuli. Finally, this basic research can be expanded to clinical trials to ameliorate and abrogate renal fibrosis with the aim of helping patients world-wide.

## 6. Bibliography

1. Kaneko Y and Szallasi A. Transient receptor potential (TRP) channels: a clinical perspective. *Br J Pharmacol.* 171, 2474-507 (2014).
2. Venkatachalam K and Montell C. TRP channels. *Annu Rev Biochem.* 76, 387-417 (2007).
3. Shekhar S, Liu Y, Wang S, Zhang H, Fang X, Zhang J, Fan L, Zheng B, Roman RJ, Wang Z, Fan F, and Booz GW. Novel Mechanistic Insights and Potential Therapeutic Impact of TRPC6 in Neurovascular Coupling and Ischemic Stroke. *Int J Mol Sci.* 22, 2074 (2021).
4. Reiser J, Polu KR, Moller CC, Kenlan P, Altintas MM, Wei C, Faul C, Herbert S, Villegas I, Avila-Casado C, McGee M, Sugimoto H, Brown D, Kalluri R, Mundel P, Smith PL, Clapham DE, and Pollak MR. TRPC6 is a glomerular slit diaphragm-associated channel required for normal renal function. *Nat Genet.* 37, 739-44 (2005).
5. Riehle M, Buscher AK, Gohlke BO, Kassmann M, Kolatsi-Joannou M, Brasen JH, Nagel M, Becker JU, Winyard P, Hoyer PF, Preissner R, Krautwurst D, Gollasch M, Weber S, and Harteneck C. TRPC6 G757D Loss-of-Function Mutation Associates with FSGS. *J Am Soc Nephrol.* 27, 2771-83 (2016).
6. Winn MP, Conlon PJ, Lynn KL, Farrington MK, Creazzo T, Hawkins AF, Daskalakis N, Kwan SY, Ebersviller S, Burchette JL, Pericak-Vance MA, Howell DN, Vance JM, and Rosenberg PB. A mutation in the TRPC6 cation channel causes familial focal segmental glomerulosclerosis. *Science.* 308, 1801-4 (2005).
7. Staruschenko A, Spires D, and Palygin O. Role of TRPC6 in Progression of Diabetic Kidney Disease. *Curr Hypertens Rep.* 21, 48 (2019).
8. Lameire NH, Bagga A, Cruz D, De Maeseneer J, Endre Z, Kellum JA, Liu KD, Mehta RL, Pannu N, Van Biesen W, and Vanholder R. Acute kidney injury: an increasing global concern. *Lancet.* 382, 170-9 (2013).
9. Hsu CY. Yes, AKI truly leads to CKD. *J Am Soc Nephrol.* 23, 967-9 (2012).
10. Chen J, You H, Li Y, Xu Y, He Q, and Harris RC. EGF Receptor-Dependent YAP Activation Is Important for Renal Recovery from AKI. *J Am Soc Nephrol.* 29, 2372-2385 (2018).
11. Bonventre JV and Yang L. Cellular pathophysiology of ischemic acute kidney injury. *J Clin Invest.* 121, 4210-21 (2011).
12. Nakazawa D, Kumar SV, Marschner J, Desai J, Holderied A, Rath L, Kraft F, Lei Y, Fukasawa Y, Moeckel GW, Angelotti ML, Liapis H, and Anders HJ. Histones and Neutrophil Extracellular Traps Enhance Tubular Necrosis and Remote Organ Injury in Ischemic AKI. *J Am Soc Nephrol.* 28, 1753-1768 (2017).
13. Devarajan P. Update on mechanisms of ischemic acute kidney injury. *J Am Soc Nephrol.* 17, 1503-20 (2006).

14. Lan R, Geng H, Singha PK, Saikumar P, Bottinger EP, Weinberg JM, and Venkatachalam MA. Mitochondrial Pathology and Glycolytic Shift during Proximal Tubule Atrophy after Ischemic AKI. *J Am Soc Nephrol.* 27, 3356-3367 (2016).
15. Sato Y and Yanagita M. Immune cells and inflammation in AKI to CKD progression. *Am J Physiol Renal Physiol.* 315, F1501-f1512 (2018).
16. Xu L, Sharkey D, and Cantley LG. Tubular GM-CSF Promotes Late MCP-1/CCR2-Mediated Fibrosis and Inflammation after Ischemia/Reperfusion Injury. *J Am Soc Nephrol.* 30, 1825-1840 (2019).
17. Volz J, Kusch C, Beck S, Popp M, Vögtle T, Meub M, Scheller I, Heil HS, Preu J, Schuhmann MK, Hemmen K, Premisler T, Sickmann A, Heinze KG, Stegner D, Stoll G, Braun A, Sauer M, and Nieswandt B. BIN2 orchestrates platelet calcium signaling in thrombosis and thrombo-inflammation. *J Clin Invest.* 130, 6064-6079 (2020).
18. Suetomi T, Willeford A, Brand CS, Cho Y, Ross RS, Miyamoto S, and Brown JH. Inflammation and NLRP3 Inflammasome Activation Initiated in Response to Pressure Overload by Ca(2+)/Calmodulin-Dependent Protein Kinase II  $\delta$  Signaling in Cardiomyocytes Are Essential for Adverse Cardiac Remodeling. *Circulation.* 138, 2530-2544 (2018).
19. Yamamoto S, Shimizu S, Kiyonaka S, Takahashi N, Wajima T, Hara Y, Negoro T, Hiroi T, Kiuchi Y, Okada T, Kaneko S, Lange I, Fleig A, Penner R, Nishi M, Takeshima H, and Mori Y. TRPM2-mediated Ca<sup>2+</sup>influx induces chemokine production in monocytes that aggravates inflammatory neutrophil infiltration. *Nat Med.* 14, 738-47 (2008).
20. Lindemann O, Umlauf D, Frank S, Schimmelpfennig S, Bertrand J, Pap T, Hanley PJ, Fabian A, Dietrich A, and Schwab A. TRPC6 regulates CXCR2-mediated chemotaxis of murine neutrophils. *J Immunol.* 190, 5496-505 (2013).
21. Lindemann O, Rossaint J, Najder K, Schimmelpfennig S, Hofschröer V, Wälte M, Fels B, Oberleithner H, Zarbock A, and Schwab A. Intravascular adhesion and recruitment of neutrophils in response to CXCL1 depends on their TRPC6 channels. *J Mol Med (Berl).* 98, 349-360 (2020).
22. Weber EW, Han F, Tauseef M, Birnbaumer L, Mehta D, and Muller WA. TRPC6 is the endothelial calcium channel that regulates leukocyte transendothelial migration during the inflammatory response. *J Exp Med.* 212, 1883-99 (2015).
23. Lv W, Booz GW, Wang Y, Fan F, and Roman RJ. Inflammation and renal fibrosis: Recent developments on key signaling molecules as potential therapeutic targets. *Eur J Pharmacol.* 820, 65-76 (2018).
24. Wu YL, Xie J, An SW, Oliver N, Barrezueta NX, Lin MH, Birnbaumer L, and Huang CL. Inhibition of TRPC6 channels ameliorates renal fibrosis and contributes to renal protection by soluble klotho. *Kidney Int.* 91, 830-841 (2017).

25. Kong W, Haschler TN, Nürnberg B, Krämer S, Gollasch M, and Markó L. Renal Fibrosis, Immune Cell Infiltration and Changes of TRPC Channel Expression after Unilateral Ureteral Obstruction in *Trpc6*<sup>-/-</sup> Mice. *Cell Physiol Biochem*. 52, 1484-1502 (2019).
26. Hafner S, Burg F, Kannler M, Urban N, Mayer P, Dietrich A, Trauner D, Broichhagen J, and Schaefer M. A (+)-Larixol Congener with High Affinity and Subtype Selectivity toward TRPC6. *ChemMedChem*. 13, 1028-1035 (2018).
27. Chai XN, Ludwig FA, Müglitz A, Schaefer M, Yin HY, Brust P, Regenthal R, and Krügel U. Validation of an LC-MS/MS Method to Quantify the New TRPC6 Inhibitor SH045 (Larixyl N-methylcarbamate) and Its Application in an Exploratory Pharmacokinetic Study in Mice. *Pharmaceuticals (Basel)*. 14, 259 (2021).
28. Mirhashemi F, Scherneck S, Kluth O, Kaiser D, Vogel H, Kluge R, Schürmann A, Neschen S, and Joost HG. Diet dependence of diabetes in the New Zealand Obese (NZO) mouse: total fat, but not fat quality or sucrose accelerates and aggravates diabetes. *Exp Clin Endocrinol Diabetes*. 119, 167-71 (2011).
29. Markó L, Szijártó IA, Filipovic MR, Kaßmann M, Balogh A, Park JK, Przybyl L, N'Diaye G, Krämer S, Anders J, Ishii I, Müller DN, and Gollasch M. Role of Cystathionine Gamma-Lyase in Immediate Renal Impairment and Inflammatory Response in Acute Ischemic Kidney Injury. *Sci Rep*. 6, 27517 (2016).
30. Restrictions in the State Office for Health and Social Affairs (LAGeSo). Animal welfare. Available from: <https://www.berlin.de/lageso/gesundheit/veterinaerwesen/tierschutz/> (Access on 17 Aug 2021).
31. Kilkeny C, Browne WJ, Cuthill IC, Emerson M, and Altman DG. Improving bioscience research reporting: the ARRIVE guidelines for reporting animal research. *PLoS Biol*. 8, e1000412 (2010).
32. Chen L, Markó L, Kaßmann M, Zhu Y, Wu K, and Gollasch M. Role of TRPV1 channels in ischemia/reperfusion-induced acute kidney injury. *PLoS One*. 9, e109842 (2014).
33. Zheng Z, Xu Y, Krügel U, Schaefer M, Grune T, Nürnberg B, Köhler MB, Gollasch M, Tsvetkov D, and Markó L. In Vivo Inhibition of TRPC6 by SH045 Attenuates Renal Fibrosis in a New Zealand Obese (NZO) Mouse Model of Metabolic Syndrome. *Int J Mol Sci*. 23, 6870 (2022).
34. Zheng Z, Tsvetkov D, Bartolomaeus TUP, Erdogan C, Krügel U, Schleifenbaum J, Schaefer M, Nürnberg B, Chai X, Ludwig FA, N'Diaye G, Köhler MB, Wu K, Gollasch M, and Markó L. Role of TRPC6 in kidney damage after acute ischemic kidney injury. *Sci Rep*. 12, 3038 (2022).
35. Chevalier RL, Forbes MS, and Thornhill BA. Ureteral obstruction as a model of renal interstitial fibrosis and obstructive nephropathy. *Kidney Int*. 75, 1145-1152 (2009).

36. Eisener-Dorman AF, Lawrence DA, and Bolivar VJ. Cautionary insights on knockout mouse studies: the gene or not the gene? *Brain Behav Immun.* 23, 318-24 (2009).
37. Ma Z, Zhu P, Shi H, Guo L, Zhang Q, Chen Y, Chen S, Zhang Z, Peng J, and Chen J. PTC-bearing mRNA elicits a genetic compensation response via Upf3a and COMPASS components. *Nature.* 568, 259-263 (2019).
38. Chu X, Tong Q, Cheung JY, Wozney J, Conrad K, Mazack V, Zhang W, Stahl R, Barber DL, and Miller BA. Interaction of TRPC2 and TRPC6 in erythropoietin modulation of calcium influx. *J Biol Chem.* 279, 10514-22 (2004).
39. Hofmann T, Schaefer M, Schultz G, and Gudermann T. Subunit composition of mammalian transient receptor potential channels in living cells. *Proc Natl Acad Sci U S A.* 99, 7461-6 (2002).
40. Schaefer M. Homo- and heteromeric assembly of TRP channel subunits. Available from: [https://research.uni-leipzig.de/pharma/main/research/schaefer/TRP\\_multimerisation.html](https://research.uni-leipzig.de/pharma/main/research/schaefer/TRP_multimerisation.html) (Access on 14 Mar 2022).
41. Dietrich A, Mederos YSM, Gollasch M, Gross V, Storch U, Dubrovskaja G, Obst M, Yildirim E, Salanova B, Kalwa H, Essin K, Pinkenburg O, Luft FC, Gudermann T, and Birnbaumer L. Increased vascular smooth muscle contractility in TRPC6<sup>-/-</sup> mice. *Mol Cell Biol.* 25, 6980-9 (2005).
42. Eder P and Molkentin JD. TRPC channels as effectors of cardiac hypertrophy. *Circ Res.* 108, 265-72 (2011).
43. Chai XN, Ludwig FA, Müglitz A, Gong Y, Schaefer M, Regenthal R, and Krügel U. A Pharmacokinetic and Metabolism Study of the TRPC6 Inhibitor SH045 in Mice by LC-MS/MS. *Int J Mol Sci.* 23, 3635 (2022).
44. Schrier RW, Arnold PE, Van Putten VJ, and Burke TJ. Cellular calcium in ischemic acute renal failure: role of calcium entry blockers. *Kidney Int.* 32, 313-21 (1987).
45. Liao W, Wang Z, Fu Z, Ma H, Jiang M, Xu A, and Zhang W. p62/SQSTM1 protects against cisplatin-induced oxidative stress in kidneys by mediating the cross talk between autophagy and the Keap1-Nrf2 signalling pathway. *Free Radic Res.* 53, 800-814 (2019).
46. Kim EY, Anderson M, Wilson C, Hagmann H, Benzing T, and Dryer SE. NOX2 interacts with podocyte TRPC6 channels and contributes to their activation by diacylglycerol: essential role of podocin in formation of this complex. *Am J Physiol Cell Physiol.* 305, C960-71 (2013).
47. Liu L, Chen M, Lin K, Xiang X, Yang J, Zheng Y, Xiong X, and Zhu S. TRPC6 Attenuates Cortical Astrocytic Apoptosis and Inflammation in Cerebral Ischemic/Reperfusion Injury. *Front Cell Dev Biol.* 8, 594283 (2020).
48. Marko L, Vigolo E, Hinze C, Park JK, Roel G, Balogh A, Choi M, Wubken A, Cording J, Blasig IE, Luft FC, Scheidereit C, Schmidt-Ott KM, Schmidt-Ullrich R,

- and Muller DN. Tubular Epithelial NF-kappaB Activity Regulates Ischemic AKI. *J Am Soc Nephrol.* 27, 2658-69 (2016).
49. Hou X, Xiao H, Zhang Y, Zeng X, Huang M, Chen X, Birnbaumer L, and Liao Y. Transient receptor potential channel 6 knockdown prevents apoptosis of renal tubular epithelial cells upon oxidative stress via autophagy activation. *Cell Death Dis.* 9, 1015 (2018).
  50. Marchant JS. Ca(2+) Signaling and Regeneration. *Cold Spring Harb Perspect Biol.* 11, a035485 (2019).
  51. Polat OK, Uno M, Maruyama T, Tran HN, Imamura K, Wong CF, Sakaguchi R, Ariyoshi M, Itsuki K, Ichikawa J, Morii T, Shirakawa M, Inoue R, Asanuma K, Reiser J, Tochio H, Mori Y, and Mori MX. Contribution of Coiled-Coil Assembly to Ca(2+)/Calmodulin-Dependent Inactivation of TRPC6 Channel and its Impacts on FSGS-Associated Phenotypes. *J Am Soc Nephrol.* 30, 1587-1603 (2019).
  52. Friedewald JJ and Rabb H. Inflammatory cells in ischemic acute renal failure. *Kidney Int.* 66, 486-91 (2004).
  53. Mizuguchi Y, Chen J, Seshan SV, Poppas DP, Szeto HH, and Felsen D. A novel cell-permeable antioxidant peptide decreases renal tubular apoptosis and damage in unilateral ureteral obstruction. *Am J Physiol Renal Physiol.* 295, F1545-53 (2008).
  54. Tadagavadi R and Reeves WB. Neutrophils in cisplatin AKI-mediator or marker? *Kidney Int.* 92, 11-13 (2017).
  55. Cao Q, Harris DC, and Wang Y. Macrophages in kidney injury, inflammation, and fibrosis. *Physiology (Bethesda).* 30, 183-94 (2015).
  56. LeBleu VS, Taduri G, O'Connell J, Teng Y, Cooke VG, Woda C, Sugimoto H, and Kalluri R. Origin and function of myofibroblasts in kidney fibrosis. *Nat Med.* 19, 1047-53 (2013).
  57. Zeisberg EM, Potenta SE, Sugimoto H, Zeisberg M, and Kalluri R. Fibroblasts in kidney fibrosis emerge via endothelial-to-mesenchymal transition. *J Am Soc Nephrol.* 19, 2282-7 (2008).
  58. Lu YA, Liao CT, and Raybould R. Single-Nucleus RNA Sequencing Identifies New Classes of Proximal Tubular Epithelial Cells in Kidney Fibrosis. *J Am Soc Nephrol.* 32, 2501-2516 (2021).
  59. Tomasek JJ, Gabbiani G, Hinz B, Chaponnier C, and Brown RA. Myofibroblasts and mechano-regulation of connective tissue remodelling. *Nat Rev Mol Cell Biol.* 3, 349-63 (2002).
  60. Davis J, Burr AR, Davis GF, Birnbaumer L, and Molkenin JD. A TRPC6-dependent pathway for myofibroblast transdifferentiation and wound healing in vivo. *Dev Cell.* 23, 705-15 (2012).
  61. Hofmann K, Fiedler S, Vierkotten S, Weber J, Klee S, Jia J, Zwickenpflug W, Flockerzi V, Storch U, Yildirim A, Gudermann T, Königshoff M, and Dietrich A.



- Classical transient receptor potential 6 (TRPC6) channels support myofibroblast differentiation and development of experimental pulmonary fibrosis. *Biochim Biophys Acta Mol Basis Dis.* 1863, 560-568 (2017).
62. Schlondorff J. TRPC6 and kidney disease: sclerosing more than just glomeruli? *Kidney Int.* 91, 773-775 (2017).
  63. Kefaloyianni E, Muthu ML, Kaeppler J, Sun X, Sabbisetti V, Chalaris A, Rose-John S, Wong E, Sagi I, Waikar SS, Rennke H, Humphreys BD, Bonventre JV, and Herrlich A. ADAM17 substrate release in proximal tubule drives kidney fibrosis. *JCI Insight.* 1, e87023 (2016).
  64. Agell N, Bachs O, Rocamora N, and Villalonga P. Modulation of the Ras/Raf/MEK/ERK pathway by Ca(2+), and calmodulin. *Cell Signal.* 14, 649-54 (2002).
  65. Liu Z, Wei Y, Zhang L, Yee PP, Johnson M, Zhang X, Gulley M, Atkinson JM, Trebak M, Wang HG, and Li W. Induction of store-operated calcium entry (SOCE) suppresses glioblastoma growth by inhibiting the Hippo pathway transcriptional coactivators YAP/TAZ. *Oncogene.* 38, 120-139 (2019).
  66. Andrikopoulos P, Kieswich J, Pacheco S, Nadarajah L, Harwood SM, O'Riordan CE, Thiernemann C, and Yaqoob MM. The MEK Inhibitor Trametinib Ameliorates Kidney Fibrosis by Suppressing ERK1/2 and mTORC1 Signaling. *J Am Soc Nephrol.* 30, 33-49 (2019).
  67. Zheng Z, Li C, Shao G, Li J, Xu K, Zhao Z, Zhang Z, Liu J, and Wu H. Hippo-YAP/MCP-1 mediated tubular maladaptive repair promote inflammation in renal failed recovery after ischemic AKI. *Cell Death Dis.* 12, 754 (2021).
  68. Chen J, Wang X, He Q, Bulus N, Fogo AB, Zhang MZ, and Harris RC. YAP Activation in Renal Proximal Tubule Cells Drives Diabetic Renal Interstitial Fibrogenesis. *Diabetes.* 69, 2446-2457 (2020).
  69. Xu J, Li PX, Wu J, Gao YJ, Yin MX, Lin Y, Yang M, Chen DP, Sun HP, Liu ZB, Gu XC, Huang HL, Fu LL, Hu HM, He LL, Wu WQ, Fei ZL, Ji HB, Zhang L, and Mei CL. Involvement of the Hippo pathway in regeneration and fibrogenesis after ischaemic acute kidney injury: YAP is the key effector. *Clin Sci (Lond).* 130, 349-63 (2016).
  70. Yu FX, Zhao B, and Guan KL. Hippo Pathway in Organ Size Control, Tissue Homeostasis, and Cancer. *Cell.* 163, 811-28 (2015).
  71. Schwartzman M, Reginensi A, Wong JS, Basgen JM, Meliambro K, Nicholas SB, D'Agati V, McNeill H, and Campbell KN. Podocyte-Specific Deletion of Yes-Associated Protein Causes FSGS and Progressive Renal Failure. *J Am Soc Nephrol.* 27, 216-26 (2016).

## 7. Statutory Declaration

“I, Zhihuang Zheng, by personally signing this document in lieu of an oath, hereby affirm that I prepared the submitted dissertation on the topic The Role of TRPC6 in Kidney Damage (Die Rolle von TRPC6 bei Nierenschäden), independently and without the support of third parties, and that I used no other sources and aids than those stated.

All parts which are based on the publications or presentations of other authors, either in letter or in spirit, are specified as such in accordance with the citing guidelines.

Furthermore, I declare that I have correctly marked all of the data, the analyses, and the conclusions generated from data obtained in collaboration with other persons, and that I have correctly marked my own contribution and the contributions of other persons (cf. declaration of contribution). I have correctly marked all texts or parts of texts that were generated in collaboration with other persons.

My contributions to any publications to this dissertation correspond to those stated in the below joint declaration made together with the supervisor. All publications created within the scope of the dissertation comply with the guidelines of the ICMJE (International Committee of Medical Journal Editors; [www.icmje.org](http://www.icmje.org)) on authorship. In addition, I declare that I shall comply with the regulations of Charité – Universitätsmedizin Berlin on ensuring good scientific practice.

I declare that I have not yet submitted this dissertation in identical or similar form to another Faculty. The significance of this statutory declaration and the consequences of a false statutory declaration under criminal law (Sections 156, 161 of the German Criminal Code) are known to me.”

Date

Signature

## Declaration of your own contribution to the publications

Zhihuang Zheng contributed the following to the below listed publications:

**Publication 1:** Zheng Z, Tsvetkov D, Bartolomaeus TUP, Erdogan C, Krügel U, Schleifenbaum J, Schaefer M, Nürnberg B, Chai X, Ludwig FA, N'Diaye G, Köhler MB, Wu K, Gollasch M, Markó L. Role of TRPC6 in Kidney Damage after Acute Ischemic Kidney Injury. *Sci Rep.* 2022; 12(1): 3038.

Contribution: I performed AKI mouse model surgery, drugs administration, organ collection and preparation, blood parameters measurements, qRT-PCR, data analysis. All the figures and tables were prepared and composed by me. Figure 1A-E, 2B, 2C, 3B-D, 4A-F, 5A, 5C-E, 6B, 6C, 7B-D, 8A-F, Figure S1-3, and Table S1-4 were created based on my data and statistical analysis. Together with co-authors, I drafted the manuscript, all authors contributed to its completion and revision.

**Publication 2:** Zheng Z, Xu Y, Krügel U, Schaefer M, Grune T, Nürnberg B, Köhler MB, Gollasch M, Tsvetkov D, Markó L. In Vivo Inhibition of TRPC6 by SH045 Attenuates Renal Fibrosis in a New Zealand Obese (NZO) Mouse Model of Metabolic Syndrome. *Int J Mol Sci.* 2022, 23(12), 6870.

Contribution: I performed UUO mouse model surgery, drugs administration, organ collection and preparation, blood parameters measurements, qRT-PCR, data analysis. All the figures and tables were prepared and composed by me. Figure 1A-G, 2B, 2D, 2E-F, 3A-F, 4B, 4D, 5A-F, 6B, 6D, 6F, Figure S1-3, Table S1-2 were created based on my data and statistical analysis. Together with co-authors, I drafted the manuscript, all authors contributed to its completion and revision.

---

Signature, date and stamp of first supervising university professor / lecturer

---

Signature of doctoral candidate

## 8. Selected Publication

### 8.1 Publication #1

The role of TRPC6 in acute kidney damage after ischemia/reperfusion-induced kidney injury.

Zhihuang Zheng, Dmitry Tsvetkov, Theda Ulrike Patricia Bartolomaeus, Cem Erdogan, Ute Krügel, Johanna Schleifenbaum, Michael Schaefer, Bernd Nürnberg, Xiaoning Chai, Friedrich-Alexander Ludwig, Gabriele N'diaye, May-Britt Köhler, Kaiyin Wu, Maik Gollasch, Lajos Markó. Role of TRPC6 in Kidney Damage after Acute Ischemic Kidney Injury. *Scientific Reports*. 2022; 12(1): 3038. **Impact Factor (2019): 3.998**

Received: 15 June 2021; Accepted: 03 Feb 2022; Published online: 22 Feb 2022.

Journal Data Filtered By: **Selected JCR Year: 2019** Selected Editions: SCIE,SSCI  
 Selected Categories: **"MULTIDISCIPLINARY SCIENCES"** Selected Category  
 Scheme: WoS

**Gesamtanzahl: 71 Journale**

Rank	Full Journal Title	Total Cites	Journal Impact Factor	Eigenfactor Score
1	NATURE	767,209	42.778	1.216730
2	SCIENCE	699,842	41.845	1.022660
3	National Science Review	2,775	16.693	0.009760
4	Science Advances	36,380	13.116	0.172060
5	Nature Human Behaviour	2,457	12.282	0.014190
6	Nature Communications	312,599	12.121	1.259510
7	Science Bulletin	5,172	9.511	0.014150
8	PROCEEDINGS OF THE NATIONAL ACADEMY OF SCIENCES OF THE UNITED STATES OF AMERICA	676,425	9.412	0.931890
9	Journal of Advanced Research	3,564	6.992	0.005470
10	GigaScience	4,068	5.993	0.016410
11	Scientific Data	5,761	5.541	0.028720
12	Research Synthesis Methods	2,572	5.299	0.006440
13	ANNALS OF THE NEW YORK ACADEMY OF SCIENCES	45,596	4.728	0.026370
14	FRACTALS-COMPLEX GEOMETRY PATTERNS AND SCALING IN NATURE AND SOCIETY	2,156	4.536	0.002210
15	iScience	1,410	4.447	0.004140
16	GLOBAL CHALLENGES	481	4.306	0.001440
17	Scientific Reports	386,848	3.998	1.231180
18	JOURNAL OF KING SAUD UNIVERSITY SCIENCE	1,640	3.819	0.002020
19	Journal of the Royal Society Interface	13,762	3.748	0.027670

Selected JCR Year: 2019; Selected Categories: "MULTIDISCIPLINARY SCIENCES"

1



OPEN

# Role of TRPC6 in kidney damage after acute ischemic kidney injury

Zhihuang Zheng<sup>1,2,3</sup>, Dmitry Tsvetkov<sup>1,2,4</sup>✉, Theda Ulrike Patricia Bartolomaeus<sup>2,12</sup>, Cem Erdogan<sup>5</sup>, Ute Krügel<sup>6</sup>, Johanna Schleifenbaum<sup>5</sup>, Michael Schaefer<sup>6</sup>, Bernd Nürnberg<sup>7</sup>, Xiaoning Chai<sup>6</sup>, Friedrich-Alexander Ludwig<sup>8</sup>, Gabriele N'diaye<sup>2,12</sup>, May-Britt Köhler<sup>2,12</sup>, Kaiyin Wu<sup>9</sup>, Maik Gollasch<sup>1,2,4</sup>✉ & Lajos Markó<sup>2,10,11,12</sup>✉

Transient receptor potential channel subfamily C, member 6 (TRPC6), a non-selective cation channel that controls influx of Ca<sup>2+</sup> and other monovalent cations into cells, is widely expressed in the kidney. *TRPC6* gene variations have been linked to chronic kidney disease but its role in acute kidney injury (AKI) is unknown. Here we aimed to investigate the putative role of TRPC6 channels in AKI. We used *Trpc6*<sup>-/-</sup> mice and pharmacological blockade (SH045 and BI-749327), to evaluate short-term AKI outcomes. Here, we demonstrate that neither *Trpc6* deficiency nor pharmacological inhibition of TRPC6 influences the short-term outcomes of AKI. Serum markers, renal expression of epithelial damage markers, tubular injury, and renal inflammatory response assessed by the histological analysis were similar in wild-type mice compared to *Trpc6*<sup>-/-</sup> mice as well as in vehicle-treated versus SH045- or BI-749327-treated mice. In addition, we also found no effect of TRPC6 modulation on renal arterial myogenic tone by using blockers to perfuse isolated kidneys. Therefore, we conclude that TRPC6 does not play a role in the acute phase of AKI. Our results may have clinical implications for safety and health of humans with *TRPC6* gene variations, with respect to mutated TRPC6 channels in the response of the kidney to acute ischemic stimuli.

Transient receptor potential (TRP) channels are a group of ion channels located mostly on the plasma membrane of numerous cell types with a relatively large non-selective permeability to cations<sup>1,2</sup>. Mammalian TRP channel family comprises 28 members, which share some structural similarity with each other<sup>2,3</sup>. Transient receptor potential canonical or classical 6 (TRPC6) are non-selective Ca<sup>2+</sup> permeable cation channels expressed in renal tissue including glomerular podocytes, mesangial cells, endothelial cells, tubulointerstitial vascular and epithelial cells, as well as in renal blood vessels<sup>4</sup>. Ca<sup>2+</sup> influx through TRPC6 maintains the integrity of glomerular filtration barrier by interacting with nephrin, podocin, CD2-associated protein, and  $\alpha$ -actinin-4 directly or indirectly<sup>5</sup>. Mutations in *TRPC6* lead to familial forms of focal segmental glomerulosclerosis (FSGS) and to end stage kidney disease<sup>6,7</sup>. Of note, TRPC6 dysregulation is also linked to progression of acquired forms of proteinuric kidney disease<sup>8,9</sup>. As a result of the TRPC6 activation, intracellular Ca<sup>2+</sup> concentration in the podocyte increases and ultimately causes programmed cell death leading to progressive kidney failure. Recent evidence strongly suggests that TRPC6 also contributes to renal fibrosis and immune cell infiltration in the unilateral ureteral obstruction mouse model of progressive renal interstitial fibrosis<sup>9,10</sup>.

Initiation of renal fibrosis is often caused by acute kidney injury (AKI), an increasingly common complication occurring in critically ill patients with high morbidity and mortality<sup>11</sup>. The outcome of AKI has been

<sup>1</sup>Department of Nephrology/Intensive Care, Charité – Universitätsmedizin Berlin, Berlin, Germany. <sup>2</sup>Experimental and Clinical Research Center (ECRC), Max Delbrück Center for Molecular Medicine in the Helmholtz Association, Charité Universitätsmedizin, Berlin, Germany. <sup>3</sup>Department of Nephrology, Shanghai General Hospital, Shanghai Jiaotong University School of Medicine, Shanghai, China. <sup>4</sup>Department of Geriatrics, University of Greifswald, University District Hospital Wolgast, Greifswald, Germany. <sup>5</sup>Institute of Vegetative Physiology, Charité–Universitätsmedizin Berlin, Berlin, Germany. <sup>6</sup>Rudolf Boehm Institute for Pharmacology and Toxicology, Leipzig University, Leipzig, Germany. <sup>7</sup>Department of Pharmacology, Experimental Therapy and Toxicology and Interfaculty Center of Pharmacogenomics and Drug Research, University of Tübingen, Tübingen, Germany. <sup>8</sup>Department of Neuroradiopharmaceuticals, Institute of Radiopharmaceutical Cancer Research, Helmholtz-Zentrum Dresden-Rossendorf, Leipzig, Germany. <sup>9</sup>Department of Pathology, Charité–Universitätsmedizin Berlin, Berlin, Germany. <sup>10</sup>DZHK (German Centre for Cardiovascular Research), Partner Site Berlin, Berlin, Germany. <sup>11</sup>Berlin Institute of Health at Charité–Universitätsmedizin Berlin, Berlin, Germany. <sup>12</sup>Charité–Universitätsmedizin Berlin, Freie Universität Berlin, Humboldt-Universität zu Berlin, Berlin, Germany. ✉email: dmitry.tsvetkov@charite.de; maik.gollasch@charite.de; lajos.marko@charite.de

primarily linked to the severity of tubular damage. In fact, most theories consider renal tubular cells as the main culprit in AKI. Ischemia/reperfusion injury (IRI)-induced epithelial damage—particularly in the outer medulla—, tubular obstruction,  $\text{Ca}^{2+}$  overload, loss of cytoskeletal integrity, and loss of cell–matrix adhesion are main consequences of ischemia and initiators of subsequent fibrosis<sup>12,13</sup>. Recent data show that in vivo TRPC6 inhibition by BI-749327 ameliorates renal fibrosis in the unilateral obstructive nephropathy (UUO) model<sup>14</sup>, where the primary feature is tubular injury as a result of obstructed urine flow. Ischemia is frequently involved in AKI and correlates with oxidative stress and inflammation<sup>15,16</sup>. Reactive oxygen species (ROS) produced by NADPH oxidases (NOX) contribute to activation of TRPC6 channels<sup>17,18</sup>. Moreover, TRPC6 is emerging as a functional element to control calcium currents in immune cells, thereby regulating transendothelial migration, chemotaxis, phagocytosis, and cytokine release<sup>19,20</sup>. In a recent study, Shen et al. found that silencing TRPC6 could prevent necroptosis of renal tubular epithelial cells upon IRI<sup>21</sup>. These findings indicate that inhibition of TRPC6 may protect the kidney from IRI making it a promising target to ameliorate AKI. This is of special interest and of potential clinical relevance as novel chemical substances selectively acting on TRPC6 have been recently developed for in vivo experiments. In particular, the diterpene (+)-larixol and its derivative SH045, as well as BI-749327 which is another known TRPC6 blocker, have been developed for selective inhibition of TRPC6 and translational treatment of TRPC6 channelopathies<sup>14,22,23</sup>.

To the best of our knowledge, no studies investigated the potential role of TRPC6 channels in AKI. Therefore, we tested the hypothesis that TRPC6 inhibition is renoprotective in AKI. We induced AKI by ischemia reperfusion injury in wild-type (WT) and *Trpc6*<sup>-/-</sup> mice. Furthermore, we used pharmacological blockers (SH045 and BI-749327) in vivo and ex vivo to verify findings from the genetical model and to evaluate effects of TRPC6 inhibition in IRI-induced AKI and intrarenal regulation of blood flow. Serum markers, renal damage marker expression, histological analysis of renal tissue damage and cellular infiltration were performed. We conclude that neither lacking nor pharmacological inhibition of TRPC6 ameliorates short-term outcomes of AKI.

## Results

**The impact of *Trpc6* deficiency on renal damage after renal IRI.** To examine a possible role of *Trpc6* deficiency in AKI, we performed comparative in vivo studies using *Trpc6*<sup>-/-</sup> and WT mice (Fig. 1A). Twenty-four hours after IRI WT mice showed similar serum creatinine level compared to *Trpc6*<sup>-/-</sup> mice ( $P=0.18$ ; Fig. 1B). Renal expression of tubular damage marker neutrophil gelatinase-associated lipocalin (*Ngal*) and kidney injury molecule 1 (*Kim1*) showed no difference between WT and *Trpc6*<sup>-/-</sup> mice (Fig. 1C,D). Additionally, *Trpc6* expression in kidneys after IRI was not altered compared to the sham kidneys (Fig. 1E). At baseline *Trpc6*<sup>-/-</sup> mice had similar blood parameters compared to WT mice (except higher but still normal concentrations of sodium and ionized  $\text{Ca}^{2+}$  (Supplementary Table S2A). After IRI, WT and *Trpc6* deficient mice developed similar hyperkalaemia and similar high serum levels of creatinine and urea nitrogen (Supplementary Table S2B). In contrast, concentrations of sodium and chloride were lower in *Trpc6*<sup>-/-</sup> mice (Supplementary Table S2B).

**The impact of *Trpc6* deficiency on renal histopathology after IRI.** To assess the degree of tubular damage in ischemic AKI kidney sections were analyzed by Periodic Acid-Schiff (PAS) staining (Fig. 2A). IRI induced severe tubular damage and necrosis such as tubular epithelial swelling, loss of brush border, luminal dilatation with simplification of the epithelium, patchy loss of tubular epithelial cells with resultant gaps and exposure of denuded basement membrane, as well as obliterated tubular hyaline and/or granular casts (Fig. 2A). Analysis of the kidney sections revealed no differences in tubular injury score and tubular necrosis score between *Trpc6*<sup>-/-</sup> and WT mice (Fig. 2B,C).

**The impact of *Trpc6* deficiency on cellular infiltration and on the expression of calcium-binding proteins in the kidneys after IRI.** Neutrophils infiltration after IRI-induced AKI contributes to inflammation and subsequent repair of injured kidneys<sup>24,25</sup>. Here, we determined neutrophils infiltration in renal IRI using immunofluorescence staining. Kidney sections were immunolabelled with the neutrophil marker Ly6B.2<sup>26</sup>. As shown in Fig. 3A, excessive Ly6B.2-positive neutrophils in renal interstitium were observed in mice underwent IRI (Fig. 3A). *Trpc6*<sup>-/-</sup> mice showed similar amount of infiltrating Ly6B.2-positive cells after IRI as WT mice (Fig. 3B). Similarly, renal expression of neutrophil markers S100 calcium-binding protein A8 (*S100a8*) and S100 calcium-binding protein A9 (*S100a9*) were not different in IRI-damaged renal tissues of *Trpc6*<sup>-/-</sup> and WT mice (Fig. 3C,D).

**Expression of inflammatory markers in WT and *Trpc6*<sup>-/-</sup> kidneys.** Expression of inflammatory molecules is low in the normal kidney but is markedly increased under pathophysiological conditions such as IRI-induced AKI<sup>27</sup>. By using qPCR, we examined the mRNA expression of cell adhesion molecules and inflammatory markers involved in renal IRI. IRI led to increased mRNA expression of all determined markers (Fig. 4A–F), however *Trpc6*<sup>-/-</sup> IRI kidneys displayed similar expression of interleukin 6 (*Il6*), tumor necrosis factor-alpha (*Tnf-a*), intercellular adhesion molecule 1 (*Icam1*), vascular cell adhesion molecule 1 (*Vcam1*) in comparison to WT IRI kidneys (Fig. 4A–D). In addition, renal expression of chemokines such as chemokine (C–C motif) ligand 2 (*Ccl2*) and chemokine (C–C motif) ligand 2 receptor (*Ccr2*), were similar between *Trpc6*<sup>-/-</sup> and WT mice (Fig. 4E,F).

**The impact of *Trpc6* pharmacological blockade on renal damage after renal IRI.** To circumvent possible bias due to the genetical approach and to examine effects of pharmacological blockade of *Trpc6* on renal damage, we used SH045 (a recently developed drug with high affinity and strong subtype selectivity toward TRPC6) in vivo in the ischemic AKI mouse model using two different ischemia time (milder with 17.5 min and



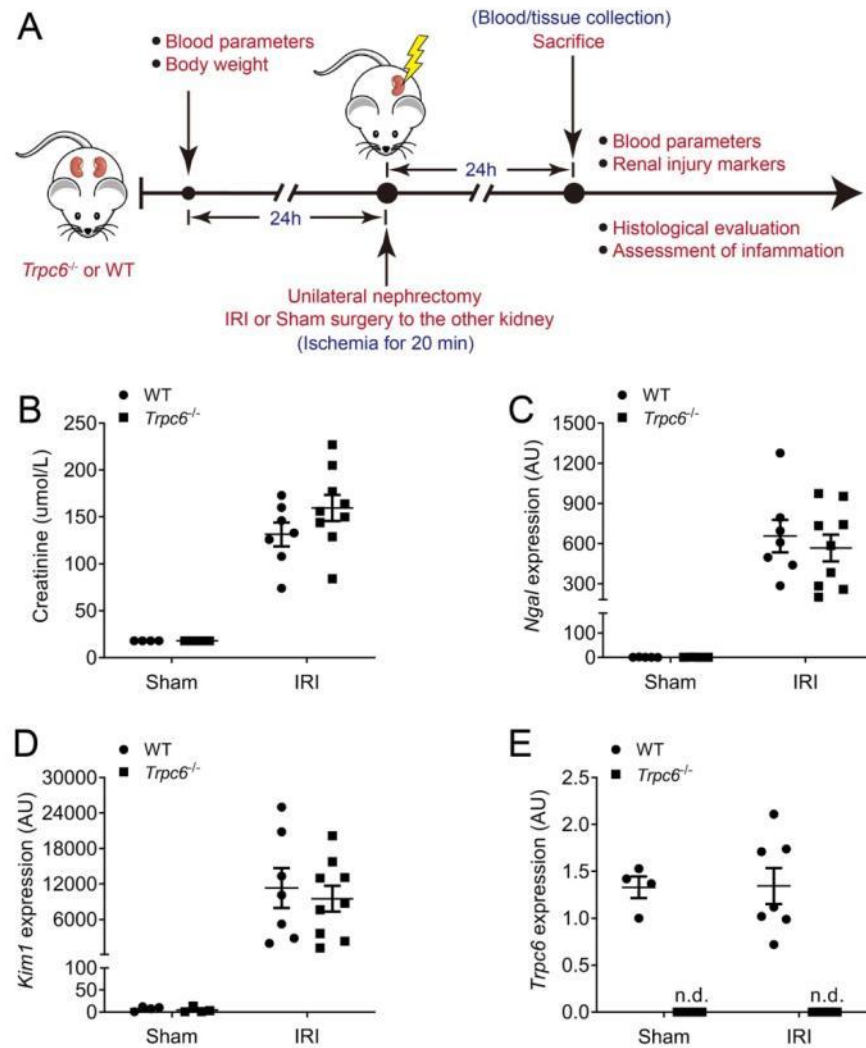


**Figure 1.** Effect of *Trpc6* deficiency on IRI-induced acute kidney injury (AKI). (A) Experimental design of ischemia reperfusion-induced AKI. (B) Serum creatinine levels in the experimental groups (Sham WT and *Trpc6*<sup>-/-</sup> n = 4 each, IRI WT n = 7, and *Trpc6*<sup>-/-</sup> n = 9, respectively). (C) Renal mRNA levels of kidney injury marker neutrophil gelatinase-associated lipocalin (*Ngai*), (D) kidney injury molecule 1 (*Kim1*) and (E) *Trpc6* (Sham WT and *Trpc6*<sup>-/-</sup> n = 4 each, IRI WT n = 7, and *Trpc6*<sup>-/-</sup> n = 9, respectively). Please note that at baseline all serum creatinine levels were below the measurement limit (18  $\mu\text{mol/L}$ ). Two-way ANOVA followed by Sidak's multiple comparisons post hoc test. *AU* arbitrary units, *n.d.* not detected.

a stronger with 20 min) (Fig. 5A). Renal concentrations of SH045 in both 30 min and 24 h after intravenous injection were similar between sham and IRI groups (Fig. 5B). Consistent with AKI data from *Trpc6*<sup>-/-</sup> and WT mice, pharmacological blockade of TRPC6 had no effects on serum creatinine levels after 17.5 min or 20 min IRI-induced AKI in comparison to vehicle injected WT IRI mice ( $P=0.23$  and  $P=0.76$ , respectively, Fig. 5C). In addition, renal mRNA expression of *Ngai* and *Kim1* was similar in SH045-treated compared to vehicle-treated kidneys after IRI (Fig. 5D,E). Furthermore, SH045 did not affect blood parameters such as sodium, potassium, chloride, ionized calcium, carbon dioxide, glucose, urea nitrogen, hematocrit, hemoglobin, and the anion gap



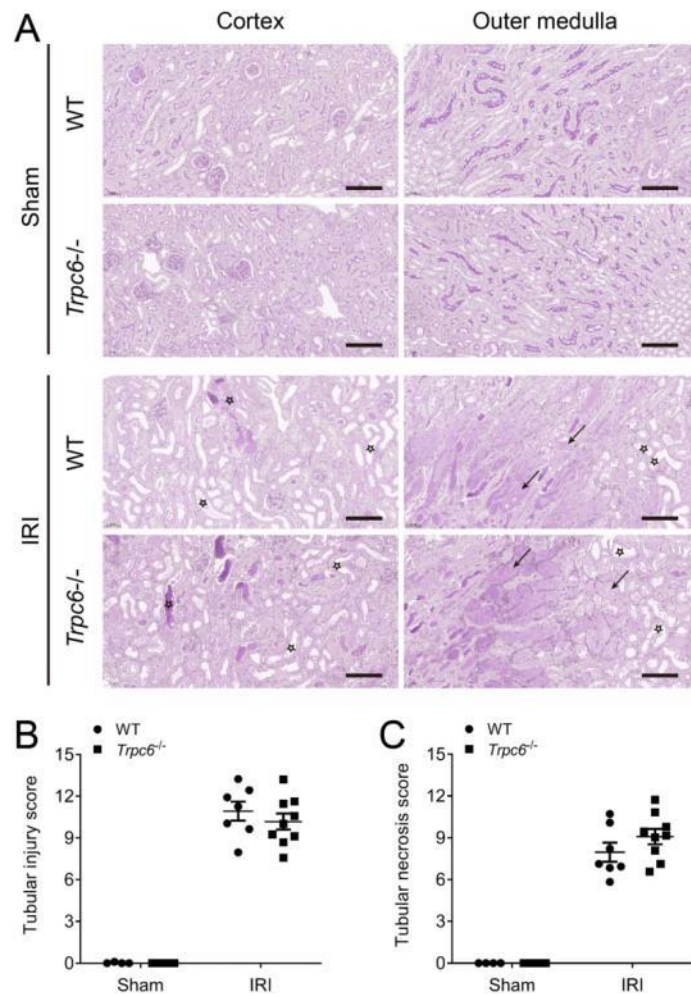


**Figure 2.** Effect of *Trpc6* deficiency on kidney histopathology after renal IRI-induced AKI. (A) Representative cortical or outer medullary images of IRI-injured kidneys isolated from *Trpc6*<sup>-/-</sup> and WT mice (magnification: 200×). Kidneys sections were stained with periodic acid-Schiff staining (PAS). Stars indicate tubular injury. Scale bars are 100 μm. (B) Semi-quantification of cortical tubular injury. (C) Semi-quantification of outer medullary tubular necrosis. Data expressed as means ± SEM (Sham WT and *Trpc6*<sup>-/-</sup> n = 4 each, IRI WT n = 7, and *Trpc6*<sup>-/-</sup> n = 9, respectively). Two-way ANOVA followed by Sidak's multiple comparisons post hoc test.

after IRI-induced AKI (Supplementary Table S3A–F). To further confirm the results of SH045, we used another TRPC6 blocker, BI-749327. In IRI-induced AKI mice, renal function parameters such as serum creatinine and renal expression of renal damage markers (*Ngal* and *Kim1*) were similar between vehicle- and BI-749327-treated mice (Supplementary Fig. S1A–D). Besides, no difference in other blood parameters was found between vehicle- and BI-749327-treated AKI mice (Supplementary Table S4A,B).

**The impact of *Trpc6* pharmacological blockade on renal histopathology after IRI.** Histological analyses and semi-quantitative scoring revealed no statistically significant differences in cortical tubular damage

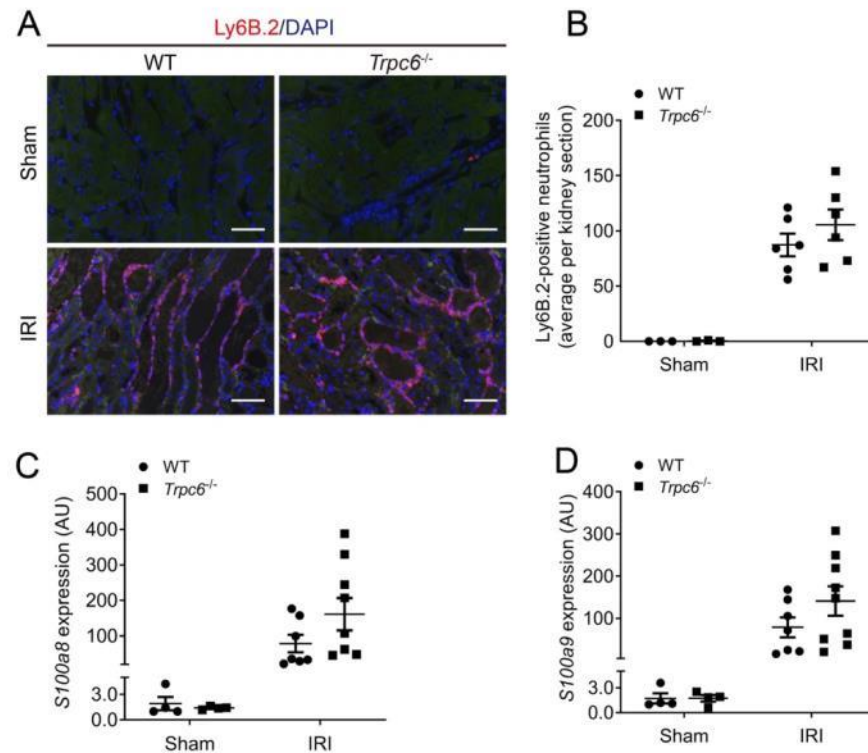


**Figure 3.** Effect of *Trpc6* deficiency on renal neutrophils infiltration and inflammatory markers in IRI-induced AKI. (A) Representative outer medullary images of IRI-injured kidneys. Kidneys were stained with Ly6B.2 (magnification: 400×). Scale bars are 100 μm. (B) The semi-quantification renal neutrophils infiltration (Sham WT and *Trpc6*<sup>-/-</sup> n = 3 each, IRI WT n = 6, and *Trpc6*<sup>-/-</sup> n = 6, respectively). (C) Renal mRNA levels of S100 calcium-binding protein A8 (*S100a8*). (D) Renal mRNA levels of S100 calcium-binding protein A9 (*S100a9*) (Sham WT and *Trpc6*<sup>-/-</sup> n = 4 each, IRI WT n = 7, and *Trpc6*<sup>-/-</sup> n = 9, respectively). Data expressed as means ± SEM. Two-way ANOVA followed by Sidak's multiple comparisons post hoc test. AU arbitrary units.

after renal 17.5 min- or 20 min-IRI in SH045 compared to vehicle-treated mice (Fig. 6A,B). Moreover, epithelial cells in the outer stripe of outer medulla, especially susceptible to ischemic injury, exhibited comparable level of tubular necrosis between SH045 treated and control mice after renal 17.5 min- or 20 min-IRI (Fig. 6A,C). Similarly, BI-749327 also did not influence tubular damage and necrosis in IRI (Supplementary Fig. S2A–C).

**The impact of *Trpc6* pharmacological blockade on cellular infiltration and calcium-binding proteins on the kidneys after IRI.** Consistent with the results in AKI-induced *Trpc6*<sup>-/-</sup> mice, SH045 treatment had no effect on renal infiltration of Ly6B.2-positive granulocytes after 17.5 min- or 20 min-IRI-induced AKI in comparison to vehicle-treated mice (Fig. 7A,B). In agreement with that, renal expression of *S100a8* and *S100a9* after 17.5 min- or 20 min-IRI is similar in mice treated with SH045 versus vehicle (Fig. 7C,D). Furthermore, similar results were also obtained in mice treated with BI-749327 compared to vehicle-treated mice (Supplementary Fig. S3G,H).

**The impact of *Trpc6* pharmacological blockade on expression of renal cytokines and chemokine after IRI.** SH045-treated mice underwent 17.5 or 20 min IRI-induced AKI showed similar renal expression of *Il6*, *Tnf-α*, *Icam1*, *Vcam1*, *Ccl2*, and *Ccr2* in comparison to vehicle-treated mice with the same IRI (Fig. 8A–F). In addition, the mRNA levels of these inflammatory markers in BI-749327-treated AKI mice were equivalent to vehicle-treated AKI mice (Supplementary Fig. S3A–F).

**Impact of pharmacological modulation of *Trpc6* on renal microcirculation.** The renal microcirculation is emerging as a key player in AKI<sup>28</sup>. To explore whether modulation of TRPC6 has impact on renal microcirculation, we evaluated myogenic tone in the mouse renal circulation using the TRPC6 blockers SH045

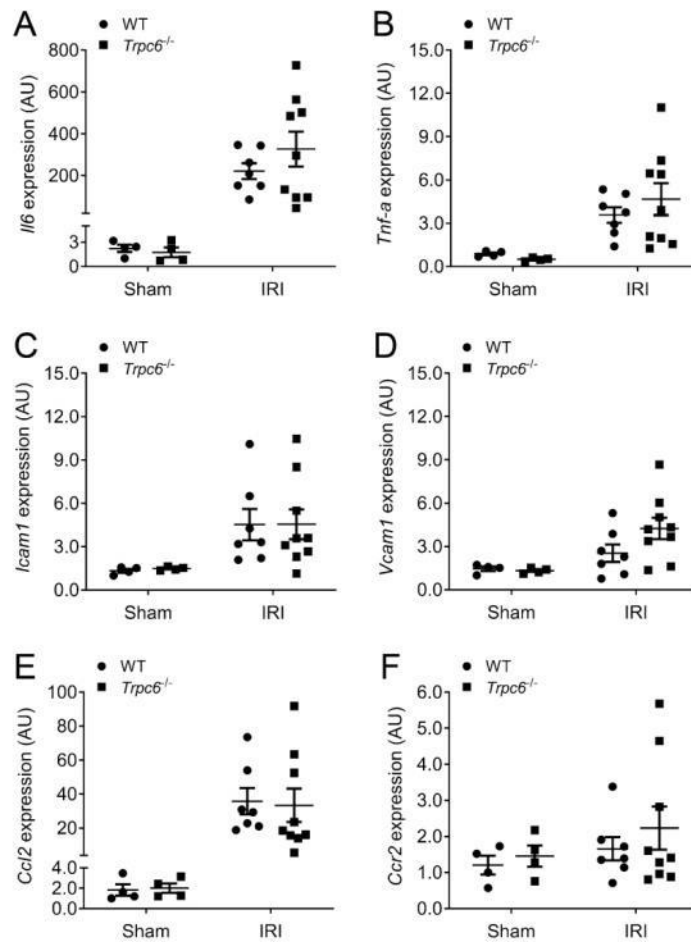


**Figure 4.** Effect of *Trpc6* deficiency on gene expression of pro-inflammatory cytokines and chemokines after renal IRI. (A) Renal mRNA levels of interleukin 6 (*Il6*) and (B) tumor necrosis factor- $\alpha$  (*Tnf-a*), (C) intercellular adhesion molecule 1 (*Icam1*) and (D) vascular cell adhesion protein 1 (*Vcam1*), (E) C-C motif chemokine 2 (*Ccl2*) and (F) C-C motif chemokine receptor 2 (*Ccr2*) (Sham WT and *Trpc6*<sup>-/-</sup> n = 4 each, IRI WT n = 7, and *Trpc6*<sup>-/-</sup> n = 9, respectively). Data expressed as means  $\pm$  SEM. Two-way ANOVA followed by Sidak's multiple comparisons post hoc test. AU arbitrary units.

and BI-749327, and the TRPC6 activator hyperforin<sup>29</sup>. Isolated kidneys perfused with SH045 or BI-749327 developed a similar decrease of perfusion pressure compared to control kidneys (Supplementary Fig. S4A–C,E). In addition, activation of TRPC6 using hyperforin resulted in similar spontaneous decrease of perfusion pressure compared to control kidneys (Supplementary Fig. S4A,D,E). Of note, there was also no difference in Angiotensin (Ang) II induced vasoconstrictions between kidneys perfused with SH045, BI-749327, or hyperforin versus control kidneys (Supplementary Fig. S4F). Together, these results indicate no effect of TRPC6 modulation on renal arterial myogenic tone.

### Discussion

In our previous study, we have shown that TRPC6 contributes to renal fibrosis and immune cell infiltration in a murine UUO model using *Trpc6*<sup>-/-</sup> mice<sup>9</sup>. Renal IRI is a common cause of CKD. IRI is associated with calcium (Ca<sup>2+</sup>) overload, ROS production, and immune responses which has been reported as crucial factors of tubular

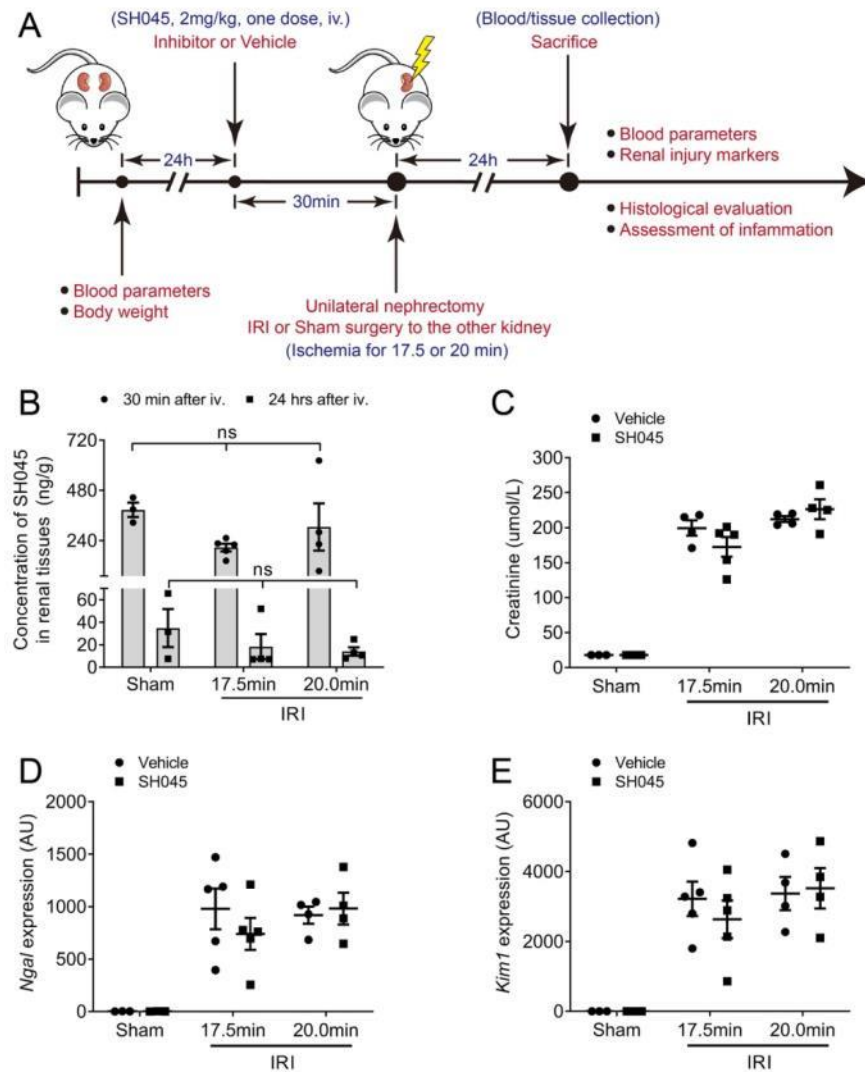


**Figure 5.** Effect of the TRPC6 inhibitor SH045 on IRI-induced acute kidney injury (AKI). **(A)** Experimental design of IRI-induced AKI. **(B)** Concentrations of SH045 in kidney tissue 30 min and 24 h after intravenous injection (Sham  $n = 3$  each, 17.5 min-IRI in vehicle and SH045  $n = 5$  each, 20 min-IRI in vehicle and SH045  $n = 4$  each, respectively). **(C)** Serum creatinine levels (Sham  $n = 3$  each, 17.5 min-IRI in vehicle and SH045  $n = 5$  each, 20 min-IRI in vehicle and SH045  $n = 4$  each, respectively). **(D)** Renal mRNA levels of kidney injury marker neutrophil gelatinase-associated lipocalin (*Ngal*) and **(E)** kidney injury molecule 1 (*Kim1*) (Sham  $n = 3$  each, 17.5 min-IRI in vehicle and SH045  $n = 5$  each, 20 min-IRI in vehicle and SH045  $n = 4$  each, respectively). Please note that at baseline all serum creatinine levels were below the measurement limit ( $18 \mu\text{mol/L}$ ). Two-way ANOVA followed by Sidak's multiple comparisons post hoc test. AU arbitrary units. Data expressed as means  $\pm$  SEM.



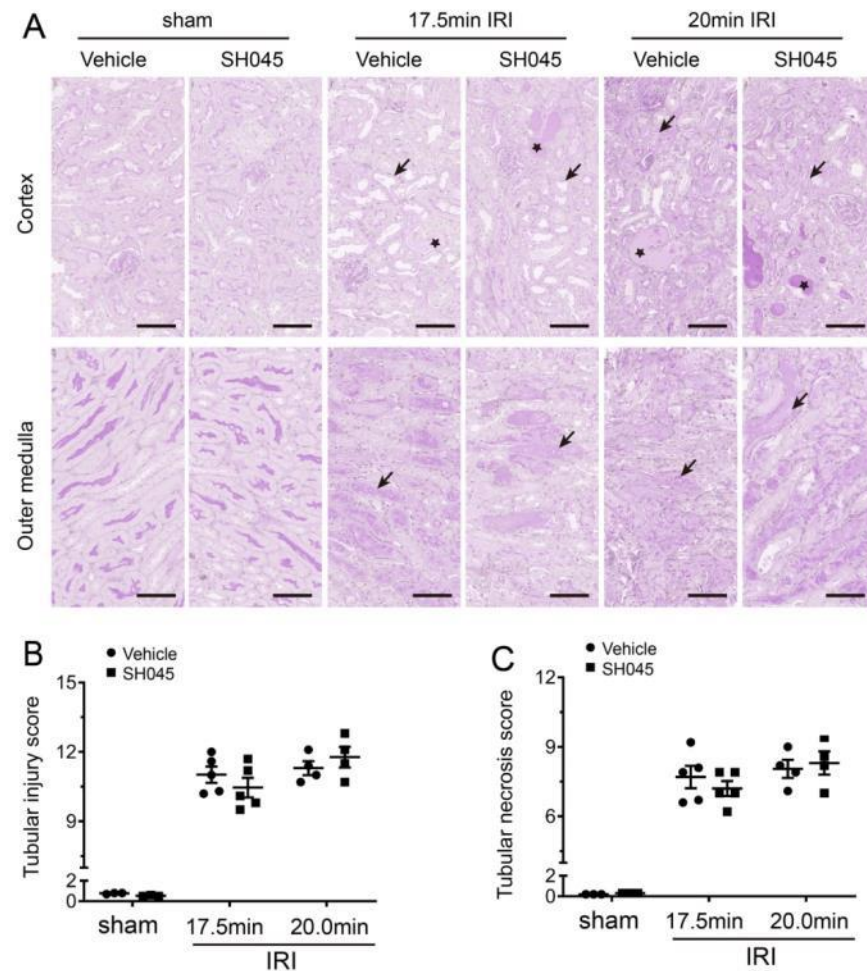


**Figure 6.** SH045 effects on kidney histopathology after renal ischemia reperfusion-induced AKI. (A) Representative cortical or outer medullary images of IRI-injured kidneys isolated from mice injected with vehicle or Trpc6 blocker SH045 (magnification: 400×). Kidneys sections/slices were stained with Periodic Acid-Schiff staining (PAS). Arrows indicate tubular injury. Stars indicate tubular casts. Scale bars are 100 μm. (B) The semi-quantification of cortical tubular injury. (C) The semi-quantification of outer medullary tubular necrosis. Data expressed as means ± SEM (Sham n = 3 each, 17.5 min-IRI in vehicle and SH045 n = 5 each, 20 min-IRI in vehicle and SH045 n = 4 each, respectively). Two-way ANOVA followed by Sidak's multiple comparisons post hoc test.

injury in IRI-induced AKI<sup>12,15,16</sup>. As a Ca<sup>2+</sup>-permeable cationic channel, TRPC6 can be activated by reactive oxygen species (ROS) and mediate podocyte injury in glomerular diseases<sup>17,18</sup>. In addition, TRPC6 is involved in immune responses regulating transendothelial migration, chemotaxis, phagocytosis, and cytokine release<sup>19,20</sup>. A recent study using pharmacological blockage of TRPC6 in mice demonstrated that decreased Ca<sup>2+</sup> entry due to TRPC6 contributed to reducing astrocytic apoptosis, cytotoxicity and inflammatory responses in cerebral ischemic/reperfusion insult<sup>20</sup>. Given that, in the present study we hypothesized that TRPC6 inhibition may also exhibit nephroprotective effects in AKI. To test this hypothesis, we applied the IRI experimental model on *Trpc6*<sup>-/-</sup> mice and employed a pharmacological approach of in vivo TRPC6 inhibition by SH045 and BI-749327 in wild-type (WT) mice.

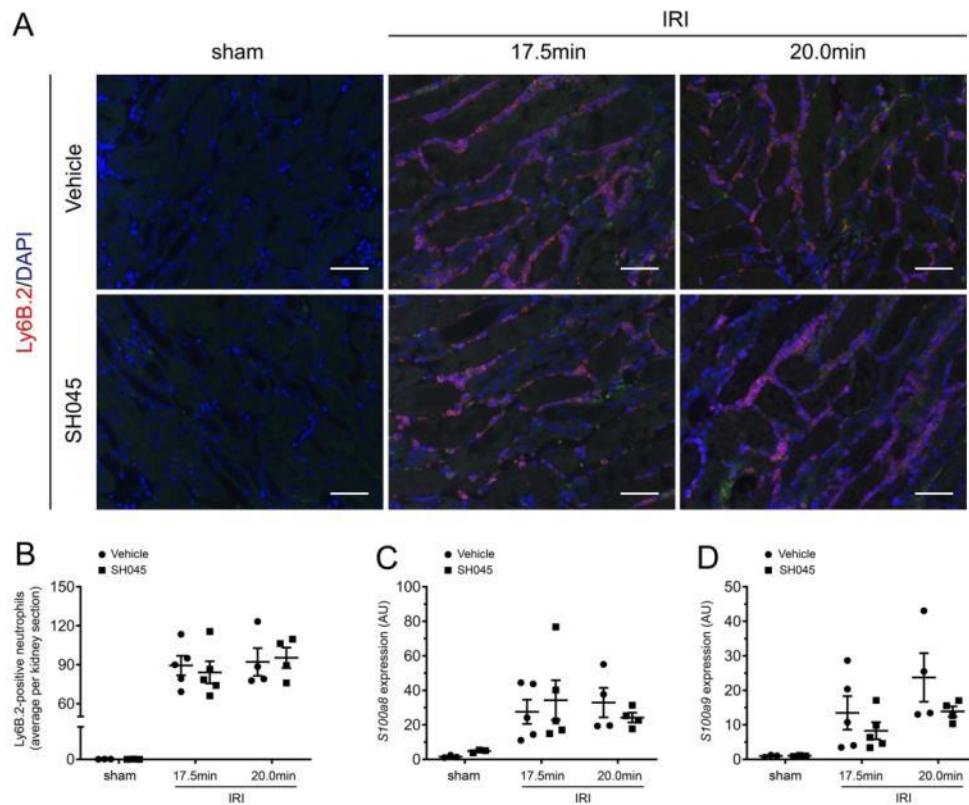


**Figure 7.** SH045 effects on renal neutrophils infiltration and inflammatory markers in ischemia reperfusion-induced AKI. (A) Representative outer medullary images of IRI-injured kidneys. Kidneys were stained with Ly6B.2 (magnification: 400 $\times$ ). Sham and IRI mice were treated with either vehicle or Trpc6 inhibitor (SH045). Scale bars are 100  $\mu$ m. (B) The semi-quantification renal neutrophils infiltration. (C) Renal mRNA levels of S100 calcium-binding protein A8 (*S100a8*). (D) Renal mRNA levels of S100 calcium-binding protein A9 (*S100a9*). Data expressed as means  $\pm$  SEM (Sham  $n = 3$  each, 17.5 min-IRI in vehicle and SH045  $n = 5$  each, 20 min-IRI in vehicle and SH045  $n = 4$  each, respectively). Two-way ANOVA followed by Sidak's multiple comparisons post hoc test. AU, arbitrary units.

In our study, *Trpc6*<sup>-/-</sup> mice subjected to acute IRI showed no difference in renal function or tubular damage when compared to WT mice which underwent IRI. The *Trpc6*<sup>-/-</sup> mouse model was established as a homozygous colony, therefore we used C57BL/6 J mice as control<sup>9</sup>. Given this limitation of our experimental approach and to account for possible confounding genomic and non-genomic effects of other TRPC channels caused by global loss of TRPC6<sup>31</sup>, we performed also studies using two different TRPC6 blockers SH045 and BI-749327 in C57BL/6 J WT mice to evaluate the role of TRPC6 in short-term AKI outcomes. Of note, TRPC6 and TRPC2, TRPC3, TRPC7 can form heteromeric channels with regulatory properties that are different from those of the homomeric TRPC channels<sup>32,33</sup>. Pharmacological inhibition allows high selectivity for inhibition of homomeric TRPC6 channels than for heteromeric channels in AKI, particularly compared to targeting TRPC6 using *Trpc6*<sup>-/-</sup> animals. Thus, using the pharmacological approach can precisely allow investigating the specific effects of TRPC6 homomeric channels on AKI. We used SH045 and BI-749327, and performed studies with two different ischemic times in order to have a model for mild (17.5 min) and moderate (20 min) renal damage. These two periods of reversible ischemia were based on our earlier IRI studies with mice<sup>34-36</sup>. However, we still found no differences with respect to serum creatinine or tubular damage between mice undergoing IRI treated with TRPC6 blocker vs. vehicle in both models.

Previously, we demonstrated that inhibition of tubular epithelial NF- $\kappa$ B activity can ameliorate IRI-induced AKI in our experimental settings<sup>36</sup>. Thus, our experimental conditions enable to observe beneficial effects of therapeutic interventions, i.e. kidney injury potentially can be ameliorated in our AKI mouse model. According to the reported IC<sub>50</sub>-values for SH045 of 6 to 60 nM<sup>37</sup> and the pharmacokinetic analysis by non-compartment

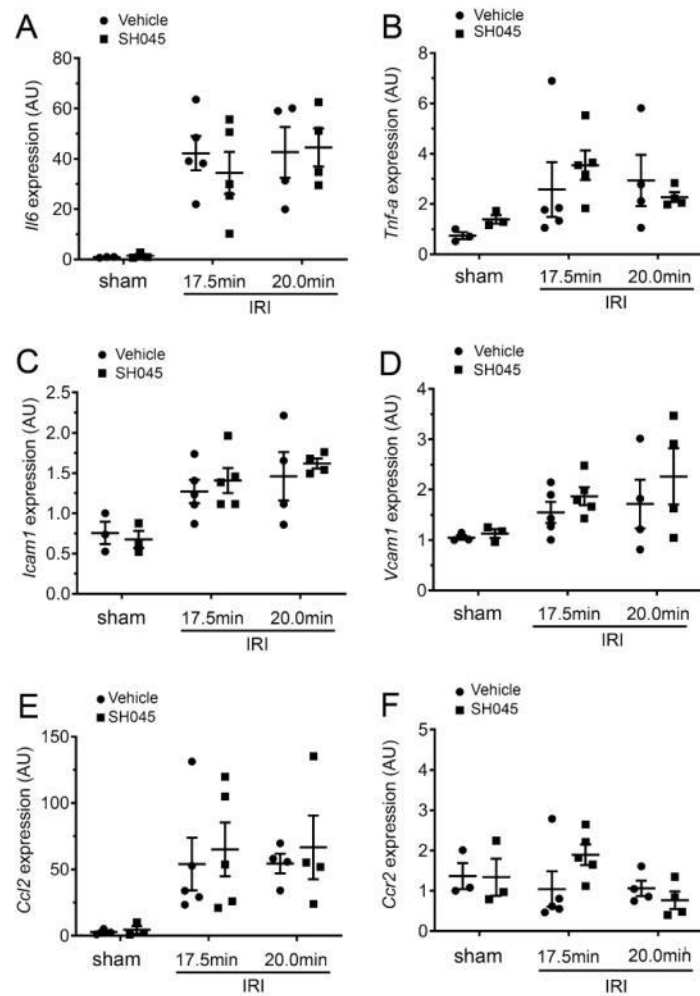


**Figure 8.** SH045 effects on gene expression of pro-inflammatory cytokines and chemokines after renal IRI. (A) Renal mRNA levels of interleukin 6 (*Il6*), (B) tumor necrosis factor- $\alpha$  (*Tnf-a*), (C) intercellular adhesion molecule 1 (*Icam1*) and (D) vascular cell adhesion protein 1 (*Vcam1*). (E) Renal mRNA levels of C-C motif chemokine 2 (*Ccl2*) and (F) C-C motif chemokine receptor 2 (*Ccr2*). Data expressed as means  $\pm$  SEM (Sham  $n = 3$  each, 17.5 min-IRI in vehicle and SH045  $n = 5$  each, 20 min-IRI in vehicle and SH045  $n = 4$  each, respectively). Two-way ANOVA followed by Sidak's multiple comparisons post hoc test. AU arbitrary units.

modeling<sup>38</sup>, SH045 can be considered as pharmacologically effective at tissue concentrations equal or higher than 22 ng/g. To confirm the drug is distributed in the kidney within the expected time, we measured the renal concentration of SH045 by using LC-MS/MS assay. As shown in Fig. 5B, the concentration of SH045 in renal tissue after 30 min post-injection ( $284.56 \text{ ng/g} \pm 144.76$ ) was much higher than 22 ng/g. In case of BI-749327, Lin et al., reported that in concentrations of 10–30 mg/kg BI-749327 has renal protective effects in the UUO mouse model<sup>14</sup>. Therefore, the concentrations of pharmacological blockers used in this study were appropriate to inhibit the TRPC6 channels in vivo in our experiments.

It is now well established that inflammation plays an important role in AKI<sup>39–42</sup>. Shortly after endothelial or tubular epithelial cell damage, activation of resident renal inflammatory cells occurs. It leads to overproduction of cytokines, followed by recruitment and subsequent infiltration with different leukocytes subsets<sup>43,44</sup>. TRPC6



is expressed in a wide range of inflammatory and vascular cell types, including neutrophils, lymphocytes and endothelium<sup>45</sup>. During the acute phase response, TRPC6 plays a crucial role in neutrophil mobilization as it enhances chemotactic responses through increasing intracellular  $Ca^{2+}$  concentration and promoting actin-based cytoskeleton remodeling<sup>20,46</sup>. Indeed, after renal IRI, we found a notable accumulation of neutrophils in the region of outer medulla. However, the infiltration of neutrophils in IRI *Trpc6*<sup>-/-</sup> kidney was equivalent to IRI WT mice as well as in SH045-treated AKI mice compared to vehicle-treated AKI mice. Accordingly, inflammatory response including cytokines and chemokine overexpression was also similar in AKI mice with or without *Trpc6* intervention. In addition, *Trpc6* was normally expressed in kidney tissue 24 h after IRI. A recent study using single-cell RNA sequencing in clusters of inflammatory cells during AKI confirms a similar renal expression of *Trpc6* mRNA in AKI versus control<sup>17</sup>. S100a8 and S100a9 are  $Ca^{2+}$  binding proteins belonging to the S100 family, which are constitutively expressed in neutrophils and monocytes as a  $Ca^{2+}$  sensor, participating in cytoskeleton rearrangement and arachidonic acid metabolism<sup>48,49</sup>. These two molecules modulate inflammatory response by stimulating recruitment of neutrophils and cytokine secretion<sup>49</sup>. We hypothesized that blocking intracellular influx of  $Ca^{2+}$  in neutrophils through genetical or pharmacological TRPC6 inhibition might affect the S100a8/9-mediated inflammation. However, we detected comparable renal expression of *S100a8/9* after AKI in WT and *Trpc6*<sup>-/-</sup> mice or in TRPC6 blockers-treated kidneys after AKI compared to respective control kidneys. Taken together, our data suggest no impact of TRPC6 to renal inflammatory reaction in the ischemic AKI.

Of note, TRPC6 is also expressed in tubular epithelial cells and plays an important role in nephron physiology<sup>50</sup>. Although one study showed functional importance of TRPC6 in autophagy regulation in vitro using proximal tubular cells of *Trpc6* deficient mice and TRPC6 overexpressing HK-2 cells<sup>50</sup>, our data argue against protective effects of TRPC6 in the tubular damage of AKI in vivo. After AKI, interstitial fibrosis formation is an important part of renal repair, yet excess leads to AKI-to-CKD transition. Wu et al., and our previous study showed that inhibition of TRPC6 function either by genetic deletion ameliorates renal interstitial fibrosis<sup>10</sup>. Besides, another study further demonstrated an obligate function for TRPC6 in promoting fibroblast transdifferentiation<sup>51</sup>. Therefore, inhibition of TRPC6 may have effects on renal fibrogenesis during AKI-to-CKD transition, and the beneficial effects of TRPC6 inhibition seen in the UUO model most likely involve fibroblast activation and transdifferentiation. Since its differentiation is an expected long-term outcome of AKI<sup>52</sup>, this might explain the lack of *Trpc6*<sup>-/-</sup> effects on the short-term outcome of AKI in present study. In addition, renal microvascular dysfunction is considered playing critical role in acute kidney injury<sup>53</sup>. Due to unchanged myogenic tone after TRPC6 modulation in vascular smooth muscle cells using isolated perfused kidneys, it is unlikely that a vascular component represents a protective mechanism of renal TRPC6 inhibition.

In summary, the present study shows that TRPC6 inhibition has no effects on short-term outcome of AKI. Our results improve the understanding of the role of TRPC6 role in kidney diseases. Future studies should investigate if TRPC6 could have a protective role on long-term outcome of AKI. Our results may have clinical implications for safety and long-term outcome of humans with *TRPC6* gene variations leading to familial forms of FSGS, with respect to the response of the kidney to acute ischemic stimuli.

## Materials and methods

**Animals.** Male *Trpc6*<sup>-/-</sup> mice (n = 10, homozygosity in a mix 129 Sv:C57BL/6J background) and wild-type (WT, C57BL/6J) control mice (n = 9) were used. *Trpc6*<sup>-/-</sup> mice have been generated and characterized previously<sup>9,31</sup>. For the pharmacological study WT mice (C57BL/6J, Jackson Laboratory) were used. Mice were held in specific-pathogen-free (SPF) condition, in a 12:12-h light-dark cycle, and with free access to purified food (E15430-047, Ssniff, Soest, Germany) and water. Experiments were approved by the Berlin Animal Review Board, Berlin, Germany (No. G0178/18) and followed the restrictions in the Berlin State Office for Health and Social Affairs (LaGeSo)<sup>54</sup>. All experiments were performed in accordance with ARRIVE guidelines<sup>55</sup>.

**Renal IRI model.** Renal IRI was induced as described earlier<sup>34</sup>. Briefly, male mice (aged 14–18 weeks) were anaesthetized by isoflurane (2.3%) in air (350 ml/min). Preemptive analgesia with buprenorphine (0.2 mg/100 g) was used<sup>56</sup>. Mice were operated individually to ensure similar exposure to isoflurane<sup>57</sup>. Body temperature was maintained at 37 °C and monitored during surgery. Ischemia was induced after right-sided nephrectomy by clipping the pedicle of the left kidney for 17.5 or 20 min with a non-traumatic aneurysm clip (FE690K, Aesculap, Germany). Reperfusion was confirmed visually and the abdomen and the skin were sutured separately with a 5/0 braided-silk suture. After surgery mice had free access to water and chow. Body-warm sterile physiological saline solution (1 ml) was applied subcutaneously to every mouse. Sham operation was performed in a similar manner, except for clamping the renal pedicle. Twenty-four hours after reperfusion, mice were sacrificed by overdose of isoflurane and additionally cervical dislocation, and kidney and blood samples were collected for further analysis. The kidneys were divided into three portions. Upper pole of the kidney tissue was frozen and used for measurement of SH045 concentration. Middle part of kidney was immersed in 4% phosphate-buffered saline (PBS)-buffered formalin for histology, and the other left tissue was snap-frozen in liquid nitrogen for RNA preparation.

**TRPC6 blocker.** Larixyl-6-N-methylcarbamate, also called SH045, is a compound with high affinity and subtype selectivity toward TRPC6 described by Häfner et al.<sup>22</sup>. SH045 was initially dissolved in DMSO (ratio of DMSO to vehicle is 0.5%) and then in 5% Cremophor EL<sup>®</sup> solution with 0.9% NaCl and used for intravenous injection (2 mg/kg) 30 min before IRI surgery in the pharmacological studies with WT mice. BI-749327 is an orally bioavailable TRPC6 antagonist as reported<sup>14</sup>. BI-749327 (MedChemExpress, New Jersey, USA) was dissolved in DMSO and then suspended in corn oil (final ratio of DMSO to corn oil is 5%). For administration, 30 mg/kg of the final dose was delivered to mice via oral gavage 60 min before IRI surgery.



**Blood measurements and drugs.** To allow repeated blood measurements of sodium, potassium, chloride, ionized calcium, total carbon dioxide, glucose, urea nitrogen, creatinine, hematocrit, hemoglobin and anion gap within a short time interval in the same mouse, 95  $\mu$ L blood was taken from the facial vein and parameters were measured using an i-STAT system with Chem8 + cartridges (Abbott, USA).

**Quantitative real-time (qRT)-PCR.** qRT-PCR was performed as described previously<sup>9</sup>. Briefly, Total RNA from snap-frozen kidneys were isolated using RNeasy RNA isolation kit (Qiagen, Australia) according to manufacturer's instruction after homogenization with a Precellys 24 homogenizer (Peqlab, Germany). RNA concentration and quality were determined by NanoDrop-1000 spectrophotometer (Thermo Fisher Scientific, USA). Two micrograms of RNA were transcribed to cDNA (Applied Biosystems, USA). Quantitative analysis of target mRNA expression was performed with qRT-PCR using the relative standard curve method. TaqMan and SYBR green analysis was conducted using an Applied Biosystems 7500 Sequence Detector (Applied Biosystems, USA). The expression levels were normalized to 18S. Primer sequences are provided in Supplementary Table S1.

**Histology and analysis.** Formalin-fixed, paraffin-embedded sections (2  $\mu$ m) of kidneys were subjected to Periodic acid Schiff (PAS) stain according to the manufacturer's protocols (Sigma, Germany). Semi-quantitative scoring of tubular damage was performed in a blinded manner in those 12 to 15 images at 200 $\times$  magnification per sample. Acute tubular injury (ATI) was observed in this study to assess the reversible tubular damage due to ischemia. The histologic features of ATI included one or more of the following lesions: tubular epithelial swelling with lucency of the cytoplasm, loss of brush border, luminal dilatation with simplification of the epithelium, and cytoplasmic vacuolization. Acute tubular necrosis (ATN) was also evaluated, which was indicated by patchy loss of tubular epithelial cells with resultant gaps and exposure of denuded basement membrane, evidence of cellular regeneration, as well as obliterated tubular hyaline and/or granular casts. The histological findings were graded from 0 to 3 according to the distribution of lesions: 0 = none; 1 = <25%; 2 = 25–50%; 3 = >50%<sup>56</sup>. The total score was calculated as sum of all morphological parameters. Tubular damage and tubular necrosis were quantified by an experienced renal pathologist who was unaware of Trpc6 genotypes or of treatment.

**HPLC and tandem mass spectrometric method (LC-MS/MS).** Concentration of SH045 in kidney homogenates was measured as previously described<sup>23</sup>. In summary, analyses were performed with an Agilent 1260 Infinity quaternary HPLC system (Agilent Technologies, Germany) consisting of a G4225A degasser, G1312B binary pump, G1367E autosampler, G1330B thermostat, G1316A column oven and G4212B diode array detector, coupled to a tandem QTRAP 5500 hybrid linear ion-trap triple quadrupole mass spectrometer (AB SCIEX, Canada). Data were acquired and processed using Analyst software (Version 1.7.1, AB SCIEX). Linear regressions and calculations were done using MultiQuant software (Version 2.1.1, AB SCIEX). Lower limit of quantification (LLOQ) and accuracy were determined for quantification of SH045 effects in kidney and both revealed as high as reported for plasma by Chai et al.<sup>38</sup>.

**Immunofluorescence and analysis.** We performed immunofluorescence similarly as previously described<sup>34</sup>. Two- $\mu$ m thick sections of IRI-injured kidneys were post-fixed in ice-cold acetone, air-dried, rehydrated and blocked with 10% normal donkey serum (Jackson ImmunoResearch, America) for 30 min. Then sections were incubated in a humid chamber overnight at 4  $^{\circ}$ C with rat anti-Ly6B.2 (Gr1) (1:300; MCA771G; Bio-Rad AbD Serotec, Germany). The bound anti-Ly6B.2 antibody was visualized using Cy3-conjugated secondary antibody (1:500; Jackson ImmunoResearch, America) by incubating the sections for 1 h in a humid chamber at room temperature. Positive cells were counted in the outer medulla on ten non-overlapping view fields at 400 $\times$  magnification and mean cell numbers were taken for analysis.

**Isolated perfused kidneys.** Isolated kidneys were perfused in an organ chamber using a peristaltic pump (Instech, USA) at constant flow (0.3–1.9 ml/min) of oxygenated (95% O<sub>2</sub> and 5% CO<sub>2</sub>) physiological salt solution (PSS) containing (in mmol/L) 119 NaCl, 4.7 KCl, 1.2 KH<sub>2</sub>PO<sub>4</sub>, 25 NaHCO<sub>3</sub>, 1.2 Mg<sub>2</sub>SO<sub>4</sub>, 11.1 glucose, 1.6 CaCl<sub>2</sub>. Hyperforin (Sigma-Aldrich, USA), BI-749327, and SH045 were dissolved in DMSO. Before application, the aliquots were dissolved 1:1000 in PSS. So, the final concentration of DMSO did not exceed 0.1%. The concentrations of hyperforin, BI-749327, SH045 were 10  $\mu$ M, 100 nM, and 100 nM, respectively. We used PSS as a solvent for Ang II (LKT Laboratories Inc., USA) and applied it at 10 nM concentration. Drugs were added to the perfusate. Perfusion pressure was detected using pressure transducer after an equilibration period of 60 min. Powerlab system (AD Instruments, Colorado Springs) was used for data acquisition and analysis. Ang II-induced pressor effects were normalized to the maximal pressor effect obtained with KCl (60 mmol/L)<sup>58</sup>. The composition of 60 mM KCl (in mmol/L) was 63.7 NaCl, 60 KCl, 1.2 KH<sub>2</sub>PO<sub>4</sub>, 25 NaHCO<sub>3</sub>, 1.2 Mg<sub>2</sub>SO<sub>4</sub>, 11.1 glucose, and 1.6 CaCl<sub>2</sub>.

**Statistics.** Statistical analysis was performed using GraphPad 5.04 software. Study groups were analyzed by one-way ANOVA using Turkey's post-hoc test or two-way ANOVA using Sidak's multiple comparisons post hoc test. Data are presented as mean  $\pm$  SEM. *P* values < 0.05 were considered as statistically significant.

**Experimental statement.** All methods were carried out in accordance with relevant guidelines and regulations.

Received: 15 June 2021; Accepted: 3 February 2022  
 Published online: 22 February 2022

## References

1. Tsagareli, M. G. & Nozadze, I. An overview on transient receptor potential channels superfamily. *Behav. Pharmacol.* **31**, 413–434 (2020).
2. Kaneko, Y. & Szallasi, A. Transient receptor potential (TRP) channels: A clinical perspective. *Br. J. Pharmacol.* **171**, 2474–2507 (2014).
3. Harteneck, C. Function and pharmacology of TRPM cation channels. *Naunyn Schmiedebergs Arch. Pharmacol.* **371**, 307–314 (2005).
4. Ma, R., Chaudhari, S. & Li, W. Canonical transient receptor potential 6 channel: A new target of reactive oxygen species in renal physiology and pathology. *Antioxid. Redox Signal.* **25**, 732–748 (2016).
5. Mulukala, S. K. N. *et al.* Structural features and oligomeric nature of human podocin domain. *Biochem. Biophys. Rep.* **23**, 100774 (2020).
6. Winn, M. P. *et al.* A mutation in the TRPC6 cation channel causes familial focal segmental glomerulosclerosis. *Science* **308**, 1801–1804 (2005).
7. Riehle, M. *et al.* TRPC6 G757D loss-of-function mutation associates with FSGS. *J. Am. Soc. Nephrol.* **27**, 2771–2783 (2016).
8. Ilatovskaya, D. V. *et al.* Angiotensin II has acute effects on TRPC6 channels in podocytes of freshly isolated glomeruli. *Kidney Int.* **86**, 506–514 (2014).
9. Kong, W. *et al.* Renal fibrosis, immune cell infiltration and changes of TRPC channel expression after unilateral ureteral obstruction in *Trpc6*<sup>-/-</sup> mice. *Cell Physiol. Biochem.* **52**, 1484–1502 (2019).
10. Wu, Y. L. *et al.* Inhibition of TRPC6 channels ameliorates renal fibrosis and contributes to renal protection by soluble klotho. *Kidney Int.* **91**, 830–841 (2017).
11. Singbartl, K. & Kellum, J. A. AKI in the ICU: Definition, epidemiology, risk stratification, and outcomes. *Kidney Int.* **81**, 819–825 (2012).
12. Schrier, R. W., Arnold, P. E., Van Putten, V. J. & Burke, T. J. Cellular calcium in ischemic acute renal failure: Role of calcium entry blockers. *Kidney Int.* **32**, 313–321 (1987).
13. Weinberg, J. M. The cell biology of ischemic renal injury. *Kidney Int.* **39**, 476–500 (1991).
14. Lin, B. L. *et al.* In vivo selective inhibition of TRPC6 by antagonist BI 749327 ameliorates fibrosis and dysfunction in cardiac and renal disease. *Proc. Natl. Acad. Sci. USA.* **116**, 10156–10161 (2019).
15. Meng, X. M. *et al.* NADPH oxidase 4 promotes cisplatin-induced acute kidney injury via ROS-mediated programmed cell death and inflammation. *Lab Invest.* **98**, 63–78 (2018).
16. Liao, W. *et al.* p62/SQSTM1 protects against cisplatin-induced oxidative stress in kidneys by mediating the cross talk between autophagy and the Keap1-Nrf2 signalling pathway. *Free Radic. Res.* **53**, 800–814 (2019).
17. Kim, E. Y. *et al.* NOX2 interacts with podocyte TRPC6 channels and contributes to their activation by diacylglycerol: Essential role of podocin in formation of this complex. *Am. J. Physiol. Cell Physiol.* **305**, C960–C971 (2013).
18. Graham, S. *et al.* Abundance of TRPC6 protein in glomerular mesangial cells is decreased by ROS and PKC in diabetes. *Am. J. Physiol. Cell Physiol.* **301**, C304–C315 (2011).
19. Weber, E. W. *et al.* TRPC6 is the endothelial calcium channel that regulates leukocyte transendothelial migration during the inflammatory response. *J. Exp. Med.* **212**, 1883–1899 (2015).
20. Lindemann, O. *et al.* TRPC6 regulates CXCR2-mediated chemotaxis of murine neutrophils. *J. Immunol.* **190**, 5496–5505 (2013).
21. Shen, B. *et al.* TRPC6 may protect renal ischemia-reperfusion injury through inhibiting necroptosis of renal tubular epithelial cells. *Med. Sci. Monit. Int. Med. J. Exp. Clin. Res.* **22**, 633 (2016).
22. Häfner, S. *et al.* A (+)-larixol congener with high affinity and subtype selectivity toward TRPC6. *ChemMedChem* **13**, 1028–1035 (2018).
23. Chai, X. N. *et al.* Validation of an LC-MS/MS Method to Quantify the New TRPC6 Inhibitor SH045 (Larixyl N-methylcarbamate) and Its Application in an Exploratory Pharmacokinetic Study in Mice. *Pharmaceuticals* **14**, 2 (2021).
24. Sato, Y. & Yanagita, M. Immune cells and inflammation in AKI to CKD progression. *Am. J. Physiol. Renal Physiol.* **315**, F1501–F1512 (2018).
25. Singbartl, K., Formeck, C. L. & Kellum, J. A. Kidney-immune system crosstalk in AKI. *Semin. Nephrol.* **39**, 96–106 (2019).
26. Kidoya, H. *et al.* APJ regulates parallel alignment of arteries and veins in the skin. *Dev. Cell.* **33**, 247–259 (2015).
27. Bonventre, J. V. & Zuk, A. Ischemic acute renal failure: an inflammatory disease? *Kidney Int.* **66**, 480–485 (2004).
28. van den Akker, J. P. C., Bakker, J., Groeneveld, A. B. J. & den Uil, C. A. Risk indicators for acute kidney injury in cardiogenic shock. *J. Crit. Care.* **50**, 11–16 (2019).
29. Thiel, G. & Rössler, O. G. Hyperforin activates gene transcription involving transient receptor potential C6 channels. *Biochem. Pharmacol.* **129**, 96–107 (2017).
30. Liu, L. *et al.* TRPC6 attenuates cortical astrocytic apoptosis and inflammation in cerebral ischemic/reperfusion injury. *Front. Cell Dev. Biol.* **8**, 594283 (2020).
31. Dietrich, A. *et al.* Increased vascular smooth muscle contractility in *TRPC6*<sup>-/-</sup> mice. *Mol. Cell Biol.* **25**, 6980–6989 (2005).
32. Chu, X. *et al.* Interaction of TRPC2 and TRPC6 in erythropoietin modulation of calcium influx. *J. Biol. Chem.* **279**, 10514–10522 (2004).
33. Hofmann, T., Schaefer, M., Schultz, G. & Gudermann, T. Subunit composition of mammalian transient receptor potential channels in living cells. *Proc. Natl. Acad. Sci. USA.* **99**, 7461–7466 (2002).
34. Markó, L. *et al.* Role of cystathionine gamma-lyase in immediate renal impairment and inflammatory response in acute ischemic kidney injury. *Sci. Rep.* **6**, 27517 (2016).
35. Mannaa, M. *et al.* Transient receptor potential vanilloid 4 channel deficiency aggravates tubular damage after acute renal ischaemia reperfusion. *Sci. Rep.* **8**, 4878 (2018).
36. Markó, L. *et al.* Tubular epithelial NF- $\kappa$ B activity regulates ischemic AKI. *J. Am. Soc. Nephrol.* **27**, 2658–2669 (2016).
37. Häfner, S. & Burg, F. A (+)-larixol congener with high affinity and subtype selectivity toward TRPC6. *ChemMedChem* **13**, 1028–1035 (2018).
38. Chai, X. N. & Ludwig, F. A. Validation of an LC-MS/MS method to quantify the new TRPC6 inhibitor SH045 (Larixyl N-methylcarbamate) and its application in an exploratory pharmacokinetic study in mice. *Pharmaceuticals* **14**, 2 (2021).
39. Rabb, H. *et al.* Inflammation in AKI: Current understanding, key questions, and knowledge gaps. *J. Am. Soc. Nephrol.* **27**, 371–379 (2016).
40. Grigoryev, D. N. *et al.* The local and systemic inflammatory transcriptome after acute kidney injury. *J. Am. Soc. Nephrol.* **19**, 547–558 (2008).
41. Ren, K. *et al.* Gasdermin D mediates inflammation-driven pathogenesis of the myelodysplastic syndromes. *Blood* **138**, 2587–2587 (2021).
42. Pang, Y. *et al.* Andrade-oliveira salvianolic acid B modulates caspase-1-mediated pyroptosis in renal ischemia-reperfusion injury via Nrf2 pathway. *Front. Pharmacol.* **11**, 541426 (2020).



43. Bonavia, A. & Singbartl, K. A review of the role of immune cells in acute kidney injury. *Pediatr. Nephrol.* **33**, 1629–1639 (2018).
44. Amrouche, L. *et al.* MicroRNA-146a in human and experimental ischemic AKI: CXCL8-dependent mechanism of action. *J. Am. Soc. Nephrol.* **28**, 479–493 (2017).
45. Ramirez, G. A. *et al.* Ion channels and transporters in inflammation: Special focus on TRP channels and TRPC6. *Cells* **7**, 2 (2018).
46. Damann, N., Owsianik, G., Li, S., Poll, C. & Nilius, B. The calcium-conducting ion channel transient receptor potential canonical 6 is involved in macrophage inflammatory protein-2-induced migration of mouse neutrophils. *Acta Physiol. (Oxf)*. **195**, 3–11 (2009).
47. Rudman-Melnick, V. *et al.* Single-cell profiling of AKI in a murine model reveals novel transcriptional signatures, profibrotic phenotype, and epithelial-to-stromal crosstalk. *J. Am. Soc. Nephrol.* **31**, 2793–2814 (2020).
48. Hiroshima, Y. *et al.* S100A8/A9 and S100A9 reduce acute lung injury. *Immunol. Cell Biol.* **95**, 461–472 (2017).
49. Dessing, M. C. *et al.* The calcium-binding protein complex S100A8/A9 has a crucial role in controlling macrophage-mediated renal repair following ischemia/reperfusion. *Kidney Int.* **87**, 85–94 (2015).
50. Hou, X. *et al.* Transient receptor potential channel 6 knockdown prevents apoptosis of renal tubular epithelial cells upon oxidative stress via autophagy activation. *Cell Death Dis.* **9**, 1015 (2018).
51. Davis, J., Burr, A. R., Davis, G. F., Birnbaumer, L. & Molkentin, J. D. A TRPC6-dependent pathway for myofibroblast transdifferentiation and wound healing in vivo. *Dev. Cell.* **23**, 705–715 (2012).
52. Kefaloyianni, E. *et al.* ADAM17 substrate release in proximal tubule drives kidney fibrosis. *JCI Insight.* **1**, 2 (2016).
53. Zafrani, L. & Ince, C. Microcirculation in acute and chronic kidney diseases. *Am. J. Kidney Dis.* **66**, 1083–1094 (2015).
54. Restrictions in the State Office for Health and Social Affairs (LAGeSo). Animal welfare. <https://www.berlin.de/lageso/gesundheitsveterinaerwesen/tierschutz/>.
55. ARRIVE guidelines. <https://arriveguidelines.org/arrive-guidelines> (2020).
56. Chen, L. *et al.* Role of TRPV1 channels in ischemia/reperfusion-induced acute kidney injury. *PLoS ONE* **9**, e109842 (2014).
57. Lee, H. T. *et al.* Isoflurane protects against renal ischemia and reperfusion injury and modulates leukocyte infiltration in mice. *Am. J. Physiol. Renal Physiol.* **293**, F713–F722 (2007).
58. Schleifenbaum, J. *et al.* Stretch-activation of angiotensin II type 1a receptors contributes to the myogenic response of mouse mesenteric and renal arteries. *Circ. Res.* **115**, 263–272 (2014).

### Acknowledgements

We thank Jana Czychi and Juliane Ulrich for their technical help. This work was supported by the Deutsche Forschungsgemeinschaft (DFG) to B.N. and M.G. (SFB1365, GO766/18-2, GO766/12-3, NU53/12-2) and M.S. (SFB-TTR152, TP18).

### Author contributions

All authors planned and designed experimental studies. Z.Z., D.T., and T.U.P.B. performed qPCRs, histological evaluation, analyzed data and drafted the manuscript. C.E. and J.S. performed the isolated kidney perfusions. U.K. and M.S. supplied the TRPC6 Blocker and provided pharmacokinetic measurements for its use in vivo. X.C. and F.-A.L. measured the concentration of SH045 in vivo. K.W. supervised the histological analysis. G.N. performed murine surgery and collected blood and tissues. M.-B.K. performed renal PAS and immunofluorescence staining. B.N., M.G. and L.M. supervised the experimental work. All authors revised the manuscript critically for important intellectual content. All authors agree to be accountable for all aspects of the work in ensuring that questions related to the accuracy or integrity of any part of the work are appropriately investigated and resolved. All authors made substantial contributions to conception, design, drafting and completion of the article.

### Funding

Open Access funding enabled and organized by Projekt DEAL.

### Competing interests

The authors declare no competing interests.


### Additional information

**Supplementary Information** The online version contains supplementary material available at <https://doi.org/10.1038/s41598-022-06703-9>.

**Correspondence** and requests for materials should be addressed to D.T., M.G. or L.M.

**Reprints and permissions information** is available at [www.nature.com/reprints](http://www.nature.com/reprints).

**Publisher's note** Springer Nature remains neutral with regard to jurisdictional claims in published maps and institutional affiliations.

 **Open Access** This article is licensed under a Creative Commons Attribution 4.0 International License, which permits use, sharing, adaptation, distribution and reproduction in any medium or format, as long as you give appropriate credit to the original author(s) and the source, provide a link to the Creative Commons licence, and indicate if changes were made. The images or other third party material in this article are included in the article's Creative Commons licence, unless indicated otherwise in a credit line to the material. If material is not included in the article's Creative Commons licence and your intended use is not permitted by statutory regulation or exceeds the permitted use, you will need to obtain permission directly from the copyright holder. To view a copy of this licence, visit <http://creativecommons.org/licenses/by/4.0/>.

© The Author(s) 2022

# Supplementary Information

## Figure S1

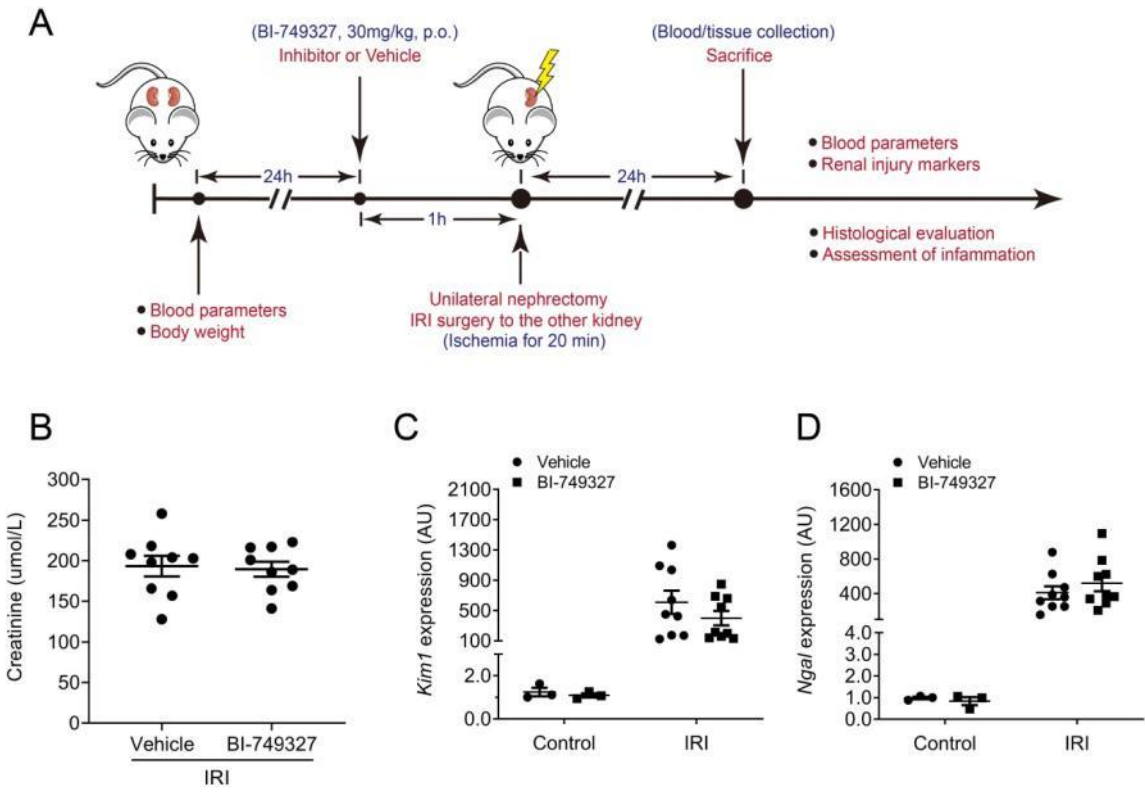


Figure S2

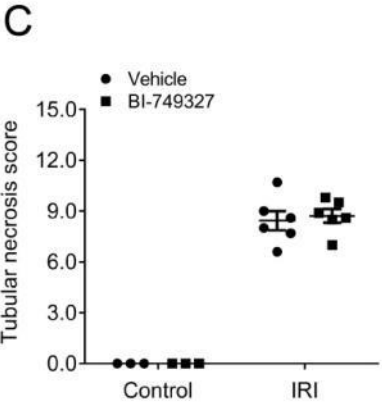
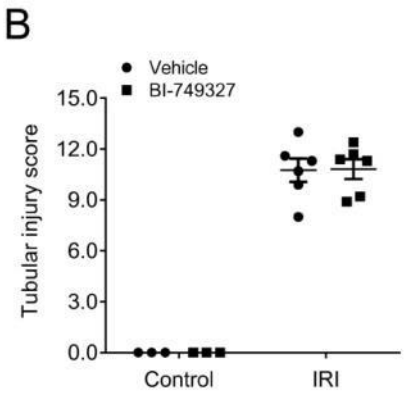
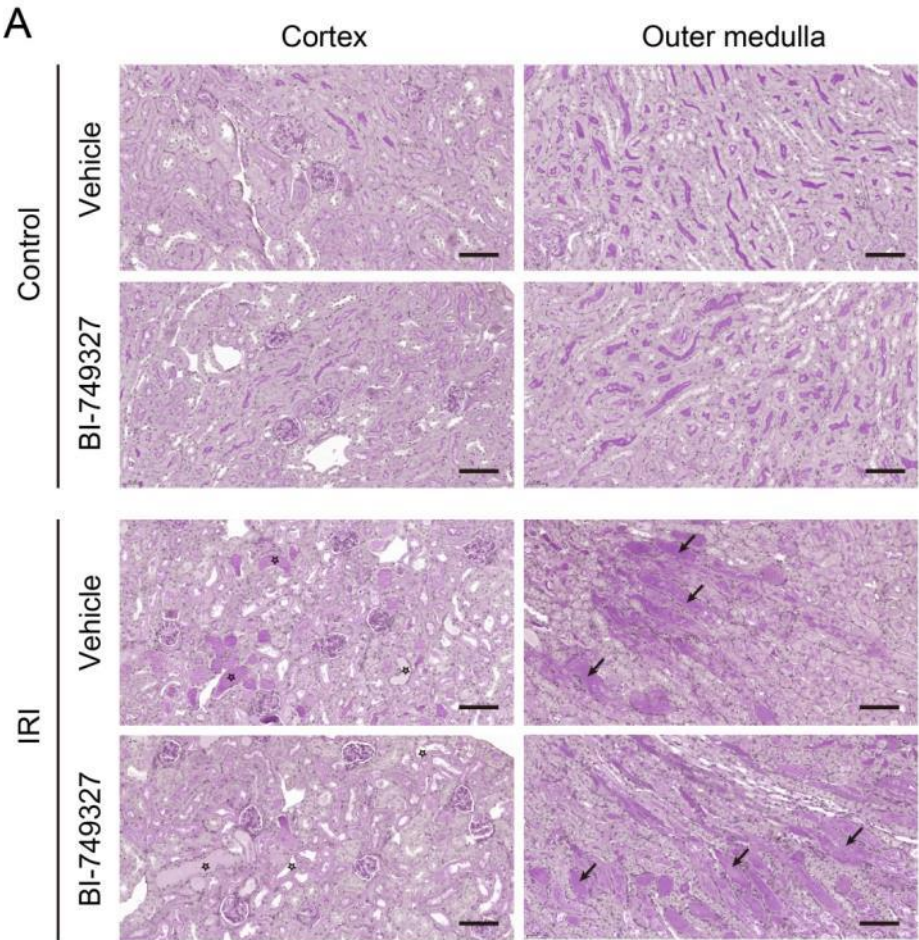
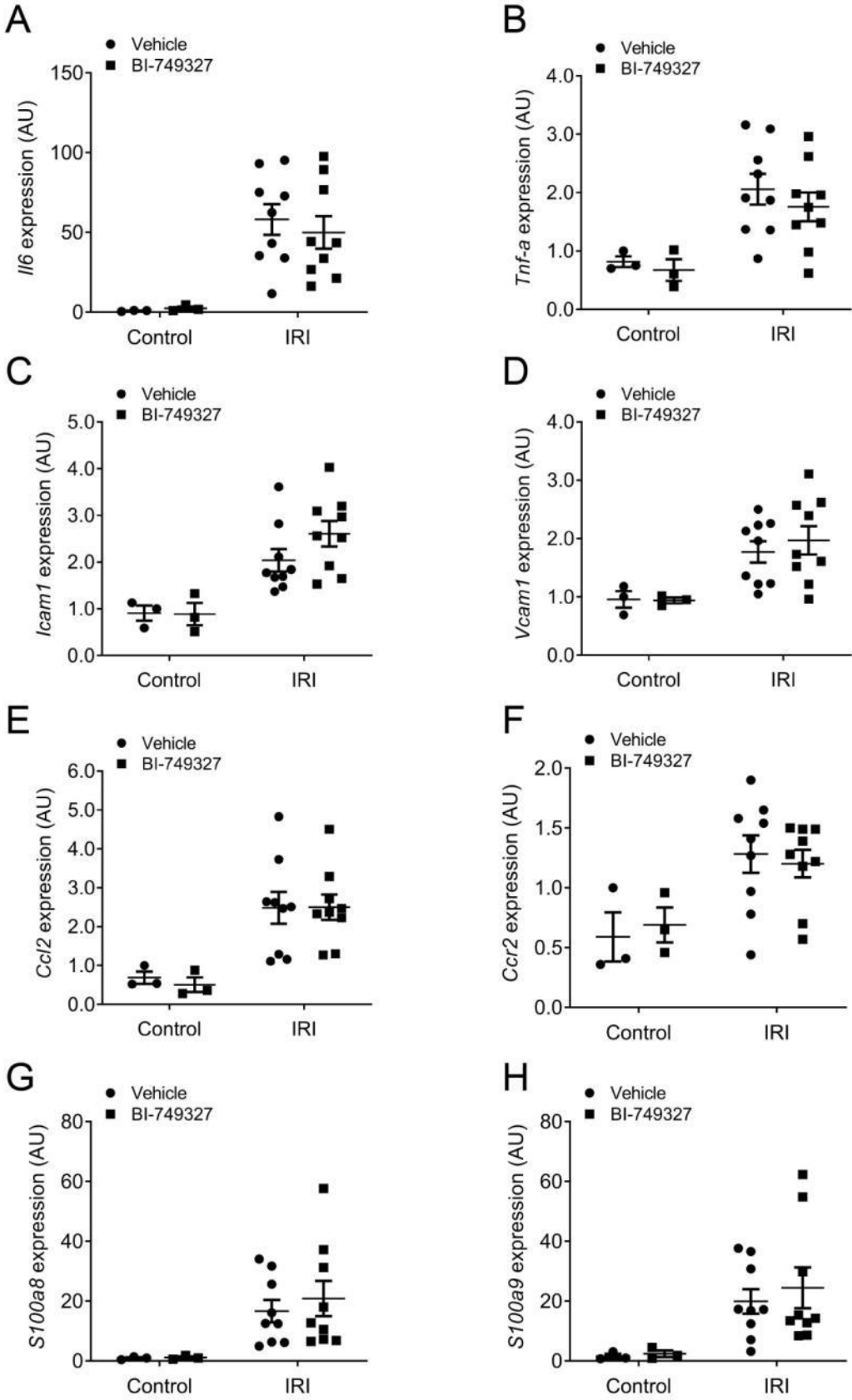
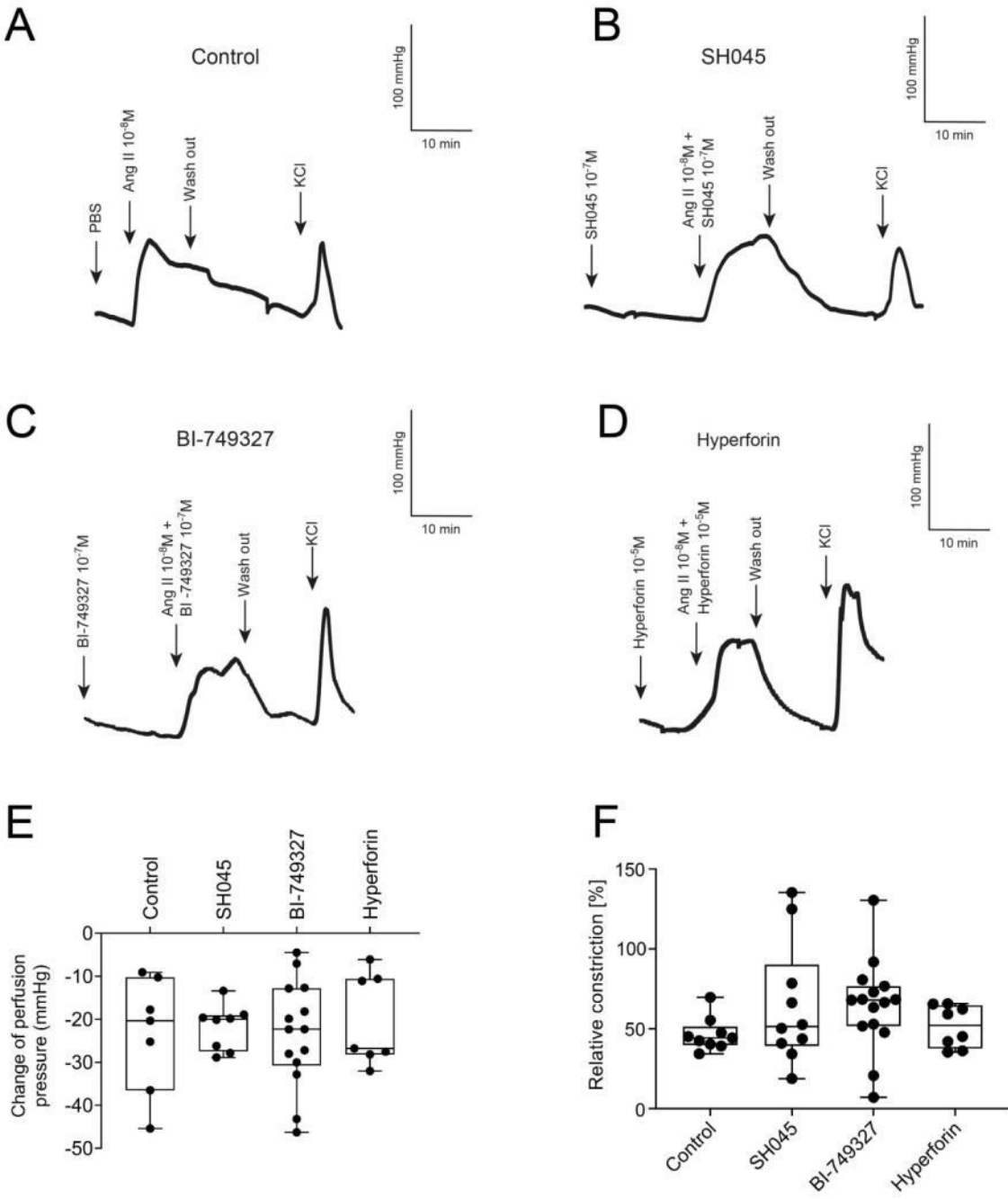


Figure S3



**Figure S4**



**Table S1**

Primers	Forward	Reverse
<i>Ngal</i>	5'-TGATCCCTGCCCCATCTCT-3'	5'-GGAAGTATCGCTCCGGAA-3'
<i>Kim1</i>	5'-CTGGAGTAATCACACTGAAGCAATG-3'	5'-GATGCCAACATAGAAGCCCTTAGT-3'
<i>Il-6</i>	5'-TGTCTCGAGCCCACCAGG-3'	5'-TGCGGAGAGAACTTCATAGCTG-3'
<i>Trpc6</i>	5'-GACCGTTCATGAAGTTTGTAGCAC-3'	5'-AGTATTCTTTGGGGCCTTGAGTCC-3'
<i>Tnf-a</i>	5'-CTGAACTTCGGGGTGATCGG-3'	5'-GGCTTGTCCTCGAATTTTGAGA-3'
<i>S1008a</i>	5'-TCACCATGCCCTCTACAAGA-3'	5'-CCAATTCTCTGAACAAGTTTTCG-3'
<i>S1009a</i>	5'-TCAGACAAATGGTGGAAGCA-3'	5'-GTCCAGGTCCTCCATGATGT-3'
<i>Icam1</i>	5'-CTGGGCTTGGGAGACTCAGTG-3'	5'-CCACTCTCCGGAAACGAA-3'
<i>Vcam1</i>	5'-CTGGGAAGCTGGAACGAAGT-3'	5'-GCCAAACACTTGACCGTGAC-3'
<i>Ccl2</i>	5'-GGCTCAGCCAGATGCAGTTAA-3'	5'-CCTACTCATTGGGATCATCTTGCT-3'
<i>Ccr2</i>	5'-GTTCTCTTCTGACCACCTTC-3'	5'-CTT CGG AAC TTC TCA CCA ACA-3'
18S	5'-ACATCCAAGGAAGGCAGCAG-3'	5'-TTTTCGTCACTACCTCCCCG-3'



**Table S2****A** Baseline

Blood parameters	WT		<i>Trpc6</i> <sup>-/-</sup>		t-test
	Mean	STD	Mean	STD	<i>P</i> -value
Sodium (mmol/L)	145.33	1.66	148.89	1.45	0.0002
Potassium (mmol/L)	4.72	0.47	4.68	0.40	0.832
Chloride (mmol/L)	113.00	1.80	113.44	2.24	0.649
Ionized Calcium (mmol/L)	1.23	0.05	1.28	0.04	0.035
Total Carbon Dioxide (mmol/L)	21.78	1.64	22.22	3.49	0.734
Glucose (mg/dl)	228.22	28.38	199.44	35.45	0.075
Urea Nitrogen (mmol/L)	7.14	1.52	8.02	1.35	0.214
Creatinine (umol/L)	<18	n.a.	<18	n.a.	n.a.
Hematocrit (%PCU)	39.89	1.36	40.78	0.67	0.098
Hemoglobin (g/dl)	13.58	0.47	13.84	0.22	0.141
Anion Gap (mmol/L)	17.33	2.65	17.78	2.39	0.713

**B** 24 h after IRI

Blood parameters	WT		<i>Trpc6</i> <sup>-/-</sup>		t-test
	Mean	STD	Mean	STD	<i>P</i> -value
Sodium (mmol/L)	147.33	2.58	142.67	2.69	0.0053
Potassium (mmol/L)	6.77	1.44	7.84	1.12	0.127
Chloride (mmol/L)	120.67	3.27	112.89	5.30	0.007
Ionized Calcium (mmol/L)	1.04	0.21	1.16	0.14	0.203
Total Carbon Dioxide (mmol/L)	16.00	2.90	18.00	2.55	0.182
Glucose (mg/dl)	106.83	28.08	121.44	53.69	0.554
Urea Nitrogen (mmol/L)	>50	n.a.	>50	n.a.	n.a.
Creatinine (umol/L)	129.00	35.744	159.56	41.723	0.166
Hematocrit (%PCU)	33.50	2.88	31.89	4.17	0.427
Hemoglobin (g/dl)	11.40	0.97	10.84	1.43	0.421
Anion Gap (mmol/L)	18.50	3.45	20.11	2.80	0.337

# Table S3

## A Baseline (Sham)

Blood parameters	Vehicle		SH045		t-test
	Mean	STD	Mean	STD	P-value
Sodium (mmol/L)	146.50	0.71	144.67	2.08	0.334
Potassium (mmol/L)	4.70	0.14	4.73	0.06	0.724
Chloride (mmol/L)	113.00	1.41	114.00	1.00	0.413
Ionized Calcium (mmol/L)	1.25	0.02	1.25	0.02	0.936
Total Carbon Dioxide (mmol/L)	21.50	0.71	22.67	1.15	0.302
Glucose (mg/dl)	193.50	7.78	188.33	19.66	0.757
Urea Nitrogen (mmol/L)	8.60	1.13	10.20	0.70	0.137
Creatinine (umol/L)	<18	n.a.	<18	n.a.	n.a.
Hematocrit (%PCU)	39.00	1.41	41.33	1.15	0.133
Hemoglobin (g/dl)	13.35	0.64	14.07	0.40	0.210
Anion Gap (mmol/L)	17.50	0.71	15.67	1.15	0.146

## B 24 h after Sham operation

Blood parameters	Vehicle		SH045		t-test
	Mean	STD	Mean	STD	P-value
Sodium (mmol/L)	147.67	0.58	147.33	0.58	0.519
Potassium (mmol/L)	4.80	0.62	4.90	0.17	0.802
Chloride (mmol/L)	116.00	4.58	117.00	1.00	0.731
Ionized Calcium (mmol/L)	1.28	0.03	1.29	0.03	0.519
Total Carbon Dioxide (mmol/L)	21.67	1.15	21.33	1.53	0.778
Glucose (mg/dl)	183.67	7.64	214.67	20.98	0.074
Urea Nitrogen (mmol/L)	9.77	0.71	10.80	1.76	0.399
Creatinine (umol/L)	<18	n.a.	<18	n.a.	n.a.
Hematocrit (%PCU)	35.33	3.06	35.00	3.61	0.909
Hemoglobin (g/dl)	12.00	1.01	11.87	1.23	0.892
Anion Gap (mmol/L)	15.67	3.21	15.00	0.00	0.738

## C Baseline (17.5min-IRI)

Blood parameters	Vehicle		SH045		t-test
	Mean	STD	Mean	STD	P-value
Sodium (mmol/L)	144.50	1.87	144.50	0.55	1.000
Potassium (mmol/L)	4.70	0.65	4.57	0.19	0.639
Chloride (mmol/L)	111.67	3.01	112.83	3.43	0.545
Ionized Calcium (mmol/L)	1.28	0.03	1.29	0.03	0.923
Total Carbon Dioxide (mmol/L)	21.33	4.03	24.00	2.61	0.204
Glucose (mg/dl)	204.17	39.67	191.00	30.24	0.532
Urea Nitrogen (mmol/L)	8.30	1.77	9.63	0.93	0.134
Creatinine (umol/L)	<18	n.a.	<18	n.a.	n.a.
Hematocrit (%PCU)	40.00	1.41	41.50	1.64	0.121
Hemoglobin (g/dl)	13.58	0.41	14.12	0.54	0.084
Anion Gap (mmol/L)	16.33	1.21	14.83	2.14	0.166

## D 24 h after 17.5min-IRI

Blood parameters	Vehicle		SH045		t-test
	Mean	STD	Mean	STD	P-value
Sodium (mmol/L)	140.75	5.12	144.20	1.64	0.194
Potassium (mmol/L)	8.05	1.32	6.92	1.31	0.242
Chloride (mmol/L)	117.25	4.79	117.80	1.92	0.819
Ionized Calcium (mmol/L)	0.95	0.12	1.00	0.13	0.548
Total Carbon Dioxide (mmol/L)	13.75	2.63	14.40	2.30	0.704
Glucose (mg/dl)	101.00	17.64	122.40	35.12	0.307
Urea Nitrogen (mmol/L)	>50	n.a.	>50	n.a.	n.a.
Creatinine (umol/L)	199.50	21.794	172.60	31.635	0.193
Hematocrit (%PCU)	31.75	1.71	34.00	2.45	0.165
Hemoglobin (g/dl)	11.55	2.05	11.56	0.85	0.992
Anion Gap (mmol/L)	18.50	0.71	19.80	1.92	0.415

## E Baseline (20 min-IRI)

Blood parameters	Vehicle		SH045		t-test
	Mean	STD	Mean	STD	P-value
Sodium (mmol/L)	144.50	3.11	144.60	0.89	0.947
Potassium (mmol/L)	4.63	0.53	4.64	0.50	0.966
Chloride (mmol/L)	114.00	2.16	115.00	2.24	0.521
Ionized Calcium (mmol/L)	1.29	0.06	1.28	0.02	0.782
Total Carbon Dioxide (mmol/L)	22.00	2.71	21.60	0.55	0.753
Glucose (mg/dl)	236.75	62.89	201.60	13.18	0.256
Urea Nitrogen (mmol/L)	9.36	1.75	8.74	2.04	0.644
Creatinine (umol/L)	<18	n.a.	<18	n.a.	n.a.
Hematocrit (%PCU)	42.25	2.75	42.00	1.00	0.854
Hemoglobin (g/dl)	14.38	0.94	14.26	0.35	0.805
Anion Gap (mmol/L)	14.75	0.50	13.80	1.92	0.374

## F 24 h after 20 min-IRI

Blood parameters	Vehicle		SH045		t-test
	Mean	STD	Mean	STD	P-value
Sodium (mmol/L)	140.00	4.32	135.75	2.36	0.135
Potassium (mmol/L)	8.53	0.36	>9.0	n.a.	n.a.
Chloride (mmol/L)	114.75	5.19	115.00	4.16	0.943
Ionized Calcium (mmol/L)	0.97	0.07	0.98	0.07	0.812
Total Carbon Dioxide (mmol/L)	14.00	1.41	13.25	1.71	0.524
Glucose (mg/dl)	91.50	11.68	86.75	12.50	0.599
Urea Nitrogen (mmol/L)	>50	n.a.	>50	n.a.	n.a.
Creatinine (umol/L)	212.25	8.421	226.25	28.605	0.384
Hematocrit (%PCU)	35.25	3.59	31.75	2.22	0.148
Hemoglobin (g/dl)	12.05	1.35	10.78	0.76	0.152
Anion Gap (mmol/L)	23.00	1.00	n.a.	n.a.	n.a.

**Table S4****A** Baseline

Blood parameters	Vehicle		BI-749327		t-test
	Mean	STD	Mean	STD	<i>P</i> -value
Sodium (mmol/L)	144.33	2.40	142.78	2.54	0.200
Potassium (mmol/L)	4.38	0.20	4.42	0.22	0.661
Chloride (mmol/L)	116.00	3.00	118.22	4.82	0.257
Ionized Calcium (mmol/L)	1.23	0.06	1.22	0.06	0.770
Total Carbon Dioxide (mmol/L)	21.00	2.12	19.67	2.45	0.235
Glucose (mg/dl)	196.67	16.28	201.00	20.51	0.626
Urea Nitrogen (mmol/L)	7.29	0.42	7.48	0.66	0.464
Creatinine (umol/L)	<18	n.a	<18	n.a	n.a
Hematocrit (%PCU)	37.00	1.80	37.67	3.00	0.576
Hemoglobin (g/dl)	12.80	0.88	12.64	0.95	0.723
Anion Gap (mmol/L)	17.44	2.51	18.67	2.29	0.296

**B** 24 h after IRI

Blood parameters	Vehicle		BI-749327		t-test
	Mean	STD	Mean	STD	<i>P</i> -value
Sodium (mmol/L)	146.00	4.56	145.67	8.50	0.919
Potassium (mmol/L)	7.53	1.33	8.80	0.14	0.067
Chloride (mmol/L)	123.44	6.69	119.78	10.95	0.404
Ionized Calcium (mmol/L)	0.98	0.29	0.75	0.18	0.059
Total Carbon Dioxide (mmol/L)	13.22	1.99	14.56	2.40	0.218
Glucose (mg/dl)	101.11	22.03	113.89	37.04	0.387
Urea Nitrogen (mmol/L)	>50	n.a	>50	n.a	n.a
Creatinine (umol/L)	193.33	38.030	189.56	27.722	0.813
Hematocrit (%PCU)	35.11	4.54	37.22	3.49	0.285
Hemoglobin (g/dl)	11.97	1.55	12.66	1.20	0.307
Anion Gap (mmol/L)	17.22	5.12	21.56	5.10	0.091

## Role of TRPC6 in Kidney Damage after Acute Ischemic Kidney Injury

Zhihuang Zheng<sup>1,2,3</sup>, Dmitry Tsvetkov<sup>1,2,4\*</sup>, Theda Bartolomaeus<sup>2,12</sup>, Cem Erdogan<sup>5</sup>, Ute Krügel<sup>6</sup>, Johanna Schleifenbaum<sup>5</sup>, Michael Schaefer<sup>6</sup>, Bernd Nürnberg<sup>7</sup>, Xiaoning Chai<sup>6</sup>, Friedrich-Alexander Ludwig<sup>8</sup>, Gabriele N'diaye<sup>2,12</sup>, May-Britt Köhler<sup>2,12</sup>, Kaiyin Wu<sup>9</sup>, Maik Gollasch<sup>1,2,4\*</sup>, Lajos Markó<sup>2,10,11,12\*</sup>

### Supplementary Information

**Supplementary Figure S1.** Effect of BI-749327 on renal function and renal damage markers. (A) Experimental design. (B) Serum creatinine levels (n=9 per group). (C) Renal expression of kidney injury molecule 1 (*Kim1*) and (D) neutrophil gelatinase-associated lipocalin (*Ngal*). Statistical testing was two-way ANOVA followed by Sidak's multiple comparisons post hoc test.

**Supplementary Figure S2.** Effect of BI-749327 on kidney histopathology after AKI. (A) Representative images from the cortico-medullar region of control and IRI-injured kidneys of vehicle or BI-749327-treated mice (magnification: 200×). Kidney sections are Periodic Acid-Schiff (PAS) stained. Arrows indicate tubular necrosis. Stars indicate tubular injury. Scale bars are 100 µm. (B) Semi-quantification of tubular injury. (C) Semi-quantification of tubular necrosis. Data expressed as mean ± SEM (Control n=3 each, and IRI n=6 each, respectively). Statistical testing was performed using two-way ANOVA followed by Sidak's multiple comparisons post hoc test.

**Supplementary Figure S3.** Effect of BI-749327 on renal gene expression of inflammatory markers. (A) Renal expression of interleukin 6 (*Il6*) and (B) tumor necrosis factor-α (*Tnf-α*), (C) intercellular adhesion molecule 1 (*Icam1*), (D) vascular cell adhesion protein 1 (*Vcam1*), (E) C-C motif chemokine 2 (*Ccl2*), (F) C-C motif chemokine receptor 2 (*Ccr2*), and (G and H) S100 calcium-binding protein A8/9 (*S100a8/9*) (Control n=3 each, and IRI n=9 each, respectively). Data expressed as mean ± SEM. Statistical testing was performed using two-way ANOVA followed by Sidak's multiple comparisons post hoc test. AU, arbitrary units.

**Supplementary Figure S4.** Vasoregulation in isolated perfused kidneys. (A) Original recordings of perfusion pressure in kidneys perfused with PSS (control), (B) TRPC6 blocker SH045, (C) another TRPC6 blocker BI-749327, and (D) TRPC6 agonist hyperforin. (E) Decrease of perfusion pressure (n = 7, 8, 14, 7 for control, SH045, BI-749327, and hyperforin, respectively). (F) Increase in perfusion pressure induced by 10 nM Ang II normalized to 60 mM KCl (n = 9, 10, 15, 8 for Control, SH045, BI-749327, and hyperforin, respectively). One-way ANOVA followed by Dunnett's multiple comparisons test.

**Supplementary Table S1.** The sequences of murine gene primer.

**Supplementary Table S2.** (A) Baseline serum parameters of WT or *Trpc6*<sup>-/-</sup> mice before IRI surgery (n=9 per group). (B) Serum parameters of sham WT or *Trpc6*<sup>-/-</sup> mice at 24 hours after IRI surgery (n=7, 9 for IRI WT and *Trpc6*<sup>-/-</sup>, respectively). Data expressed as means ± STD. Two-tailed unpaired t-test. n.a. = not applicable.

**Supplementary Table S3.** (A) Baseline serum parameters of sham mice before surgery (n=3 per group). (B) Serum parameters of sham mice after surgery (n=3 per group). (C) Baseline serum parameters of 17.5 min-IRI mice before surgery (n=5 per group). (D) Serum parameters of 17.5 min-IRI mice after surgery (n=4, 5 for 17.5 min-IRI in vehicle and SH045, respectively). (E) Serum parameters of 20 min-IRI mice before surgery (n=4 per group). (F) (E) Serum parameters of 20 min-IRI mice after surgery (n=4 per group). Data expressed as means ± STD. Two-tailed unpaired t-test. n.a. = not applicable.

**Supplementary Table S4.** (A) Baseline serum parameters of sham mice before surgery (n=9 per group). (B) Serum parameters of IRI mice after surgery (n=9 per group). Data expressed as means ± STD. Two-tailed unpaired t-test. n.a. = not applicable.

## 8.2 Publication #2

The role of TRPC6 in subchronic kidney damage after unilateral ureteral obstruction-induced kidney injury.

Zhihuang Zheng, Yao Xu, Ute Krügel, Michael Schaefer, Tilman Grune, Bernd Nürnberg, May-Britt Köhler, Maik Gollasch, Dmitry Tsvetkov, Lajos Markó. In Vivo Inhibition of TRPC6 by SH045 Attenuates Renal Fibrosis in a New Zealand Obese (NZO) Mouse Model of Metabolic Syndrome. *International Journal of Molecular Sciences*. 2022, 23(12), 6870. **Impact Factor (2020): 5.923**

Received: 18 Mar 2022; Accepted: 16 June 2022; Published online: 20 June 2022.

Journal Data Filtered By: **Selected JCR Year: 2020** Selected Editions: SCIE,SSCI  
 Selected Categories: **"BIOCHEMISTRY and MOLECULAR BIOLOGY"** Selected  
 Category Scheme: WoS

**Gesamtanzahl: 297 Journale**

Rank	Full Journal Title	Total Cites	Journal Impact Factor	Eigenfactor Score
1	NATURE MEDICINE	114,401	53.440	0.184050
2	CELL	320,407	41.582	0.526960
3	Molecular Cancer	24,931	27.401	0.030030
4	Annual Review of Biochemistry	24,394	23.643	0.021450
5	Signal Transduction and Targeted Therapy	3,848	18.187	0.005730
6	MOLECULAR CELL	86,299	17.970	0.161840
7	TRENDS IN MICROBIOLOGY	17,553	17.079	0.022820
8	NUCLEIC ACIDS RESEARCH	248,139	16.971	0.387070
9	MOLECULAR BIOLOGY AND EVOLUTION	61,557	16.240	0.082270
10	PROGRESS IN LIPID RESEARCH	7,328	16.195	0.004530
11	MOLECULAR PSYCHIATRY	28,622	15.992	0.046220
12	CELL DEATH AND DIFFERENTIATION	27,701	15.828	0.028730
13	NATURE STRUCTURAL & MOLECULAR BIOLOGY	32,038	15.369	0.051210
14	Nature Chemical Biology	27,428	15.040	0.047880
15	MOLECULAR ASPECTS OF MEDICINE	8,136	14.235	0.006640
16	TRENDS IN BIOCHEMICAL SCIENCES	22,003	13.807	0.025760
17	NATURAL PRODUCT REPORTS	13,293	13.423	0.011160
18	Molecular Plant	15,778	13.164	0.026860
19	Advances in Carbohydrate Chemistry and Biochemistry	752	12.200	0.000200
20	TRENDS IN MOLECULAR MEDICINE	13,213	11.951	0.014720

Rank	Full Journal Title	Total Cites	Journal Impact Factor	Eigenfactor Score
21	Redox Biology	15,982	11.799	0.024930
22	EMBO JOURNAL	76,189	11.598	0.055000
23	MATRIX BIOLOGY	8,972	11.583	0.011010
24	Molecular Systems Biology	10,149	11.429	0.016300
25	PLANT CELL	64,794	11.277	0.036260
26	CURRENT BIOLOGY	78,289	10.834	0.116100
27	BIOCHIMICA ET BIOPHYSICA ACTA-REVIEWS ON CANCER	7,025	10.680	0.007000
28	Cell Systems	5,813	10.304	0.035330
29	ONCOGENE	77,576	9.867	0.059180
30	CELLULAR AND MOLECULAR LIFE SCIENCES	34,003	9.261	0.033790
31	GENOME RESEARCH	47,141	9.043	0.064690
32	CURRENT OPINION IN CHEMICAL BIOLOGY	12,240	8.822	0.014190
33	EMBO REPORTS	19,502	8.807	0.027490
34	EXPERIMENTAL AND MOLECULAR MEDICINE	8,780	8.718	0.013260
35	ANTIOXIDANTS & REDOX SIGNALING	26,971	8.401	0.016700
36	CRITICAL REVIEWS IN BIOCHEMISTRY AND MOLECULAR BIOLOGY	4,576	8.250	0.005370
37	Science Signaling	15,954	8.192	0.023910
38	Cell Chemical Biology	5,236	8.116	0.018050
39	PLOS BIOLOGY	39,598	8.029	0.059920
40	Essays in Biochemistry	3,629	8.000	0.006450
41	BIOINORGANIC CHEMISTRY AND APPLICATIONS	1,406	7.778	0.000890

Selected JCR Year: 2020; Selected Categories: "BIOCHEMISTRY and MOLECULAR BIOLOGY"



Rank	Full Journal Title	Total Cites	Journal Impact Factor	Eigenfactor Score
42	Acta Crystallographica Section D-Structural Biology	23,670	7.652	0.020190
43	CYTOKINE & GROWTH FACTOR REVIEWS	7,650	7.638	0.005850
44	FREE RADICAL BIOLOGY AND MEDICINE	52,714	7.376	0.034180
45	Computational and Structural Biotechnology Journal	3,620	7.271	0.006770
46	AMYLOID-JOURNAL OF PROTEIN FOLDING DISORDERS	2,202	7.141	0.003280
47	Cell and Bioscience	3,184	7.133	0.004320
48	Genes & Diseases	1,850	7.103	0.003170
49	Molecular Ecology Resources	13,390	7.090	0.016690
50	Journal of Integrative Plant Biology	6,749	7.061	0.006430
51	BIOMACROMOLECULES	45,724	6.988	0.026020
52	INTERNATIONAL JOURNAL OF BIOLOGICAL MACROMOLECULES	79,246	6.953	0.073720
53	AMERICAN JOURNAL OF RESPIRATORY CELL AND MOLECULAR BIOLOGY	15,280	6.914	0.015050
54	International Review of Cell and Molecular Biology	3,057	6.813	0.004320
55	CURRENT OPINION IN STRUCTURAL BIOLOGY	12,448	6.809	0.018970
56	PROTEIN SCIENCE	16,581	6.725	0.021220
57	International Journal of Biological Sciences	10,778	6.580	0.010540
58	Open Biology	4,059	6.411	0.010280
59	MOLECULAR MEDICINE	6,239	6.354	0.004460
60	Antioxidants	9,076	6.312	0.009480
61	JOURNAL OF PHOTOCHEMISTRY AND PHOTOBIOLOGY B-BIOLOGY	17,015	6.252	0.012740

Rank	Full Journal Title	Total Cites	Journal Impact Factor	Eigenfactor Score
62	MOLECULAR ECOLOGY	44,625	6.185	0.040470
63	HUMAN MOLECULAR GENETICS	47,192	6.150	0.047520
64	BIOFACTORS	5,004	6.113	0.002810
65	Biomedicines	2,391	6.081	0.003650
66	JOURNAL OF NUTRITIONAL BIOCHEMISTRY	14,446	6.048	0.010580
67	INTERNATIONAL JOURNAL OF MOLECULAR SCIENCES	139,463	5.923	0.195430
68	JOURNAL OF LIPID RESEARCH	28,376	5.922	0.019290
69	CELLULAR & MOLECULAR BIOLOGY LETTERS	2,216	5.787	0.002190
70	EXPERT REVIEWS IN MOLECULAR MEDICINE	2,042	5.600	0.000790
71	Reviews of Physiology Biochemistry and Pharmacology	865	5.545	0.000390
72	FEBS Journal	23,493	5.542	0.022540
73	Nucleic Acid Therapeutics	1,392	5.486	0.003070
74	JOURNAL OF MOLECULAR BIOLOGY	65,163	5.469	0.038400
75	BIOCHEMICAL SOCIETY TRANSACTIONS	14,862	5.407	0.014350
76	Food & Function	19,700	5.396	0.021550
77	BIOELECTROCHEMISTRY	6,107	5.373	0.004870
78	JOURNAL OF NEUROCHEMISTRY	40,281	5.372	0.019170
79	BIOORGANIC CHEMISTRY	10,576	5.275	0.010220
80	GENE THERAPY	8,112	5.250	0.004130
81	Frontiers in Molecular Biosciences	3,140	5.246	0.007660
82	CHROMOSOME RESEARCH	2,752	5.239	0.002250
83	CHEMICO-BIOLOGICAL INTERACTIONS	16,208	5.192	0.011950

Selected JCR Year: 2020; Selected Categories: "BIOCHEMISTRY and MOLECULAR BIOLOGY"



Article

# In Vivo Inhibition of TRPC6 by SH045 Attenuates Renal Fibrosis in a New Zealand Obese (NZO) Mouse Model of Metabolic Syndrome

Zhihuang Zheng <sup>1,2</sup> , Yao Xu <sup>3</sup>, Ute Krügel <sup>4</sup> , Michael Schaefer <sup>4</sup>, Tilman Grune <sup>5,6</sup>, Bernd Nürnberg <sup>7</sup> , May-Britt Köhler <sup>2</sup>, Maik Gollasch <sup>1,3,\*</sup>, Dmitry Tsvetkov <sup>3,\*</sup> and Lajos Markó <sup>2,6,8,9,\*</sup>

- <sup>1</sup> Department of Nephrology/Intensive Care, Charité—Universitätsmedizin Berlin, Corporate Member of Freie Universität Berlin and Humboldt-Universität zu Berlin, 10117 Berlin, Germany; zhihuang.zheng@charite.de
- <sup>2</sup> Experimental and Clinical Research Center, a Joint Cooperation of the Charité—University Medicine Berlin and Max Delbrück Center for Molecular Medicine in the Helmholtz Association, 13125 Berlin, Germany; may-britt.koehler@charite.de
- <sup>3</sup> Department of Internal Medicine and Geriatrics, University Medicine Greifswald, 17475 Greifswald, Germany; yao.xu@med.uni-greifswald.de
- <sup>4</sup> Rudolf Boehm Institute for Pharmacology and Toxicology, Leipzig University, 04107 Leipzig, Germany; ute.kruegel@medizin.uni-leipzig.de (U.K.); michael.schaefer@medizin.uni-leipzig.de (M.S.)
- <sup>5</sup> Department of Molecular Toxicology, German Institute of Human Nutrition Potsdam-Rehbruecke (DIfE), 14558 Nuthetal, Germany; tilman.grune@dife.de
- <sup>6</sup> DZHK (German Centre for Cardiovascular Research), Partner Site, 10785 Berlin, Germany
- <sup>7</sup> Department of Pharmacology, Experimental Therapy and Toxicology and Interfaculty Center of Pharmacogenomics and Drug Research, University of Tübingen, 72076 Tübingen, Germany; bernd.nuernberg@uni-tuebingen.de
- <sup>8</sup> Berlin Institute of Health at Charité-Universitätsmedizin Berlin, 10178 Berlin, Germany
- <sup>9</sup> Charité-Universitätsmedizin Berlin, Corporate Member of Freie Universität Berlin and Humboldt-Universität zu Berlin, 10117 Berlin, Germany
- \* Correspondence: maik.gollasch@med.uni-greifswald.de (M.G.); dmitry.tsvetkov@med.uni-greifswald.de (D.T.); lajos.marko@charite.de (L.M.)



**Citation:** Zheng, Z.; Xu, Y.; Krügel, U.; Schaefer, M.; Grune, T.; Nürnberg, B.; Köhler, M.-B.; Gollasch, M.; Tsvetkov, D.; Markó, L. In Vivo Inhibition of TRPC6 by SH045 Attenuates Renal Fibrosis in a New Zealand Obese (NZO) Mouse Model of Metabolic Syndrome. *Int. J. Mol. Sci.* **2022**, *23*, 6870. <https://doi.org/10.3390/ijms23126870>

Academic Editors: Luís Belo and Márcia Carvalho

Received: 18 March 2022

Accepted: 16 June 2022

Published: 20 June 2022

**Publisher's Note:** MDPI stays neutral with regard to jurisdictional claims in published maps and institutional affiliations.



**Copyright:** © 2022 by the authors. Licensee MDPI, Basel, Switzerland. This article is an open access article distributed under the terms and conditions of the Creative Commons Attribution (CC BY) license (<https://creativecommons.org/licenses/by/4.0/>).

**Abstract:** Metabolic syndrome is a significant worldwide public health challenge and is inextricably linked to adverse renal and cardiovascular outcomes. The inhibition of the transient receptor potential cation channel subfamily C member 6 (TRPC6) has been found to ameliorate renal outcomes in the unilateral ureteral obstruction (UUO) of accelerated renal fibrosis. Therefore, the pharmacological inhibition of TRPC6 could be a promising therapeutic intervention in the progressive tubulo-interstitial fibrosis in hypertension and metabolic syndrome. In the present study, we hypothesized that the novel selective TRPC6 inhibitor SH045 (larixyl N-methylcarbamate) ameliorates UUO-accelerated renal fibrosis in a New Zealand obese (NZO) mouse model, which is a polygenic model of metabolic syndrome. The in vivo inhibition of TRPC6 by SH045 markedly decreased the mRNA expression of pro-fibrotic markers (*Col1a1*, *Col3a1*, *Col4a1*, *Acta2*, *Ccn2*, *Fn1*) and chemokines (*Cxcl1*, *Ccl5*, *Ccr2*) in UUO kidneys of NZO mice compared to kidneys of vehicle-treated animals. Renal expressions of intercellular adhesion molecule 1 (ICAM-1) and  $\alpha$ -smooth muscle actin ( $\alpha$ -SMA) were diminished in SH045- versus vehicle-treated UUO mice. Furthermore, renal inflammatory cell infiltration (F4/80+ and CD4+) and tubulointerstitial fibrosis (Sirius red and fibronectin staining) were ameliorated in SH045-treated NZO mice. We conclude that the pharmacological inhibition of TRPC6 might be a promising antifibrotic therapeutic method to treat progressive tubulo-interstitial fibrosis in hypertension and metabolic syndrome.

**Keywords:** TRPC6; UUO; NZO mice; inflammation; fibrosis; CKD; SH045

## 1. Introduction

Chronic kidney disease (CKD) is characterized by progressive loss of kidney function. The main risk factors of developing CKD are the combination of obesity, diabetes and hypertension, which is commonly referred to as metabolic syndrome. Other contributors are autoimmune diseases (e.g., glomerulonephritis), environmental exposures and genetic risk factors [1,2]. Morphologically, persistent low-grade renal inflammation and tubulointerstitial fibrosis are key hallmarks of CKD [3,4]. The complex interplay of fibroblasts, lymphocytes, tubular, and other cell types in the kidney lead to excessive extracellular matrix deposition and the further deterioration of renal function [5,6]. Although unspecific treatments strategies are available (e.g., medications lowering blood pressure), CKD progression is still poorly controlled.

In recent years, novel drug targets, such as transient receptor potential cation channel, subfamily C, and member 6 (TRPC6), emerged [7,8]. TRPC6 mutations lead to glomerular injury and proteinuria, presumably involving the Ca<sup>2+</sup> signaling pathway and resulting in progressive kidney failure [9–12]. Both TRPC6 gain-of-function and loss-of-function cause familial forms of focal segmental glomerulosclerosis (FSGS) [11,13]. Interestingly, in a murine model of kidney injury (unilateral ureteral obstruction (UUO)), *Trpc6*<sup>-/-</sup> deficiency and pharmacological blockade with BI-749327 ameliorated renal fibrosis in C57BL/6J mice [7,8]. Remarkably, these beneficial effects were not observed in the acute stage of kidney injury (AKI) [14]. Thus, TRPC6 inhibition may have effects on renal fibrogenesis during AKI-to-CKD transition. Given this state of affairs, TRPC6 inhibition seems to represent a promising new therapeutic approach to combat progressive renal failure since it potentially affects CKD at later stages after kidney injury. However, it is unknown whether TRPC6 inhibition is effective for inhibiting progressive tubulo-interstitial fibrosis in hypertension and metabolic syndrome.

Recently, by the chemical diversification of (+)-larixol originating from *Larix decidua* resin traditionally used for inhalation, its methylcarbamate congener, named SH045, was developed as a novel, highly potent, subtype-selective inhibitor of TRPC6 [15]. In the present study, we hypothesized that this novel selective TRPC6 inhibitor (SH045) [15] could ameliorate renal fibrogenesis in the New Zealand obese (NZO) mouse model, which is a polygenic model of metabolic syndrome [16]. We studied the therapeutic effects of the in vivo inhibition of TRPC6 by the novel blocker SH045 in the UUO mouse model of accelerated renal fibrogenesis utilizing these mice.

## 2. Results

### 2.1. SH045 Treatment Does Not Affect Renal Function and *Trpc* Expression in UUO Model

To investigate the impact of in vivo TRPC6 inhibition on renal function, target molecules and fibrosis, we performed UUO in the NZO mice. During the one week period, we administered SH045 (TRPC6 inhibitor) or vehicle once daily (Figure 1A). After 7 days, urinary tract obstruction led to hydronephrosis (Figure S1). Consistent with our previous findings, *Trpc6* expression significantly increased in UUO kidneys. SH045 affected neither *Trpc6* mRNA expression nor the expression of other TRPC channels, including *Trpc1*, *Trpc2*, *Trpc3* and *Trpc4* (Figure 1B and Figure S2A–D). SH045 had no impact on renal function. Serum creatinine ( $p = 0.1098$ ; Figure 1B) and blood urea nitrogen (BUN) ( $p = 0.928$ ; Figure 1C), serum cystatin C, urine albumin, and urine albumin-to-creatinine ratio in SH045-treated mice were unchanged (Figure 1D–F). In addition, we found no differences in serum levels of glucose, sodium, potassium, ionized calcium, total CO<sub>2</sub>, hemoglobin, hematocrit, and anion gap in SH045-treated animals compared to the vehicle group (Table S1). SH045-treated mice exhibited a slightly higher serum chloride concentration ( $p = 0.047$ ), albeit within the normal physiological range.

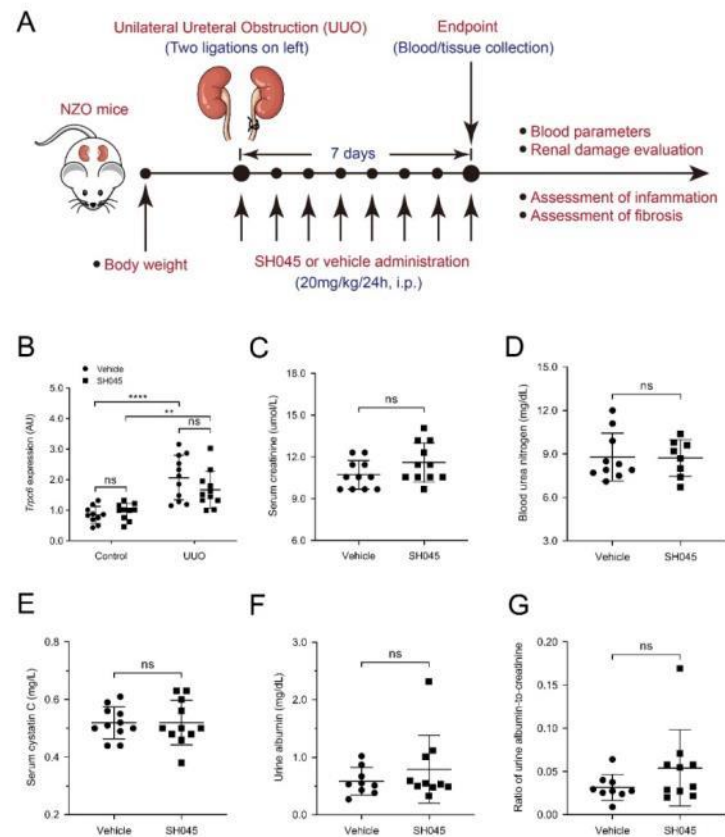


**Figure 1.** Impact of SH045 administration on renal function and *Trpc6* expression in UUO model. (A) Experimental design of unilateral ureteral obstruction (UUO) model. NZO mice were subjected to UUO and then injected with SH045 ( $n = 11$ ) or vehicle ( $n = 11$ ) once every 24 h between day 0 and day 7. All mice were euthanized on day 7 after UUO surgery. (B) Renal mRNA levels of *Trpc6* (control  $n = 10$ , UUO  $n = 11$ ). Control group includes kidneys that were not subjected to the UUO. (C) Serum levels of creatinine, (D) blood urea nitrogen, and (E) cystatin C in the experimental UUO groups. (F) Urine albumin and (G) ratio of albumin to creatinine in the experimental UUO groups (UUO vehicle  $n = 10$ –11, UUO SH045  $n = 8$ –11). Data expressed as means  $\pm$  SD. Two-way ANOVA followed by Sidak's multiple comparisons post hoc test. \*\*  $p < 0.01$  and \*\*\*\*  $p < 0.0001$  defined as significant. ns, not statistically significant. AU, arbitrary units.

## 2.2. SH045 Treatment Does Not Alter Kidney Parenchymal Damage

Morphologically, UUO increased mesangial matrix deposition, leading to glomerular hypertrophy, and tubular dilatation (Figure 2A–D). The expressions of renal damage markers, kidney injury molecule-1 (*Havcr1*) and Lipocalin-2 (*Lcn2*), were increased in UUO kidneys compared to control (Figure 2E,F). However, SH045 did not affect these parameters in both UUO and control kidneys (Figure 2A–F). These results indicate that TRPC6 inhibition per se has no impact on the damage to renal parenchyma (glomerular or tubular) caused by UUO.



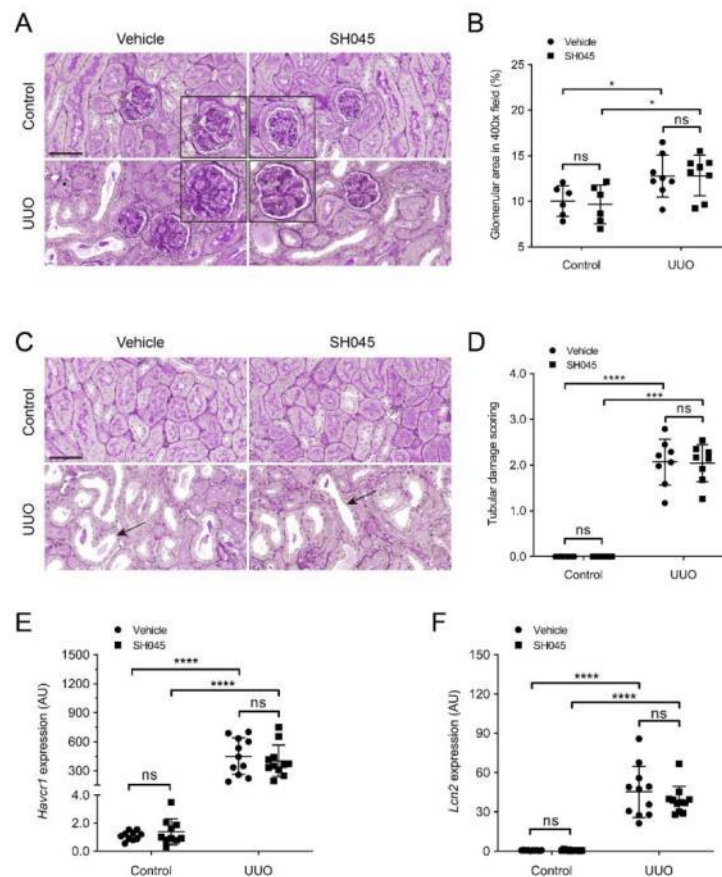


**Figure 2.** SH045 impact on kidney histopathology after UUO. **(A)** Representative images of UUO-injured glomerulus (magnification: 400 $\times$ ). Kidney sections were stained with periodic acid–Schiff staining (PAS). **(B)** Quantification of glomerular damage (control  $n = 6$ , UUO  $n = 8$ ). **(C)** Representative images of UUO-injured tubules (magnification: 400 $\times$ ). Kidneys sections were stained with periodic acid–Schiff staining (PAS). Arrows indicate tubular injury. Scale bars are 50  $\mu$ m. **(D)** Semi-quantification of tubular damage (control  $n = 6$ , UUO  $n = 8$ ). **(E)** Renal mRNA levels of kidney injury molecule 1 (*Haver1*) and **(F)** Lipocalin 2 (*Lcn2*) (control  $n = 10$ , UUO  $n = 11$ ). Data expressed as means  $\pm$  SD. Two-way ANOVA followed by Sidak’s multiple comparisons post hoc test. \*  $p < 0.05$ , \*\*\*  $p < 0.001$  and \*\*\*\*  $p < 0.0001$  defined as significant. ns, not statistically significant. AU, arbitrary units.

### 2.3. SH045 Treatment Ameliorates Renal Expression of Inflammatory Markers

Next, we measured the renal mRNA expression of inflammatory cytokines and chemokines using qRT-PCR. The expression of inflammatory molecules was markedly increased in kidneys subjected to UUO compared to control groups (Figure 3). The mRNA expression of chemokine (C-X-C motif) ligand 1 (*Cxcl1*), chemokine (C-C motif) ligand 5 (*Ccl5*), and chemokine (C-C motif) receptor 2 (*Ccr2*) was significantly lower in UUO kidneys of SH045-treated mice (SH045 UUO kidneys) compared to UUO kidneys of vehicle-treated mice (vehicle UUO kidneys) (Figure 3A–C). The expressions of chemokine (C-C

motif) ligand 2 (*Ccl2*), chemokine (C-X-C motif) ligand 2 (*Cxcl2*), and intercellular adhesion molecule 1 (*Icam1*) were increased in both SH045 UUO and vehicle UUO kidneys compared to control kidneys, although there were no differences between SH045 UUO and vehicle UUO kidneys ( $p = 0.056$ ,  $p = 0.068$  and  $p = 0.076$ , respectively) (Figure 3D–F). Furthermore, immunofluorescence staining of ICAM-1 markedly increased in UUO kidneys in comparison to control kidneys (Figure S3A–C). Additionally, the pharmacological inhibition of TRPC6 by SH045 decreased ICAM-1 expression after UUO in comparison to vehicle-treated kidneys (Figure S3A–C). Whereas ICAM1 expression was similar in the vessels of UUO kidneys, vehicle-treated kidneys had a much higher expression in SH045-treated UUO kidneys due to more ICAM-1-positive immune cell infiltration (Figure S3A).

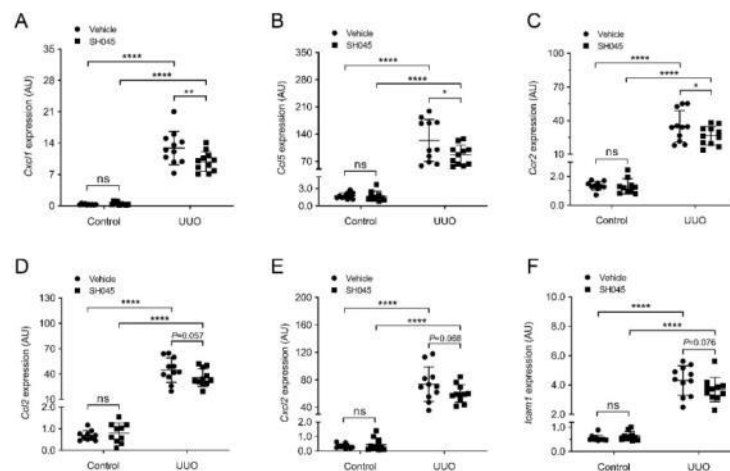


**Figure 3.** SH045 impact on renal expression of inflammatory markers. (A) Renal mRNA levels of chemokine (C-X-C motif) ligand 1 (*Cxcl1*), (B) chemokine (C-C motif) ligand 5 (*Ccl5*), (C) chemokine (C-C motif) receptor 2 (*Ccr2*), (D) chemokine (C-C motif) ligand 2 (*Ccl2*), (E) chemokine (C-X-C motif) ligand 2 (*Cxcl2*), and (F) intercellular adhesion molecule-1 (*Icam1*) (control  $n = 10$ , UUO  $n = 11$ ). Data expressed as means  $\pm$  SD. Two-way ANOVA followed by Sidak's multiple comparisons post hoc test. \*  $p < 0.05$ , \*\*  $p < 0.01$ , and \*\*\*\*  $p < 0.0001$  defined as significant. ns, not statistically significant. AU, arbitrary units.

#### 2.4. SH045 Treatment Leads to Less Renal Immune Cell Infiltration

To evaluate inflammatory cell infiltration in UUO kidneys, we examined macrophages and T cell presence using immunofluorescence. Kidney cross sections were immunolabelled with the macrophage marker F4/80 and T cell marker CD4 as described previously [17]. As shown in Figure 4A,B, excessive CD4-positive cells infiltration was observed in renal interstitium of UUO kidneys in comparison to control kidneys (Figure 4A,B). Similarly, the number of F4/80-positive cells in UUO kidneys was also markedly increased compared to control kidneys (Figure 4C,D). In accordance with ameliorated inflammatory cytokine and chemokine expression, SH045 treatment decreased UUO-induced macrophage and T cell infiltration (Figure 4A–D). Thus, these data suggest that TRPC6 inhibition reduces renal inflammation in the UUO model of NZO mice.

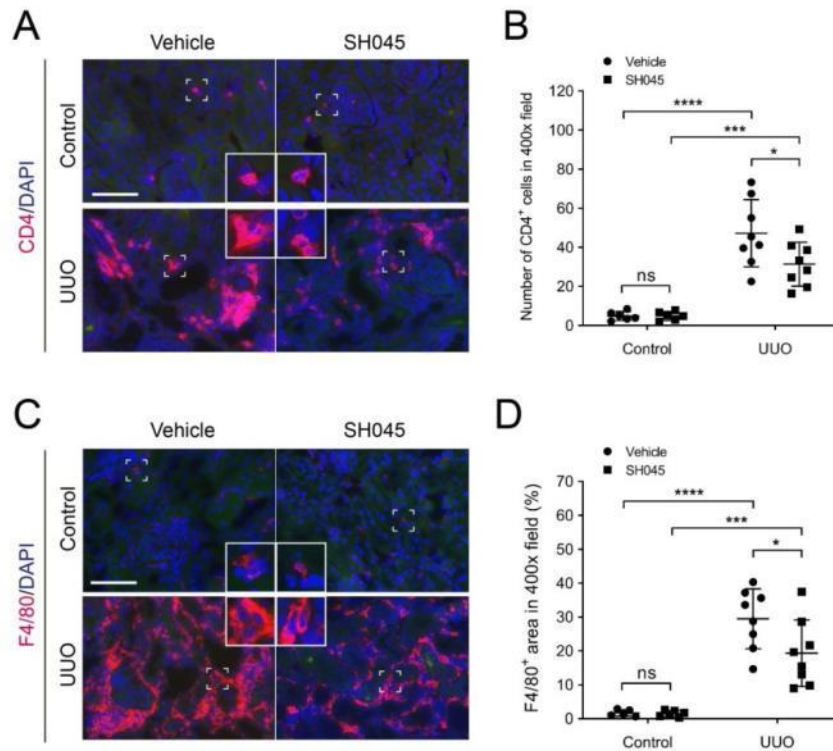


**Figure 4.** SH045 impact on renal inflammatory cell accumulation after UUO. (A) Representative images of control and UUO-injured kidneys stained with CD4<sup>+</sup> T cells (magnification: 400 $\times$ ). Rectangles represent single-cell magnifications. Scale bars are 50  $\mu$ m. (B) Quantification in renal infiltration of CD4<sup>+</sup> T cells (control  $n = 6$ , UUO  $n = 8$ ). (C) Representative images of control and UUO-injured kidneys stained with F4/80<sup>+</sup> macrophages (magnification: 400 $\times$ ). Rectangles represent single-cell magnifications. Scale bars are 50  $\mu$ m. (D) Quantification in renal infiltration of F4/80<sup>+</sup> macrophages (control  $n = 6$ , UUO  $n = 8$ ). Data expressed as means  $\pm$  SD. Two-way ANOVA followed by Sidak's multiple comparisons post hoc test. \*  $p < 0.05$ , \*\*\*  $p < 0.001$ , and \*\*\*\*  $p < 0.0001$  defined as significant. ns, not statistically significant. AU, arbitrary units.

#### 2.5. SH045 Treatment Reduces Renal Expression of Fibrotic Markers

Since progressive fibrosis is a typical lesion occurring after UUO [18], we examined the impact of SH045 administration on renal fibrosis. We measured the renal mRNA expression of pro-fibrotic markers, including collagen I (*Col1a2*), collagen III (*Col3a1*), collagen IV (*Col4a3*),  $\alpha$ -smooth muscle actin (*Acta2*), connective tissue growth factor (*Ccn2*), and fibronectin (*Fn1*). All these fibrosis-associated genes were upregulated after UUO (Figure 5A–F). Notably, SH045 treatment significantly reduced *Col1a2*, *Col3a1*, *Col4a3*, *Acta2*, *Ccn2*, and *Fn1* expressions in the UUO kidney (Figure 5A–F).



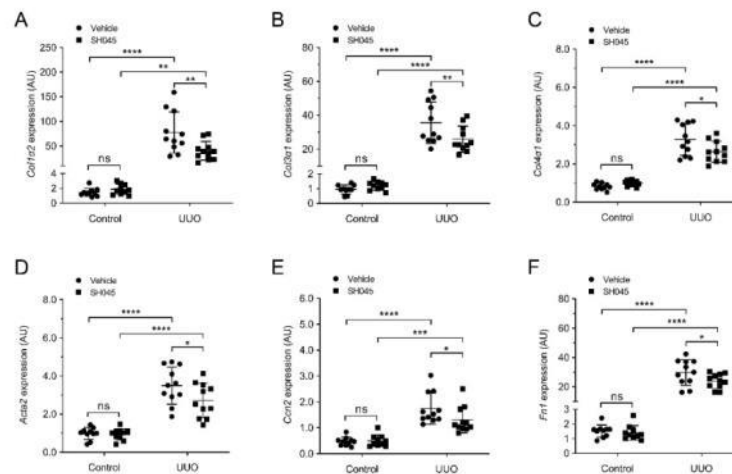


**Figure 5.** SH045 impact on expression of renal fibrotic markers UUO. (A) Renal mRNA levels of collagen type I  $\alpha$  1 (*Col1a2*), (B) Collagen type III  $\alpha$  1 (*Col3a1*), (C) Collagen type IV  $\alpha$  1 (*Col4a1*), (D)  $\alpha$ -Smooth muscle actin (*Acta2*), (E) Connective tissue growth factor (*Ccn2*), and (F) Fibronectin (*Fn1*) (Control  $n = 10$ , UUO  $n = 11$ ). Data expressed as means  $\pm$  SD. Two-way ANOVA followed by Sidak's multiple comparisons post hoc test. \*  $p < 0.05$ , \*\*  $p < 0.01$ , \*\*\*  $p < 0.001$  and \*\*\*\*  $p < 0.0001$  defined as significant. ns, not statistically significant. AU, arbitrary units.

To further confirm our qPCR data, Sirius red (SR) and fibronectin immunofluorescence staining was performed. Control kidneys exhibited small SR-positive (+) areas. In contrast, UUO kidneys displayed markedly increased SR<sup>+</sup> areas compared to control kidneys, indicating that UUO caused considerable collagen deposition (Figure 6A,B). SH045 effectively decreased this collagen deposition (Figure 6A,B). Similarly, immunofluorescence staining revealed increased fibronectin deposition and chromogenic immunohistochemistry increased  $\alpha$ -smooth muscle actin ( $\alpha$ -SMA) expression in UUO kidneys in comparison to control kidneys, which were reduced by SH045 treatment (Figure 6C–F). Taken together, these data suggest that renal fibrosis and inflammatory reactions are ameliorated in response to *in vivo* TRPC6 inhibition by SH045.

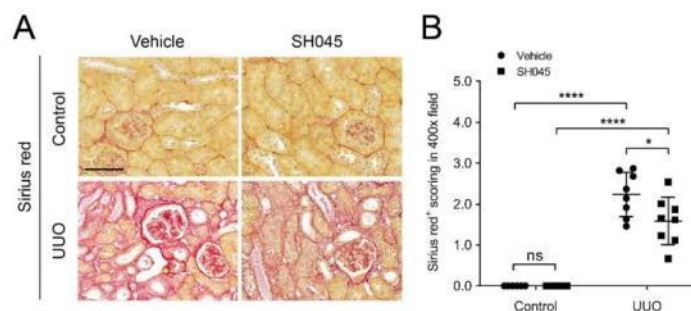


**Figure 6.** Cont.

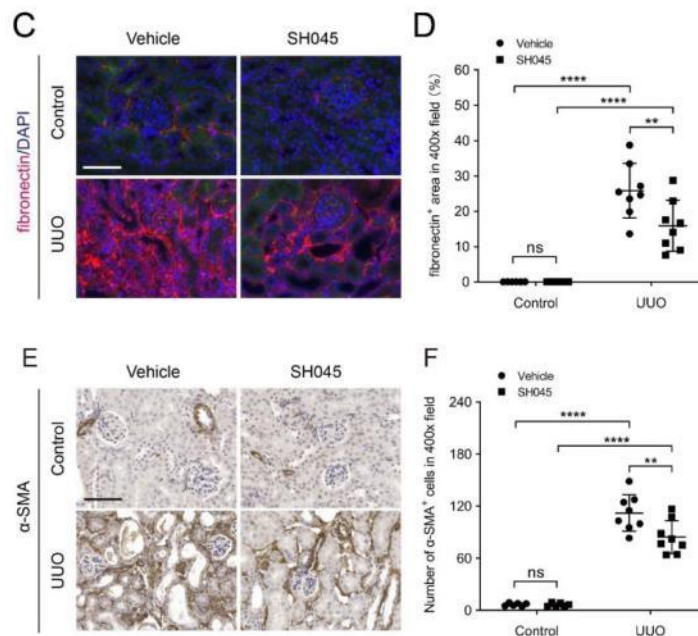


**Figure 6.** SH045 impact on renal fibrogenesis after UUO. (A) Representative images of control and UUO-injured kidneys stained with Sirius red (magnification: 400 $\times$ ). Scale bars are 50  $\mu$ m. (B) Semi-quantification in renal Sirius red+ area proportion (control  $n = 6$ , UUO  $n = 8$ ). (C) Representative images of control and UUO-injured kidneys stained with fibronectin (magnification: 400 $\times$ ). Scale bars are 50  $\mu$ m. (D) Quantification in fibronectin+ area (control  $n = 6$ , UUO  $n = 8$ ). (E) Representative images of control and UUO-injured kidneys stained with  $\alpha$ -SMA (magnification: 400 $\times$ ). Scale bars are 50  $\mu$ m. (F) Quantification of  $\alpha$ -SMA+ staining (control  $n = 6$ , UUO  $n = 8$ ). Data expressed as means  $\pm$  SD. Two-way ANOVA followed by Sidak's multiple comparisons post hoc test. \*  $p < 0.05$ , \*\*  $p < 0.01$ , and \*\*\*\*  $p < 0.0001$  defined as significant. ns, not statistically significant.

### 3. Discussion

Renal fibrosis is the final common outcome of progressive CKD, which is often observed in metabolic syndrome [19]. To date, there are few clinical treatments that successfully target fibrosis in CKD. Thus, developing new drug treatments is the current focus. Increasing evidence indicates that TRPC6 could play a critical role in kidney fibrosis [20]. In our previous study using *Trpc6*<sup>-/-</sup> mice, we found that TRPC6 deficiency ameliorated renal fibrosis and immune cellular infiltration in the UUO model [7]. However, the results were difficult to interpret due to confounding genomic and non-genomic effects of other TRPC channels, e.g., TPRC1, TRPC3, TRPC4 and TRPC5. Previous studies identified SH045 (larixyl N-methylcarbamate) as a novel, highly potent, subtype-selective inhibitor of TRPC6 channels [15]. In our previous study, we found that the in vivo inhibition of TRPC6 by SH045 had no effects on acute kidney injury (AKI) [14]. However, there are no studies on the effects of SH045 in kidney fibrosis. In the present study, we tested the hypothesis that SH045 ameliorates UUO-accelerated renal fibrosis in NZO mice.

Our results show that SH045 ameliorates fibrotic processes in UUO kidneys. Expressions of all investigated fibrosis or fibrosis-related genes were ameliorated by SH045 treatment. The histological assessment of deposited collagen and extracellular matrix protein confirmed the expression data of the genes. Of note, renal fibrosis arises after an insult, whereas resident kidney fibroblasts and cells of hematopoietic origin differentiate

into myofibroblasts [21–23]. Myofibroblasts acquire a contractile/proliferative phenotype upon activation by profibrotic factors and become principal kidney collagen-producing cells [24]. Considerable evidence indicates that renal inflammation plays a central role in the initiation and progression of fibrosis [19]. Myofibroblasts are regulated by a variety of means, including paracrine signals derived from lymphocytes and macrophages. Critical chemokines recruiting macrophages and lymphocytes are CCL2/CCR2, CCL5, and CXCL1/2. ICAM-1 is an endothelial- and leukocyte-associated transmembrane protein in facilitating leukocyte endothelial transmigration [25]. Interestingly, our results show that SH045 inhibits the overexpression of these chemokines and the infiltration of numerous immune cells, suggesting that TRPC6 inhibition may antagonize renal fibrosis by affecting inflammatory processes. TRPC6 is expressed in a wide range of cell types, including neutrophils, lymphocytes, platelets and the endothelium, which might be a modulator of tissue susceptibility to inflammatory injuries [26,27]. Some studies suggested that TRPC6 channels may enhance chemotactic responses by increasing  $Ca^{2+}$  concentration, which promotes actin-based cytoskeleton remodeling [28,29]. Furthermore,  $Ca^{2+}$  currents within T-lymphocytes are influenced by TRPC6, which can affect the function of T-lymphocytes [30]. Novel myeloid cell subsets could be targeted to ameliorate injury or enhance repair, including an *Arg1+* monocyte subset present during injury and *Mmp12+* macrophages present during repair [31]. It is intriguing to speculate that TRPC6 inhibition might ameliorate fibrotic processes in UUO kidneys by modulating the function(s) of these cell types.

On the other hand, TRPC6 was also reported to contribute to fibroblast transdifferentiation and healing in vivo [32]. Thus, the beneficial effects of TRPC6 inhibition seen in the UUO model might also involve fibroblasts. A TRPC6 blockade may decrease  $Ca^{2+}$  dependent activation of MEK/ERK signaling pathway [33]. Of note, this pathway was implemented in the detrimental differentiation and expansion of kidney fibroblasts [34]. The inhibition of the ERK1/2 pathway by trametinib ameliorated UUO-induced fibrosis through the mammalian target of rapamycin complex 1 (mTORC1) and its downstream targets.

In the present study, SH045 did not affect renal function parameters in 7-day-UUO mice, which is not surprising. In this short-term UUO model, the kidney function of contralateral undamaged kidney remained preserved and compensated for the loss of the obstructed kidney at the early stage [35]. We used the NZO inbred obese mouse strain, which carries susceptibility genes for diabetes and hypertension, conditions similar to metabolic syndrome and CKD in humans [36]. Our data observed in UUO induced fibrosis in NZO mice, and thus might be of importance in mimicking human CKD pathophysiology.

Renal fibrosis involves complex interactions among multiple cells and cytokine signaling pathways. Further studies of the TRPC6 modulation of renal fibrosis using single-cell RNA sequencing could help to better understand the exact mechanism(s) of action in the different cell types. Single-cell RNA sequencing enables the precise discrimination of specific cell type(s) or cell state(s) enriched in certain conditions (e.g., UUO) [31]. Thus, selecting cellular labels based on gene expression markers could represent a novel approach to determine cell type(s) or cell state(s) predominantly influenced by the inhibition of TRPC6 (by SH045) in the UUO model. Understanding the mechanisms behind TRPC6-induced fibrogenesis is essential for developing novel therapies to slow the progression of CKD.

Our study demonstrates that the in vivo administration of SH045 ameliorates immune cell infiltration and fibrosis in NZO mice subjected to UUO, which makes SH045 a promising therapeutic drug strategy in CKD treatment for metabolic syndrome.

## 4. Materials and Methods

### 4.1. Animals

Male NZO mice ( $n = 22$ , NZO/BomHIDife genetic background) from Max-Rubner-Laboratory, German Institute of Human Nutrition Potsdam-Rehbrücke (Nuthetal, Germany) were used. These mice had increased weight ( $45.90 \pm 4.11$  g b.w) and were previously characterized [7]. Mice were held in specific-pathogen-free (SPF) condition, in a 12:12 h



light–dark cycle, with free access to food and drinking water. All experimental procedures were approved by the Berlin Animal Review Board, Berlin, Germany and followed the restrictions in the Berlin State Office for Health and Social Affairs (LaGeSo) [37]. All experiments were performed in accordance with ARRIVE guidelines [38].

#### 4.2. UUO Model

UUO mouse model was performed as described earlier [7]. Briefly, NZO mice were anaesthetized by isoflurane (2.2%) supplied with air flow at approximately 350 mL/min. During the surgery mice were placed on a heating pad to prevent hypothermia. Preemptive analgesia with carprofen (5–10 mg/kg b.w) was subcutaneously used. Body temperature was maintained at 37.5 °C and monitored during surgery using a temperature controller with a heating pad (TCAT-2, Physitemp Instruments, Clifton, NJ, USA). In deep anesthesia, the anterior abdominal skin was shaved. Then, a midline laparotomy was conducted via an incision of the avascular linea alba, and the left ureter was exposed from left side. The ureter was then ligated twice close to the renal pelvis using a 5–0 polyglycolic acid (PGA) suture wire (Resorba®, Nürnberg, Germany). The linea alba and skin were closed separately. The wound was sanitized with a silver aluminium spray (Henry Schein®, Berlin, Germany), and 0.5 mL of warm (37 °C) isotonic sodium chloride solution was intraperitoneally injected. Subsequently, each mouse was placed in a cage in front of an infrared (IR) lamp and monitored until they recovered consciousness. For the following two days, mice received carprofen (2.5 mg/mL) in their drinking water (1:50) with a final concentration of 0.05 mg/mL. After surgery mice had free access to drinking water and chow. Seven days after UUO surgery, mice were sacrificed by overdose of isoflurane and cervical dislocation. The blood samples were collected for further analysis and left kidneys were removed immediately. The kidneys were divided into three portions. Upper part of the kidney tissue was frozen in isophane. Middle part of kidney was immersed in 4% phosphate-buffered saline (PBS)-buffered formalin for histological assessment. The other left tissue was snap frozen in liquid nitrogen for RNA preparation.

#### 4.3. TRPC6 Inhibitor

SH045 (Larixyl-6-N-methylcarbamate) was previously described [15]. SH045 was initially dissolved in DMSO (final concentration of DMSO is 0.5%) and then in 5% Cremophor EL® solution with 0.9% NaCl and used for intraperitoneal injection (i.p.). Mice subjected to UUO were treated with SH045 (20 mg/kg once per day, i.p.) or vehicle daily until day 7 after surgery.

#### 4.4. Blood Measurements and Drugs

The blood measurements of sodium, potassium, chloride, ionized calcium, total carbon dioxide, glucose, urea nitrogen, creatinine, hematocrit, hemoglobin, and anion gap were performed at endpoint. Ninety-five microliters of blood were taken from the facial vein, and parameters were measured using i-STAT system with Chem8+ cartridges (Abbott GmbH, Wiesbaden, Germany).

#### 4.5. Quantitative Real-Time (qRT)-PCR

The qRT-PCR was performed as previously described [7]. Briefly, total mRNA from mice was isolated from snap-frozen kidneys using RNeasy RNA isolation kit (Qiagen, Australia), according to the manufacturer's instructions. The concentration and quality of RNA were determined by NanoDrop-1000 spectrophotometer (Thermo Fisher Scientific, Waltham, MA, USA). Next, RNA was transcribed to cDNA using a reaction kit (Applied Biosystems, Waltham, MA, USA). Quantitative analysis of target marker was performed with qRT-PCR using the relative standard curve method. TaqMan or SYBR green analysis was conducted by using an Applied Biosystems 7500 Sequence Detector (Applied Biosystems, Waltham, MA, USA). The expression levels were normalized to 18S rRNA. All primer sequences are provided in Table S2.

#### 4.6. Kidney Histopathology

Histological kidney assessment was performed as previously reported [39]. Formalin-fixed, paraffin-embedded sections (2  $\mu\text{m}$ ) of kidneys were subjected to periodic acid–Schiff (PAS) and Sirius red (SR) staining. The PAS reaction visualized the basement membranes of the capillary loops of the glomeruli, through which the glomerular damage can be evaluated [7]. In each group, 10 fields of view were randomly selected from each kidney sample section under a 400 $\times$  magnification, and the average ratio of glomerular section area to total area within the view was calculated using the software ImageJ. SR staining allows for a quantification of interstitial fibrosis. The severity of tubule interstitial fibrosis was graded from 0 to 3 according to the distribution of lesions: 0, no lesion; 1, less than 20%; 2, 20–50%; 3, more than 50% [40]. Semi-quantitative glomerular damage and renal fibrotic scoring were performed in a blinded manner at 400 $\times$  magnification per sample. All measurements were repeated three times.

#### 4.7. Immunofluorescence and Immunohistochemistry

We performed immunostaining as previously described [7,41]. Immunofluorescence or immunohistochemistry was performed on 3- $\mu\text{m}$  ice-cold acetone-fixed cryosections of kidneys using the following primary antibodies: anti-fibronectin, anti-CD4, anti-F4/80, anti-ICAM-1, anti- $\alpha$ -SMA (AbD Serotec, Oxford, UK). For indirect immunostaining, non-specific binding sites were blocked with 10% normal donkey serum for 30 min. Then, sections were incubated with the primary antibody for 1 h at room temperature or overnight at 4  $^{\circ}\text{C}$ . All incubations were performed in a humid chamber. For fluorescence visualization of bound primary antibodies, sections were further incubated with Cy3-conjugated secondary antibodies (Jackson Immuno Research, WG, USA) for 1 h in a humid chamber at room temperature. Slides were analyzed using a Zeiss Axioplan-2 imaging microscope with the computer program AxioVision 4.8 (Zeiss, Jena, Germany). For immunohistochemistry, after incubation with the primary antibody directed against  $\alpha$ -SMA, biotinylated secondary antibody (Dako REAL<sup>TM</sup> EnVision<sup>TM</sup>; Dako Denmark A/S, Glostrup, Denmark) was used. Immunohistochemical positive staining was consecutively revealed by the 3,3'-Diaminobenzidine Peroxidase Substrate Kit (Dako REAL<sup>TM</sup> EnVision<sup>TM</sup>; Dako Denmark A/S, Glostrup, Denmark) in accordance with the manufacturer's instructions.

Quantitative analyses of infiltrating cells (CD4+ and F4/80+) and fibroblasts ( $\alpha$ -SMA+) were counted in 15 non-overlapping, randomly chosen fields per kidney section under a 400 $\times$  magnification. The average ratio of the fibronectin or ICAM-1-labeled area to the total area in the view (400 $\times$ ) was calculated using the software ImageJ (NIH, Bethesda, MD, USA). In addition, ICAM-1 expression was also analyzed using software ImageJ to calculate the mean gray value (integrated density to area).

#### 4.8. Statistics

Statistical analysis was performed using GraphPad 5.04 software. Study groups were analyzed by two-way ANOVA using Sidak's multiple comparisons post hoc test. Data are presented as mean  $\pm$  SD.  $p$  values < 0.05 were considered statistically significant.

**Supplementary Materials:** The following are available online at: <https://www.mdpi.com/article/10.3390/ijms23126870/s1>.

**Author Contributions:** Conceptualization, M.G., D.T. and L.M.; Data curation, Z.Z.; Formal analysis, Z.Z. and Y.X.; Funding acquisition, M.S., B.N. and M.G.; Investigation, Z.Z. and Y.X.; Methodology, Z.Z., U.K., M.S., B.N. and M.-B.K.; Project administration, M.G., D.T. and L.M.; Resources, U.K., T.G., M.G. and L.M.; Software, Z.Z., D.T. and L.M.; Supervision, M.G., D.T. and L.M.; Validation, D.T. and L.M.; Writing—original draft, Z.Z.; Writing—review and editing, M.G., D.T. and L.M. All authors agree to be accountable for all aspects of the work in ensuring that questions related to the accuracy or integrity of any part of the work are appropriately investigated and resolved. All authors made substantial contributions to conception, design, drafting and completion of the article. All authors have read and agreed to the published version of the manuscript.



**Funding:** This work was supported by the Deutsche Forschungsgemeinschaft (DFG) to M.G. (GO766/18-2, GO 766/12-3, SFB 1365), B.N. (NU 53/12-2) and M.S. (TRR 152) and Werner Jackstädt-Stiftung.

**Institutional Review Board Statement:** The animal study protocol was approved by the Berlin Animal Review Board, Berlin, Germany and followed the restrictions in the Berlin State Office for Health and Social Affairs (Landesamt für Gesundheit und Soziales, LaGeSo) (license No. G0175/18, 11 Sep. 2018). All experiments were performed in accordance with ARRIVE guidelines.

**Informed Consent Statement:** Not applicable.

**Data Availability Statement:** Represented data are publicly archived datasets. For further information, please contact the corresponding author.

**Acknowledgments:** We thank Mario Kaßmann for his administrative support. We thank Jana Czuchi, Gabriele N'diaye, and Juliane Ulrich for their technical help. We acknowledge financial support from the Open Access Publication Fund of Charité—Universitätsmedizin Berlin and the German Research Foundation (DFG).

**Conflicts of Interest:** The authors declare no conflict of interest.

## References

- Jha, V.; Garcia-Garcia, G.; Iseki, K.; Li, Z.; Naicker, S.; Plattner, B.; Saran, R.; Wang, A.Y.; Yang, C.W. Chronic kidney disease: Global dimension and perspectives. *Lancet* **2013**, *382*, 260–272. [\[CrossRef\]](#)
- Genovese, G.; Friedman, D.J.; Ross, M.D.; Lecordier, L.; Uzureau, P.; Freedman, B.I.; Bowden, D.W.; Langefeld, C.D.; Oleksyk, T.K.; Uscinski Knob, A.L.; et al. Association of trypanolytic ApoL1 variants with kidney disease in African Americans. *Science* **2010**, *329*, 841–845. [\[CrossRef\]](#)
- Li, X.; Pan, J.; Li, H.; Li, G. DsbA-L mediated renal tubulointerstitial fibrosis in UUO mice. *Nat. Commun.* **2020**, *11*, 4467. [\[CrossRef\]](#)
- Black, L.; Lever, J.M.; Traylor, A.M.; Chen, B.; Yang, Z.; Esmen, S.; Jiang, Y.; Cutter, G.; Boddu, R.; George, J.; et al. Divergent effects of AKI to CKD models on inflammation and fibrosis. *Am. J. Physiol. Ren. Physiol.* **2018**, *315*, F1107–F1118. [\[CrossRef\]](#)
- Schlondorff, J. TRPC6 and kidney disease: Sclerosing more than just glomeruli? *Kidney Int.* **2017**, *91*, 773–775. [\[CrossRef\]](#) [\[PubMed\]](#)
- Eddy, A.A. Overview of the cellular and molecular basis of kidney fibrosis. *Kidney Int Suppl* (2011). **2014**, *4*, 2–8. [\[CrossRef\]](#) [\[PubMed\]](#)
- Kong, W.; Haschler, T.N.; Nürnberg, B.; Krämer, S.; Gollasch, M.; Markó, L. Renal Fibrosis, Immune Cell Infiltration and Changes of TRPC Channel Expression after Unilateral Ureteral Obstruction in *Trpc6*<sup>-/-</sup> Mice. *Cell Physiol. Biochem.* **2019**, *52*, 1484–1502. [\[PubMed\]](#)
- Lin, B.L.; Matera, D.; Doerner, J.F.; Zheng, N.; Del Camino, D.; Mishra, S.; Bian, H.; Zeveleva, S.; Zhen, X.; Blair, N.T.; et al. In vivo selective inhibition of TRPC6 by antagonist BI 749327 ameliorates fibrosis and dysfunction in cardiac and renal disease. *Proc. Natl. Acad. Sci. USA* **2019**, *116*, 10156–10161. [\[CrossRef\]](#)
- Ilatovskaya, D.V.; Staruschenko, A. TRPC6 channel as an emerging determinant of the podocyte injury susceptibility in kidney diseases. *Am. J. Physiol. Ren. Physiol.* **2015**, *309*, F393–F397. [\[CrossRef\]](#)
- Dryer, S.E.; Roshanravan, H.; Kim, E.Y. TRPC channels: Regulation, dysregulation and contributions to chronic kidney disease. *Biochim. Biophys. Acta Mol. Basis Dis.* **2019**, *1865*, 1041–1066. [\[CrossRef\]](#)
- Winn, M.P.; Conlon, P.J.; Lynn, K.L.; Farrington, M.K.; Creazzo, T.; Hawkins, A.F.; Daskalakis, N.; Kwan, S.Y.; Ebersviller, S.; Burchette, J.L.; et al. A mutation in the TRPC6 cation channel causes familial focal segmental glomerulosclerosis. *Science* **2005**, *308*, 1801–1804. [\[CrossRef\]](#) [\[PubMed\]](#)
- Reiser, J.; Polu, K.R.; Moller, C.C.; Kenlan, P.; Altintas, M.M.; Wei, C.; Faul, C.; Herbert, S.; Villegas, I.; Avila-Casado, C.; et al. TRPC6 is a glomerular slit diaphragm-associated channel required for normal renal function. *Nat. Genet.* **2005**, *37*, 739–744. [\[CrossRef\]](#) [\[PubMed\]](#)
- Riehle, M.; Buscher, A.K.; Gohlke, B.O.; Kassmann, M.; Kolatsi-Joannou, M.; Brasen, J.H.; Nagel, M.; Becker, J.U.; Winyard, P.; Hoyer, P.F.; et al. TRPC6 G757D Loss-of-Function Mutation Associates with FSGS. *J. Am. Soc. Nephrol.* **2016**, *27*, 2771–2783. [\[CrossRef\]](#) [\[PubMed\]](#)
- Zheng, Z.; Tsvetkov, D.; Bartolomaeus, T.U.P.; Erdogan, C.; Krügel, U.; Schleifenbaum, J.; Schaefer, M.; Nürnberg, B.; Chai, X.; Ludwig, F.A.; et al. Role of TRPC6 in kidney damage after acute ischemic kidney injury. *Sci. Rep.* **2022**, *12*, 3038. [\[CrossRef\]](#) [\[PubMed\]](#)
- Häfner, S.; Burg, F.; Kannler, M.; Urban, N.; Mayer, P.; Dietrich, A.; Trauner, D.; Broichhagen, J.; Schaefer, M. A (+)-Larixol Congener with High Affinity and Subtype Selectivity toward TRPC6. *ChemMedChem* **2018**, *13*, 1028–1035. [\[CrossRef\]](#) [\[PubMed\]](#)
- Breyer, M.D.; Böttinger, E.; Brosius, F.C., 3rd; Coffman, T.M.; Harris, R.C.; Heilig, C.W.; Sharma, K. Mouse models of diabetic nephropathy. *J. Am. Soc. Nephrol.* **2005**, *16*, 27–45. [\[CrossRef\]](#)
- Markó, L.; Park, J.K.; Henke, N.; Rong, S.; Balogh, A.; Klamer, S.; Bartolomaeus, H.; Wilck, N.; Ruland, J.; Forslund, S.K.; et al. B-cell lymphoma/leukaemia 10 and angiotensin II-induced kidney injury. *Cardiovasc. Res.* **2020**, *116*, 1059–1070. [\[CrossRef\]](#)

18. Chevalier, R.L.; Forbes, M.S.; Thornhill, B.A. Ureteral obstruction as a model of renal interstitial fibrosis and obstructive nephropathy. *Kidney Int.* **2009**, *75*, 1145–1152. [CrossRef]
19. Lv, W.; Booz, G.W.; Wang, Y.; Fan, F.; Roman, R.J. Inflammation and renal fibrosis: Recent developments on key signaling molecules as potential therapeutic targets. *Eur. J. Pharmacol.* **2018**, *820*, 65–76. [CrossRef]
20. Wu, Y.L.; Xie, J.; An, S.W.; Oliver, N.; Barrezaeta, N.X.; Lin, M.H.; Birnbaumer, L.; Huang, C.L. Inhibition of TRPC6 channels ameliorates renal fibrosis and contributes to renal protection by soluble klotho. *Kidney Int.* **2017**, *91*, 830–841. [CrossRef] [PubMed]
21. LeBleu, V.S.; Taduri, G.; O’Connell, J.; Teng, Y.; Cooke, V.G.; Woda, C.; Sugimoto, H.; Kalluri, R. Origin and function of myofibroblasts in kidney fibrosis. *Nat. Med.* **2013**, *19*, 1047–1053. [CrossRef]
22. Zeisberg, E.M.; Potenta, S.E.; Sugimoto, H.; Zeisberg, M.; Kalluri, R. Fibroblasts in kidney fibrosis emerge via endothelial-to-mesenchymal transition. *J. Am. Soc. Nephrol.* **2008**, *19*, 2282–2287. [CrossRef] [PubMed]
23. Lu, Y.A.; Liao, C.T.; Raybould, R. Single-Nucleus RNA Sequencing Identifies New Classes of Proximal Tubular Epithelial Cells in Kidney Fibrosis. *J. Am. Soc. Nephrol.* **2021**, *32*, 2501–2516. [CrossRef] [PubMed]
24. Tomasek, J.J.; Gabbiani, G.; Hinz, B.; Chaponnier, C.; Brown, R.A. Myofibroblasts and mechano-regulation of connective tissue remodelling. *Nat. Rev. Mol. Cell Biol.* **2002**, *3*, 349–363. [CrossRef]
25. Shlipak, M.G.; Fried, L.F.; Crump, C.; Bleyer, A.J.; Manolio, T.A.; Tracy, R.P.; Furberg, C.D.; Psaty, B.M. Elevations of inflammatory and procoagulant biomarkers in elderly persons with renal insufficiency. *Circulation* **2003**, *107*, 87–92. [CrossRef]
26. Chen, Q.; Zhou, Y.; Zhou, L.; Fu, Z.; Yang, C.; Zhao, L.; Li, S.; Chen, Y.; Wu, Y.; Ling, Z.; et al. TRPC6-dependent Ca(2+) signaling mediates airway inflammation in response to oxidative stress via ERK pathway. *Cell Death Dis.* **2020**, *11*, 170. [CrossRef] [PubMed]
27. European Bioinformatics Institute (EMBL-EBI); SIB Swiss Institute of Bioinformatics (PIR). P.I.R. Universal Protein Resource (Uniprot). Available online: <http://www.uniprot.org/> (accessed on 17 March 2022).
28. Damann, N.; Owsianik, G.; Li, S.; Poll, C.; Nilius, B. The calcium-conducting ion channel transient receptor potential canonical 6 is involved in macrophage inflammatory protein-2-induced migration of mouse neutrophils. *Acta Physiol.* **2009**, *195*, 3–11. [CrossRef] [PubMed]
29. Lindemann, O.; Umlauf, D.; Frank, S.; Schimmelpfennig, S.; Bertrand, J.; Pap, T.; Hanley, P.J.; Fabian, A.; Dietrich, A.; Schwab, A. TRPC6 regulates CXCR2-mediated chemotaxis of murine neutrophils. *J. Immunol.* **2013**, *190*, 5496–5505. [CrossRef]
30. Carrillo, C.; Hichami, A.; Andreoletti, P.; Cherkaoui-Malki, M.; del Mar Cavia, M.; Abdoul-Azize, S.; Alonso-Torre, S.R.; Khan, N.A. Diacylglycerol-containing oleic acid induces increases in [Ca(2+)](i) via TRPC3/6 channels in human T-cells. *Biochim. Biophys. Acta* **2012**, *1821*, 618–626. [CrossRef]
31. Conway, B.R.; O’Sullivan, E.D. Kidney Single-Cell Atlas Reveals Myeloid Heterogeneity in Progression and Regression of Kidney Disease. *J. Am. Soc. Nephrol.* **2020**, *31*, 2833–2854. [CrossRef]
32. Davis, J.; Burr, A.R.; Davis, G.F.; Birnbaumer, L.; Molkentin, J.D. A TRPC6-dependent pathway for myofibroblast transdifferentiation and wound healing in vivo. *Dev. Cell* **2012**, *23*, 705–715. [CrossRef] [PubMed]
33. Agell, N.; Bachs, O.; Rocamora, N.; Villalonga, P. Modulation of the Ras/Raf/MEK/ERK pathway by Ca(2+), and calmodulin. *Cell Signal* **2002**, *14*, 649–654. [CrossRef]
34. Andrikopoulos, P.; Kieswich, J.; Pacheco, S.; Nadarajah, L.; Harwood, S.M.; O’Riordan, C.E.; Thiemermann, C.; Yaqoob, M.M. The MEK Inhibitor Trametinib Ameliorates Kidney Fibrosis by Suppressing ERK1/2 and mTORC1 Signaling. *J. Am. Soc. Nephrol.* **2019**, *30*, 33–49. [CrossRef] [PubMed]
35. Zeng, F.; Miyazawa, T.; Kloepfer, L.A.; Harris, R.C. ErbB4 deletion accelerates renal fibrosis following renal injury. *Am. J. Physiol. Ren. Physiol.* **2018**, *314*, F773–F787. [CrossRef] [PubMed]
36. Mirhashemi, F.; Scherneck, S.; Kluth, O.; Kaiser, D.; Vogel, H.; Kluge, R.; Schürmann, A.; Neschen, S.; Joost, H.G. Diet dependence of diabetes in the New Zealand Obese (NZO) mouse: Total fat, but not fat quality or sucrose accelerates and aggravates diabetes. *Exp. Clin. Endocrinol. Diabetes* **2011**, *119*, 167–171. [CrossRef]
37. Restrictions in the State Office for Health and Social Affairs (LAGeSo). Animal Welfare. Available online: <https://www.berlin.de/lageso/gesundheit/veterinaerwesen/tierschutz/> (accessed on 17 August 2021).
38. Kilkeny, C.; Browne, W.J.; Cuthill, I.C.; Emerson, M.; Altman, D.G. Improving bioscience research reporting: The ARRIVE guidelines for reporting animal research. *PLoS Biol.* **2010**, *8*, e1000412. [CrossRef]
39. Manna, M.; Markó, L.; Balogh, A.; Vigolo, E.; N’Diaye, G.; Kaßmann, M.; Michalick, L.; Weichelt, U.; Schmidt-Ott, K.M.; Liedtke, W.B.; et al. Transient Receptor Potential Vanilloid 4 Channel Deficiency Aggravates Tubular Damage after Acute Renal Ischaemia Reperfusion. *Sci. Rep.* **2018**, *8*, 4878. [CrossRef]
40. Zheng, Z.; Li, C.; Shao, G.; Li, J.; Xu, K.; Zhao, Z.; Zhang, Z.; Liu, J.; Wu, H. Hippo-YAP/MCP-1 mediated tubular maladaptive repair promote inflammation in renal failed recovery after ischemic AKI. *Cell Death Dis.* **2021**, *12*, 754. [CrossRef]
41. Zheng, Z.; Deng, G.; Qi, C.; Xu, Y.; Liu, X.; Zhao, Z.; Zhang, Z.; Chu, Y.; Wu, H.; Liu, J. Porous Se@SiO2 nanospheres attenuate ischemia/reperfusion (I/R)-induced acute kidney injury (AKI) and inflammation by antioxidative stress. *Int. J. Nanomed.* **2019**, *14*, 215–229. [CrossRef]



## Supplementary Information

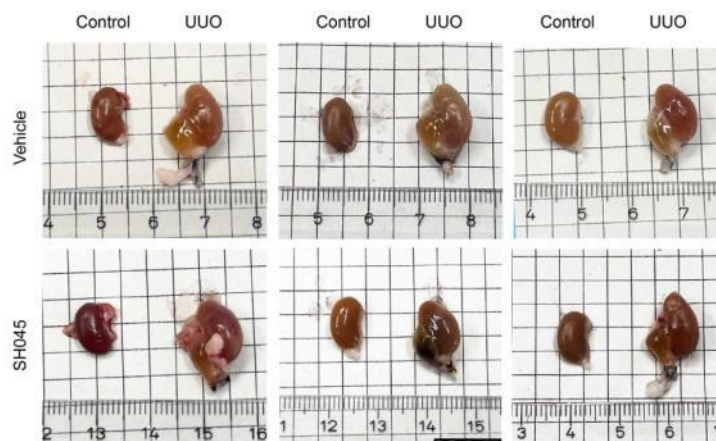
### *In vivo* inhibition of TRPC6 by SH045 attenuates renal fibrosis in the New Zealand obese (NZO) mouse model of metabolic syndrome

Zhihuang Zheng<sup>1,2,3</sup>, Yao Xu<sup>4</sup>, Ute Krügel<sup>5</sup>, Michael Schaefer<sup>5</sup>, Tilman Grune<sup>6,7</sup>, Bernd Nürnberg<sup>8</sup>, May-Britt Köhler<sup>2</sup>, Maik Gollasch<sup>1,4\*</sup>, Dmitry Tsvetkov<sup>4\*</sup> and Lajos Markó<sup>2,7,9,10\*</sup>

- <sup>1</sup> Department of Nephrology/Intensive Care, Charité - Universitätsmedizin, Corporate Member of Freie Universität Berlin, Humboldt-Universität zu Berlin, Berlin, Germany.
- <sup>2</sup> Experimental and Clinical Research Center, a cooperation of Charité - Universitätsmedizin Berlin and Max Delbrück Center for Molecular Medicine, Berlin, Germany.
- <sup>3</sup> Department of Nephrology, Shanghai General Hospital, Shanghai Jiaotong University School of Medicine, Shanghai, China.
- <sup>4</sup> Department of Geriatrics, University of Greifswald, University District Hospital Wolgast, Greifswald, Germany.
- <sup>5</sup> Rudolf Boehm Institute for Pharmacology and Toxicology, Leipzig University, Leipzig, Germany.
- <sup>6</sup> Department of Molecular Toxicology, German Institute of Human Nutrition Potsdam-Rehbruecke (DIfE), Nuthetal, Germany.
- <sup>7</sup> DZHK (German Centre for Cardiovascular Research), partner site Berlin, Germany.
- <sup>8</sup> Department of Pharmacology, Experimental Therapy and Toxicology and Interfaculty Center of Pharmacogenomics and Drug Research, University of Tübingen, Tübingen, Germany.
- <sup>9</sup> Berlin Institute of Health at Charité - Universitätsmedizin Berlin, Berlin, Germany.
- <sup>10</sup> Charité - Universitätsmedizin Berlin, Corporate Member of Freie Universität Berlin and Humboldt-Universität zu Berlin, Berlin, Germany.

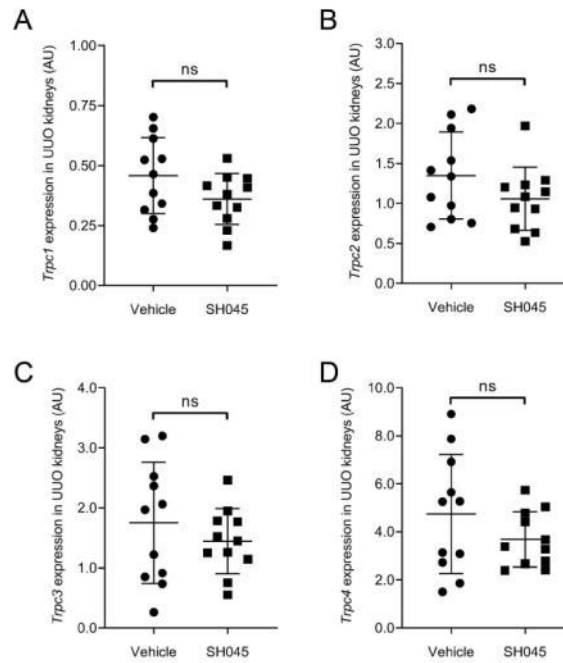
\*The corresponding authors: M.G., maik.gollasch@med.uni-greifswald.de ; D.T., dmitry.tsvetkov@med.uni-greifswald.de; L.M., lajos.marko@charite.de .

#### Figure S1

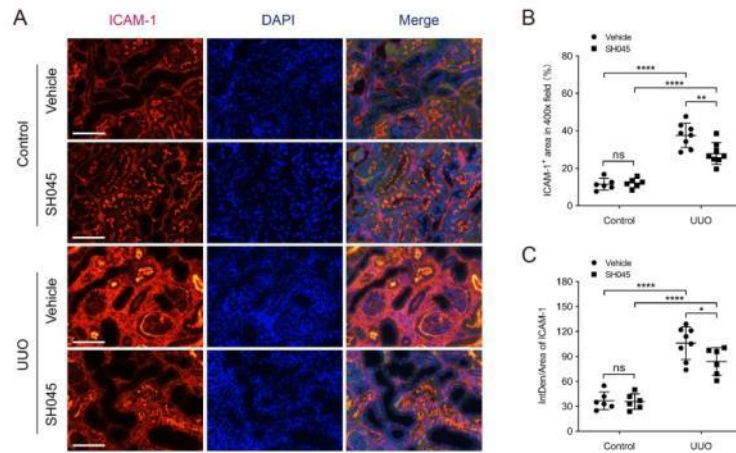


**Figure S1.** Macroscopic comparison of the kidneys. Images of control kidneys (left) and UUO kidneys (right). The UUO kidney increased in size (hydronephrosis) compared to control kidney. Scale bar: 1cm.

Figure S2



**Figure S2.** The impact of SH045 on renal *Trpc* gene expression in UJO kidneys. (A) Renal mRNA levels of *Trpc1*, (B) *Trpc2*, (C) *Trpc3*, and (D) *Trpc4* (n=11 each). Data expressed as means ± SD. Two-way ANOVA followed by Sidak's multiple comparisons post hoc test. ns, not statistically significant. AU, arbitrary units.

**Figure S3**

**Figure S3.** SH045 impact on renal ICAM-1 expression after UUO. (A) Renal immunofluorescence of ICAM-1. (B) Quantification of renal ICAM-1 expression in area proportion (Control n=6 each, UUO n=8 each, respectively). (C) Quantification of renal ICAM-1 expression in mean density (Control n=6 each, UUO n=8 each, respectively). Data expressed as means  $\pm$  SD. Two-way ANOVA followed by Sidak's multiple comparisons post hoc test. \* $p < 0.05$ , \*\* $p < 0.01$ , and \*\*\*\* $p < 0.0001$  defined as significant. ns, not statistically significant. IntDen, integrated density.

## Table S1

**Table S1.** SH045 impact on blood parameters in NZO-UUO mice. Blood parameters after 7-days UUO (n=9, 8 for UUO vehicle and UUO SH045, respectively). Data expressed as means  $\pm$  SD. Two-tailed unpaired t-test. n.a. = not applicable.

Serum parameter	Unit	UUO+Vehicle		UUO+SH045		p-value
		Mean	SD	Mean	SD	t-test
Sodium	mmol/L	147.30	1.25	146.88	2.17	0.608
Potassium	mmol/L	4.57	0.30	4.49	0.78	0.760
Chloride	mmol/L	109.40	1.17	110.75	1.49	0.047
Ionized Calcium	mmol/L	1.38	0.20	1.33	0.05	0.563
Total Carbon Dioxide	mmol/L	27.20	1.40	26.44	1.81	0.320
Glucose	mg/dL	240.10	43.83	229.56	62.19	0.672
Hematocrit	% PCV	40.10	4.43	41.63	3.62	0.444
Hemoglobin	g/dL	13.63	1.51	14.16	1.22	0.432
Anion Gap	mmol/L	16.40	2.27	15.25	1.28	0.221

## Table S2

**Table S2.** Primers used in qRT-PCR experiments.

Primers	Forward	Reverse
<i>Havcr1 (KIM-1)</i>	5'-CTGGAGTAATCACACTGAAGCAATG-3'	5'-GATGCCAACATAGAAGCCCTTAGT-3'
<i>Lcn2 (NGAL)</i>	5'-ATGTCACTCCATCCTGGTCAG-3'	5'-GCCACTTGCACATTGTAGCTCTG-3'
<i>Tpct1</i>	5'-CATCTAGCGATGAGCCTTTGAC-3'	5'-CCAAACCGTGTTCAGGAAGTGC-3'
<i>Tpct2</i>	5'-AAGACTGCGGTTGGCTGTCAAC-3'	5'-GGCAACAAGAGCTTCCAGATGG-3'
<i>Tpct3</i>	5'-ATTCTCGCCATCGGCTATTGG-3'	5'-GAGGCGTTGAATACAAGCAGACC-3'
<i>Tpct4</i>	5'-CTTGAACAGGCAAGGTCACCA-3'	5'-TGTAATCCTGGAGTCCGCCATC-3'
<i>Tpct6</i>	5'-GACCGTTCATGAAGTTGTAGCAC-3'	5'-AGTATCTTTGGGCCCTTGAGTCC-3'
<i>Col1a1</i>	5'-CATGTTCCAGCTTTGTGGACCT-3'	5'-GCAGCTGACTTCAGGGATGT-3'
<i>Col3a1</i>	5'-CTCACCCCTTTCATCCCACCTCTTA-3'	5'-ACATGGTTCTGGCTCCAGACAT-3'
<i>Col4a1</i>	5'-TTAAAGGACTCCAGGGACAC-3'	5'-CCACTGAGCCTGTACAC-3'
<i>Acta2 (<math>\alpha</math>-SMA)</i>	5'-ACTGGGACGACATGGAAAAG-3'	5'-CATCTCCAGAGTCCAGACA-3'
<i>Ccn2 (CTGF)</i>	5'-TGCGAAGCTGACCTGGAGGAAA-3'	5'-CCGCAGAAGTTCAGCCGTGATG-3'
<i>Fn1 (Fibronectin)</i>	5'-CCCTATCTCTGATACCGTTGTCC-3'	5'-TGCCGCAACTACTGTGATCCGG-3'
<i>Col2</i>	5'-GCTACAAGAGGATCACCAGCAG-3'	5'-GTCTGGACCCATTCTCTTGG-3'
<i>Col5</i>	5'-CCTGCTGTTTGCCTACCTCTC-3'	5'-ACACACTTGGCGGTTCCCTCGA-3'
<i>Ccr2</i>	5'-GCTGTGTTTGCCTCTCTACCAG-3'	5'-CAAGTAGAGGCAGGATCAGGCT-3'
<i>Cxcl1</i>	5'-TCCAGAGCTGAAGGTGTGCC-3'	5'-AACCAAGGGAGCTTCAGGGTCA-3'
<i>Cxcl2</i>	5'-CATCCAGAGCTTGAGTGTGACG-3'	5'-GGCTTCAGGGTCAAGGCAACT-3'
<i>Icam1</i>	5'-CTGGGCTTGAGACTCAGTG-3'	5'-CCACACTCTCCGAAACGAA-3'
<i>18S</i>	5'-ACATCCAAGGAAGGACGAG-3'	5'-TTTTCGTCACTACCTCCCG-3'

## **9. Curriculum Vitae**

My curriculum vitae does not appear in the electronic version of my paper for reasons of data protection.

My curriculum vitae does not appear in the electronic version of my paper for reasons of data protection.

## 10. Complete list of publications

1. **Zheng Z**, Xu Y, Krügel U, Schaefer M, Grune T, Nürnberg B, Köhler MB, Gollasch M, Tsvetkov D, Markó L. In Vivo Inhibition of TRPC6 by SH045 Attenuates Renal Fibrosis in a New Zealand Obese (NZO) Mouse Model of Metabolic Syndrome. *Int J Mol Sci.* 2022, 23(12), 6870. **IF: 5.923 (2020)**
2. **Zheng Z**, Tsvetkov D, Bartolomaeus TUP, Erdogan C, Krügel U, Schleifenbaum J, Schaefer M, Nürnberg B, Chai X, Ludwig FA, N'Diaye G, Köhler MB, Wu K, Gollasch M, Markó L. Role of TRPC6 in Kidney Damage after Acute Ischemic Kidney Injury. *Sci Rep.* 2022; 12(1): 3038. **IF: 3.998 (2019)**
3. **Zheng Z**, Xu K, Li C, Qi C, Fang Y, Zhu N, Bao J, Zhao Z, Yu Q, Wu H, Liu J. NLRP3 associated with chronic kidney disease progression after ischemia/reperfusion-induced acute kidney injury. *Cell Death Discov.* 2021; 7: 324. **IF: 4.114 (2019)**
4. **Zheng Z**, Li C, Shao G, Li J, Xu K, Zhao Z, Zhang Z, Liu J, Wu H. Hippo-YAP/MCP-1 mediated tubular maladaptive repair promote inflammation in renal failed recovery after ischemic AKI. *Cell Death Dis.* 2021; 12(8): 1-13. **IF: 6.304 (2019)**
5. **Zheng Z**, Deng G, Qi C, Xu Y, Liu X, Zhao Z, Zhang Z, Chu Y, Wu H, Liu J. Porous Se@SiO<sub>2</sub> nanospheres attenuate ischemia/reperfusion (I/R)-induced acute kidney injury (AKI) and inflammation by antioxidative stress. *Int J Nanomedicine.* 2019; 14: 215–229. **IF: 4.37 (2017)**
6. Li C, **Zheng Z** (co-first author), Xie Y, Zhu N, Bao J, Yu Q, Zhou Z, Liu J. Protective effect of taraxasterol on ischemia/reperfusion-induced acute kidney injury via inhibition of oxidative stress, inflammation, and apoptosis. *Int Immunopharmacol.* 2020; 89: 107169. **IF: 3.361 (2018)**
7. Chu Y, Wang Y, **Zheng Z**, Lin Y, He R, Liu J, Yang X. Proinflammatory Effect of High Glucose Concentrations on HMrSV5 Cells via the Autocrine Effect of HMGB1. *Front Physiol.* 2017; 8: 762. **IF: 4.134 (2016)**
8. Chen J, Zhou M, Wang H, **Zheng Z**, Rong W, He B, Zhao L. Risk factors for left atrial thrombus or spontaneous echo contrast in non-valvular atrial fibrillation patients with low CHA<sub>2</sub>DS<sub>2</sub>-VASc score. *J Thromb Thrombolysis.* 2022; 53: 523-531. **IF: 2.3 (2020)**



## 11. Acknowledgements

At this moment, I would like to express my thanks to all those who have ever given me assistance and support in this work.

Firstly, my sincere and hearty thanks and appreciations go to my supervisor, Prof. Dr. Maik Gollasch, for offering the precious opportunity to join his group. He gave me much help and advice in every stage of my doctoral studying, which has made my accomplishments possible. It has been a great privilege and joy to study under his guidance and supervision. Likewise, I would like to express my gratitude to Dr. Lajos Markó and Dr. Dmitry Tsvetkov for their supervision, dedicated support, and patient guidance. Without their help I could not complete my thesis. I am also extremely grateful to Dr. Kaiyin Wu, Dr. Mario Kaßmann, and other colleagues, who helped me a lot both in my work as well as in my life. Sincere gratitude should also go to all collaborators from AG Müller and other labs for their professional assistance. Furthermore, I would like to express my thanks to Prof. Dr. Friedrich C. Luft for his wonderful weekly lecture and guidance to me.

Importantly, I am very grateful to all my friends in Germany. With all of you, I had a perfect time and enjoyable memories. Though we may be a world apart, friendship makes us neighbours at heart. Here I sincerely appreciate my Chinese tutors Prof. Dr. Jun Liu and Prof. Huijuan Wu for their long-term care and encouragement. Of course, I also want to thank Charité – Universitätsmedizin Berlin, a great place where I learned knowledge and gained a huge growth over three years. In addition, my much appreciation would go to China Scholarship Council (CSC) for financial support in these years overseas.

Finally, I hold my sincerest gratitude to my family, especially my parents and my wife, for their deep love, sincere encouragement, and unreserved support all the time. My gratitude to them knows no bounds. Of note, here I would like to give heartfelt thanks to my sweet son Thomas Berlin Zheng (Bolin Zheng in Chinese). He gave me a tremendous glory when I become his father since 05.11.2020.

I am a slow walker, but I never walk backwards. All of you make me better. Thank and love you all!